Aging Behavior of Polymeric Absorber Materials for Solar Thermal Collectors

Dissertation

by

Susanne Kahlen

prepared at the

Polymer Competence Center Leoben GmbH

and the

Institute of Materials Science and Testing of Plastics

submitted to the

University of Leoben

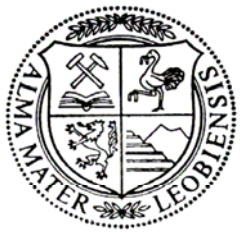

Academic Advisor

O.Univ.-Prof. Dr.mont. Reinhold W. Lang
University of Leoben, Austria

Supervisor

Ao.Univ.-Prof. Dr.mont. Gernot M. Wallner
University of Leoben, Austria

Referees

O.Univ.-Prof. Dr.mont. Reinhold W. Lang
University of Leoben, Austria

Univ.-Prof. Dr.phil. John B. Rekstad
University of Oslo, Norway

Leoben, May 2009

I declare in lieu of oath, that I wrote this dissertation and performed the associated research myself, using only the support indicated in the acknowledgements and the literature cited.

Leoben, May 2009 *Dipl.-Ing. Susanne Kahlen*

ACKNOWLEDGEMENTS

First, I would like to thank Prof. Reinhold W. Lang for his efforts in reviewing the papers and the dissertation and for his permanent interest in my work. The discussions with him offered me the possibility to look into my investigations differently. I further profited from his guidance to improve my scientific writing style. I am also very grateful to Prof. John B. Rekstad, for his acceptance as second referee of my doctoral committee. I would like to thank him for the critical discussions about polymers and for the knowledge about solar systems I learnt from him.

My best thanks go to Dr. Gernot M. Wallner who offered me this challenging possibility to work with polymers in the renewable energy research field. He contributed considerably to the scientific quality of this works and I learned from him the fundamental basics of scientific working. I am very thankful for the numerous discussions and fruitful inputs for my work.

Special thanks go to Dipl.-Ing. Jörg Fischer and Stefan Lemmerer who supported me in my work and have been beneficially for the thesis.

I would also like to express my thanks to my former colleague Dr. Robin Steinberger, who contributed with his expertise to the measurements for Paper 1 and helped me in preparing the manuscript.

I am also indebted to the companies providing me the raw materials for my research work and for performing analytical tests. In this regard special thanks go to Dr. Collin GmbH (Ebersberg, D) and Solarnor AS (Oslo, N) for the film extrusion and the supply of numerous absorber sheets.

Furthermore I would like to thank Dr. Michaela Meir, Dr. Andres Olivares and Jeanette Schackenda for the construction and supervision of the testing site at the University of Oslo.

I would like to thank all the staff from the Polymer Competence Center Leoben GmbH and from the Institute of Materials Science and Testing of Plastics for their support in solving the problems that have encountered during the last years.

Finally I wish to express my gratitude to my long lasting partner Michael Jerabek who not only contributed to Paper 1 but also encouraged me in difficult situations. I thank him also for his generous optimistic attitude in solving problems.

This research work was performed at the Polymer Competence Center Leoben GmbH (PCCL) within the research projects I-S.9 and II-S.11 in cooperation with the Institute of Materials Science and Testing of Plastics at the University of Leoben. The PCCL is funded by the Austrian Government and the State Governments of Styria and Upper Austria within the K_{plus} program of the Austrian Ministry of Traffic, Innovation and Technology.

ABSTRACT

Plastics offer a high potential for use in solar thermal absorbers, in particular also for flat plate collectors. For such applications, high temperatures in air and water represent the most harmful service conditions. Hence, the investigation of aging phenomena in such materials at elevated temperatures in water and air is of enormous importance to characterize their performance and to identify possible limitations. So far, no comprehensive characterization has been reported, and therefore the main objective of this dissertation was to investigate the aging behavior of plastics for solar thermal absorbers using various methods of polymer science. Special focus was given to the determination of physical and chemical aging processes, and to the establishment of structure-property relationships and of correlations between the results obtained on the level of laboratory specimens, and the sub-component and component level.

For this dissertation, eight different potential polymers for solar thermal absorbers, including four engineering-type plastics (a blend of polyphenylene ether and polystyrene (PPE+PS), polycarbonate (PC), high-impact polyamide 12 (PA12-HI), high-temperature PA12 (PA12-HT)) and four commodity-type plastics (two types of crosslinked polyethylene (PE-X1, PE-X2), two types of polypropylene (PP-1, PP-2)), were selected. According to northern climate conditions, 140 °C in air (during stagnation) and 80 °C in water (during operation) with aging times up to 500 h and 16000 h, respectively, were assumed as typical aging conditions corresponding to an accumulated lifetime of 20 year in service. On the laboratory specimen level, two different analytical methods (differential scanning calorimetry (DSC) and size exclusion chromatography (SEC)) and a mechanical method (monotonic tensile test) were applied to investigate the aging behavior. On the sub-component and component level, DSC and a mechanical indentation test were performed. Furthermore, for three selected polymers (PPE+PS, PC, PP-2) three different lifetime prediction models based on the Arrhenius relationship and results obtained on the laboratory specimen level were used to determine service time endurance limits.

Based on the experimental results generated and the data analysis applied (direct data reduction and/or Arrhenius based lifetime assessment models), only one of the investigated materials, i.e. PA12-HI, was found to be a promising solar thermal absorber material candidate to be applied over the full range of temperatures in air and water as indicated above. Several other materials, offer the potential for absorber applications under more specific conditions. For example, PE-X1 and PP-2 may be applied when proper measures to limit the maximum temperature rise under stagnation are taken (e.g., overheating protection by thermotropic layers). PC was found to be susceptible to hot water, thus constraining its application to air collectors and to components not directly exposed to hot water (e.g., collector glazings). For the investigated PPE+PS, significant chemical aging occurred already during film extrusion step, so that an unambiguous interpretation of the true aging behavior of this material under service near conditions is not possible.

In any case, as this dissertation is the first polymer science based study of the aging behavior of potential material candidates for solar thermal absorbers, further investigations are necessary to substantiate all of the results obtained prior to applying these materials to commercial products. Moreover, future investigations should also broaden the spectrum of material candidates by either proper modification of the polymer material classes included in this dissertation (e.g., stabilization towards the application specific conditions) or by selecting further and new potential polymer types.

KURZFASSUNG

Kunststoffe bieten ein hohes Potential für solar-thermische Absorber, im speziellen auch für Flachkollektoren. Bei derartigen Anwendungen stellen die hohen Temperaturen in Luft und Wasser die gravierendsten Servicebedingungen dar. Daher ist die Untersuchung von Alterungsphänomenen bei erhöhten Temperaturen unter diesen Bedingungen von enormer Wichtigkeit um das jeweilige Verhalten potentieller Polymermaterialien zu charakterisieren und um mögliche Einschränkungen der gewählten Materialien für diese Anwendungen zu identifizieren. Da bisher noch keine systematische Studie zu dieser Thematik durchgeführt wurde, war das Hauptziel dieser Dissertation, das Alterungsverhalten von ausgewählten, potentiellen Kunststoffe für solar-thermische Absorberanwendungen mit polymerwissenschaftlichen Methoden zu untersuchen. Ein spezieller Fokus lag dabei auf der Charakterisierung von physikalischen und chemischen Alterungsprozessen und der Ableitung von Struktur/Eigenschafts-Beziehungen, sowie der Entwicklung von Korrelationen zwischen den Resultaten auf der Laborprüfkörper-Ebene und den Ergebnissen der Sub-Komponenten- und Komponenten-Ebene.

Für diese Arbeit wurden insgesamt acht verschiedene potentielle Polymere für solar-thermische Absorber ausgewählt. Dazu gehörten vier sogenannte technische Kunststoffe (ein Blend aus Polyphenylen Ether und Polystyrol (PPE+PS), Polykarbonat (PC), ein schlagzähmodifiziertes Polyamid 12 (PA12-HI) und ein hochtemperaturmodifiziertes PA12 (PA12-HT)) und vier Standard-Kunststoffe (zwei unterschiedlich vernetzte Polyethylentypen (PE-X1, PE-X2), zwei Polypropylentypen (PP-1, PP-2)). Abgeleitet von nördlichen Klimaverhältnissen und einer Kollektoreinsatzdauer von 20 Jahren wurden für den Stagnationsfall 140 °C in Luft mit einer kumulierten Beanspruchungszeit bis zu 500 h und für den operativen Betrieb 80 °C in Wasser mit einer kumulierten Beanspruchungszeit bis zu 16000 h als Auslagerungsbedingungen für die Alterungsuntersuchungen festgelegt. Auf Laborprüfkörper-Ebene waren zwei analytische Meßmethoden (Differential Thermoanalyse (DSC) und Größenausschlußchromatographie (SEC)) und eine mechanische Methode

(monotoner Zugversuch) Teil des experimentellen Untersuchungsprogramms zur Charakterisierung des Alterungsverhaltens. Auf Sub-Komponenten- und Komponenten-Ebene wurden DSC-Untersuchungen und ein mechanischer Eindruckversuch durchgeführt. Zur Modellierung und Vorhersage der Lebensdauer unter verschiedenen Einsatzbedingungen, wurden für drei ausgewählte Kunststoffe (PPE+PS, PC, PP-2) jeweils drei verschiedene Modelle basierend auf der Arrhenius-Beziehung und Ergebnissen der Laborprüfkörper-Ebene herangezogen.

Basierend auf den experimentellen Ergebnissen und der Datenanalyse bzw. den Modellvorhersagen (einfache Datenreduktion und/oder Arrhenius basierende Lebensdauerabschätzung) hat sich nur ein Material, PA12-HI, als möglicher Kandidat für den vollen Einsatzbereich eines solar-thermischen Absorbers inklusive Stagnation herausgestellt. Weitere Materialien eignen sich möglicherweise für Absorberanwendungen unter speziellen Bedingungen. So kommen PE-X1 und PP-2 für den Absorbereinsatz in Frage, wenn entsprechende Vorkehrungen zur Limitierung der Maximaltemperatur im Stagnationsfall getroffen werden (z.B. Überhitzungsschutz durch thermotrope Schichten). Aufgrund seiner hohen Empfindlichkeit gegenüber heißem Wasser ist PC als Absorbermaterial nur für Luftkollektoren bzw. für sonstige Komponenten die nicht direkt heißem Wasser ausgesetzt sind geeignet (z.B. Kollektorabdeckungen). Das Polymerblend PPE+PS wurde bereits im Verarbeitungsschritt bei der Filmextrusion deutlich chemisch abgebaut, so dass eine eindeutige Interpretation der Ergebnisse bezüglich des tatsächlichen Alterungsverhaltens dieses Materials unter anwendungsnahen Bedingungen nicht möglich ist.

Da diese Dissertation die erste polymerphysikalische Untersuchung in Hinblick auf das Alterungsverhalten potentieller Materialkandidaten für solar-thermische Absorber darstellt, sind sicherlich noch weitere Untersuchungen notwendig um die erzielten Ergebnisse zu bestätigen, bevor die entsprechenden Werkstoffe für kommerzielle Produkte eingesetzt werden. Darüber hinaus sollte in künftigen Untersuchungen das Spektrum der Materialkandidaten durch Miteinbeziehung weiterer Modifizierungen der hier untersuchten Polymerklassen durch spezifische Stabilisierung auf die vorherrschenden Alterungsbedingungen bzw. auch neuer Polymertypen erweitert werden.

TABLE OF CONTENT

PART I:

OUTLINE AND SUMMARY

1 INTRODUCTION AND SCOPE

1.1 Background and Overall Objectives

The importance of energy to human society has changed dramatically over the past decades. While in the early stages wood was used as primary energy source, followed by fossil fuels (first coal, then oil and now increasingly natural gas), more recently numerous limits to the fossil fuel based energy system become increasingly apparent. One aspect related to energy resources is a projected increase in world energy consumption up to 50 % from 2005 to 2030 according to the US Energy Information Administration (EIA). While OECD countries are expected to raise their demand by 0.7 % per year, energy consumption in non-OECD countries is estimated to expand by 2.5 % per year (EIA, 2008). These prospects of energy consumption are of common interest for various reasons (IPCC, 2007). Most importantly it has to be considered that conventional energy resources not only cause air pollution but also exhibit a potential threat of global climate change accompanied by the influence on the terrain of many countries. Therefore, the importance of renewable energy has to be addressed much more seriously in the future.

In 2006, 18 % of the world wide primary energy was covered by renewables (IPCC, 2007). Within renewable energy technologies, the photovoltaic sector has had a tremendous upward trend in technology during the last decades leading to a worldwide installed capacity of 7.8 GW in 2007 (IEA, 2007). But also solar thermal applications in the low temperature range exhibit a promising alternative to conventional energy resources (Sayigh, 1999). For example, in the EU the energy demand in buildings for heating and cooling is 49 %, mainly at medium and low temperatures (up to 250 °C) (ESTTP, 2009). Within the EU, a remarkable growth of about 20 % was achieved in Austria over the last 10 years (ESTEC, 2009). Future scenarios are also very ambitious for Europe. Accordingly, in 2030 50 % of the low temperature heating and cooling demand should be covered by renewable energies (ESTTP, 2009).

To achieve these ambitious goals, further cost reductions are needed (Koehl, 2005). Thus, to reduce expenses in purchase and installation, light-weight plastics exhibit a potential alternative for conventional solar thermal collectors (Raman et al., 2000; Davidson et al., 2003; Wallner and Lang, 2006; Meir, 2008). According to a recent study, the use of plastics in solar thermal collectors, specifically as absorbers, also offers ecological advantages (Kicker, 2009). Moreover, the high flexibility and the related benefits of polymers for the use in solar thermal systems were also already pointed out in several publications (Lang, 1995; Lang, 1999, Wallner and Lang, 2005; Wallner and Lang, 2006).

Currently different types of solar thermal collector types are on the market. These include swimming pool absorbers (without glazing), storage collectors, flat plate collectors, vacuum-tube collectors and concentrating collectors. As heat carrier usually water or a water/glycol mixture are used in pressurized or pressureless (drain-back) systems. Flat plate collectors are furthermore classified into selective and non-selective collectors. The selective coating is applied on the absorber (Streicher, 2005). As the collector systems have different requirements according to their applications, different operating and stagnation temperatures are obtained. Except for unglazed swimming pool absorbers and storage collectors, operating temperatures ranging from 80 °C to 130 °C and stagnation temperatures ranging from 150 to 250 °C are achieved (Hausner, 2009). In a solar thermal collector system the main functional component is the absorber. Currently, mainly aluminum and copper are used. With a replacement by plastics the above-mentioned goal of cost reduction may be achieved.

For the application of polymers in solar thermal absorbers, the selection of a potential polymeric material plays a major role, and suitable test methods have to be established to evaluate the respective polymers as to their aging behavior. Freeman et al. (2005) and Wu et al. (2004) performed aging tests on the laboratory specimen level to evaluate the aging behavior of different polymers for the application as solar thermal absorber. A main focus was put on the mechanical properties of different engineering polymers including polysulfone, polybutylene and polyamide 6, 6. Therefore the long-term creep behavior examining the creep deformation and tensile tests to determine the tensile strength were evaluated.

Furthermore the change in molecular mass after aging was analyzed. Raman et al. (2000) compared the high temperature performance of different polymers based on technical data sheets available from the respective raw material supplier considering the thermal index, the heat deflection temperature and the glass transition temperatures as criteria for the application as solar thermal absorber. In contrast, Olivares et al. (2008) developed a test procedure to examine the aging behavior of relevant polymeric materials on the component level. Indentation tests were performed on solar thermal absorber sheets provided by Solarnor® and the load at indentation at break was defined as criterion to indicate aging. And yet, so far no sound characterization of the aging behavior of polymeric materials for the application as solar thermal absorber material has been reported. Furthermore, in the investigations performed so far aspects of polymer science in particular with regard to specific mechanisms of aging were hardly accounted for. Hence, the overall objectives of this dissertation are:

- to evaluate the potential of plastics for solar thermal absorbers,
- to characterize the aging behavior of a selected group of potential material candidates for plastics absorber and to clarify the physical and chemical aging mechanisms for service relevant conditions,
- to deduce potential limitations for various plastics for such applications,
- to assess the lifetime of various plastics for solar thermal absorbers under service-near conditions based on polymer-physics models, and
- to compare the aging behavior of potential plastics at different levels of material states to establish property-performance relationships.

1.2 Structure of the Thesis

This dissertation consists of 2 major parts. Part I provides an overview of the thesis outlining the introduction and scope along with the background and overall objectives in Chapter 1. Chapter 2 describes the methodology and work program. Major results are summarized and discussed in Chapter 3. Chapter 4 focuses on conclusions and provides an outlook to further work. Part II consists of a collection of 5 papers and represents the scientific essence of this dissertation. The 5 papers

cover various aspects of the overall goals defined above and are entitled as follows:

Paper 1: Characterization of Physical and Chemical Aging of Polymeric Solar Materials by Mechanical Testing

Paper 2: Aging behavior of Polymeric Solar Absorber Materials – Part 1: Engineering Plastics

Paper 3: Aging Behavior of Polymeric Solar Absorber Materials – Part 2: Commodity Plastics

Paper 4: Aging Behavior and Lifetime Modeling for Polymeric Solar Absorber Materials

Paper 5: Aging Behavior of Polymeric Solar Absorber Materials: Aging on the Component Level

All papers are currently being submitted to scientific journals as is indicated in the footnote of each paper.

2 METHODOLOGY AND WORK PROGRAM

The methodology and the major elements of the work program of the dissertation are shown in Fig. 1 (structure-property-performance pyramid). The figure illustrates the various levels of material states from the constituent level via the specimen level to the sub-component level and to the component level and the system level. The 3 levels of characterization and testing also carried in this dissertation are indicated along with information on details of the characterization and test program. To obtain a comprehensive understanding of the aging behavior of polymers for solar thermal absorber applications, various characterization and test methods at the different levels of the material state are necessary. This includes analytical methods such as differential scanning calorimetry (DSC) to obtain information on the thermal properties and the morphology of the material, size exclusion chromatography (SEC) to characterize the molecular mass distribution and the associated mean values, and mechanical tests to determine performance parameters. As to aging, laboratory and outdoor aging have to be applied preferably at maximum operation and/or stagnation conditions.

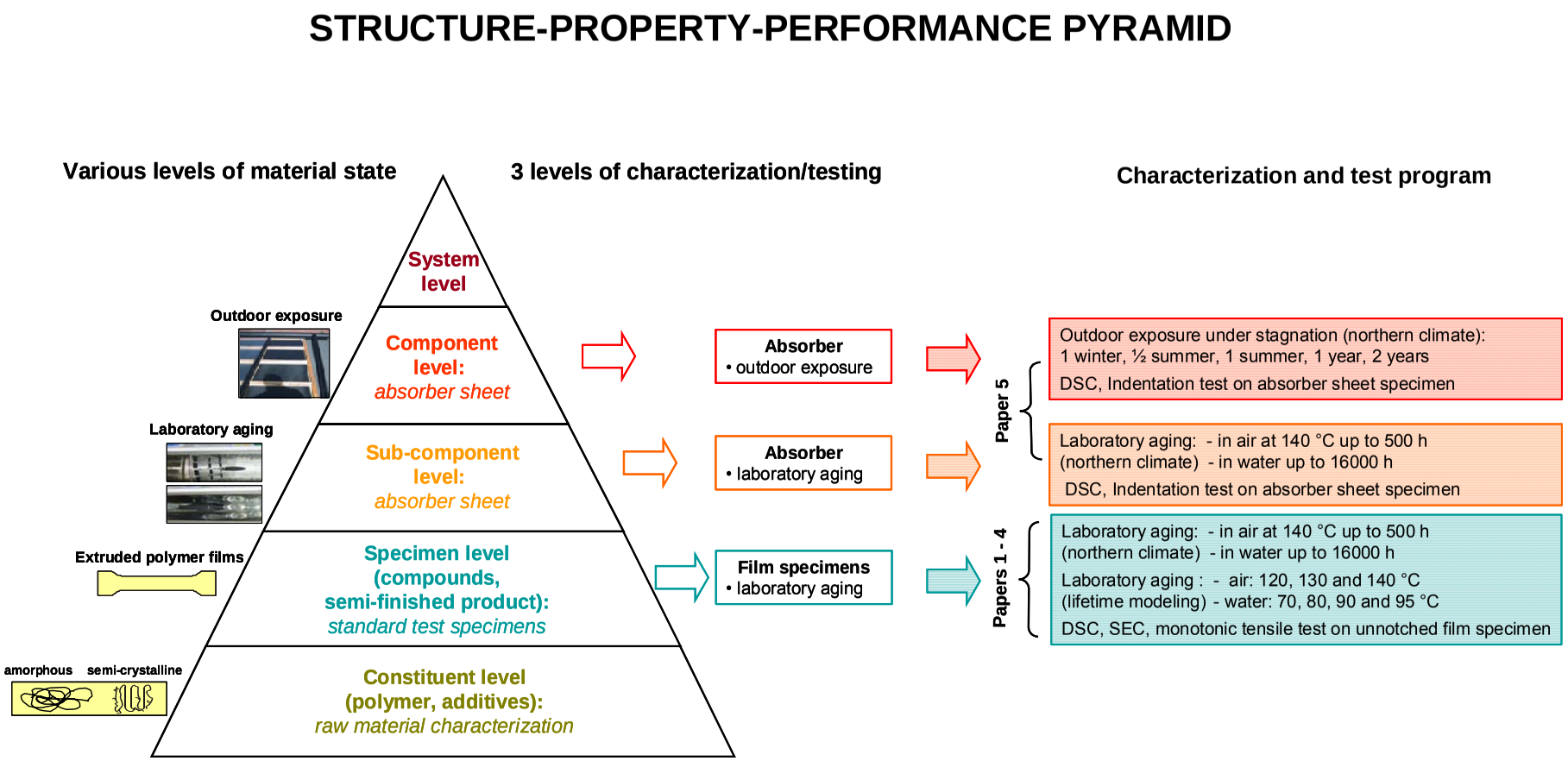

Fig. 1: Structure-property-performance pyramid and various levels of material states and of characterization and testing.

2.1 Material Selection and Definition of Specimen Configuration

Potential engineering and commodity-type plastics were selected, and according to recommendations provided by the respective supplier the most promising candidates were chosen. While some polymers were directly supplied by the company as 500 μm films, the majority of the polymers investigated was supplied as granules and extruded to 500 μm films on a single screw extruder followed by a chill roll unit. On the specimen level, thin films were preferred to accelerate aging related to the volume. The film thickness was then chosen according to the minimum wall thickness of the investigated absorber sheet in terms of practical aspects. For material characterization on the sub-component and component level, extruded absorber sheets with a thickness of approximately 10 mm were directly provided by Solarnor®.

2.2 Aging Conditions

Film specimens were tested in the unaged state and in various states of laboratory aging. Reflecting northern climate conditions, specimens were either heat aged in air at 140 °C representing stagnation conditions (“dry load”) or exposed to water at 80 °C representing operating conditions (“wet load”). Accumulated for a lifetime of 20 years, the “wet load” occurs for up to 16000 h. When in stagnation, the water is drained back into the storage tank, and an accumulated “dry load” of up to 500 h in air is deduced for the collector lifetime (Kahlen et al., 2009a). For lifetime modeling, further aging experiments in air at 120 °C up to 4500 h and at 130 °C up to 1500 h and in water at 70 °C up to 4000 h, at 90 °C up to 2000 h and at 95 °C up to 4000 h were carried out with film specimens.

On the sub-component and component level, absorber sheet specimens were either aged under laboratory aging conditions according to northern climate as described above or exposed on the roof of the laboratory site (Sollab) at the University of Oslo in Norway under service stagnation conditions to simulate real outdoor applications (latitude 59.98 °, azimuth 17 °, tilt angle 32 °; no water running through the absorber). The absorber sheets were placed on the roof at the Sollab according to the Solarnor® installation standards and were exposed to

solar irradiation for different time intervals, i.e. ½ winter, ½ summer, 1 winter, 1 summer, 1 year and 2 years.

Both laboratory aging conditions (air and water) were carried out using an air-circulating oven (type Kendro 6000; Kendro Laboratory Products GmbH; Langenselbold; D). The specimens exposed to hot air were placed on a metal grid, the specimens exposed to hot water were placed in a water filled glass jar covered by a screw top (film specimens) or a clip-on top (absorber sheet specimens). The distilled water was changed in intervals of 2000 h to reduce and avoid saturation effects in the water by leaching out additives. Following the aging exposure and prior to testing, the samples were stored in a climatized room (23 °C, 50 % r.h.). No re-drying was carried out for the samples exposed to hot water. After outdoor exposure, the absorber sheets were removed from the experimental site and cut into respective segments prior to testing.

2.3 Characterization Methods

The different amorphous and semi-crystalline laboratory aged and unaged film specimens were investigated on the constituent level by material characterization using differential scanning calorimetry (DSC) and size exclusion chromatography (SEC). With DSC, physical and chemical aging phenomena were detected. SEC was applied to determine any molecular mass changes by degradation or crosslinking (chemical aging). Mechanical characterization was used to provide information on any effects of aging on performance properties. Tensile tests were performed with film specimens covering the small and large strain regime (pre-yield, yield and post-yield), to draw any conclusions with regard to physical and chemical aging phenomena in combination with the analytical results.

Finally, laboratory aged, outdoor exposure aged and unaged absorber sheet specimens were characterized by DSC to study the material and aging state (physical and chemical aging). In addition, mechanical tests in terms of an indentation test were performed to evaluate performance properties and to correlate the mechanical results with the analytical results.

3 MAJOR RESULTS AND DISCUSSION

In this chapter the major results of this dissertation in terms of the 5 individual papers of Part II are briefly discussed. The results are further described in detail in the papers collected in Part II of the dissertation.

3.1 Characterization of Physical and Chemical Aging of Polymeric Solar Materials by Mechanical Testing (Paper 1)

Based on contactless optical strain measurement, effects of physical and chemical aging on the mechanical properties of polymeric films for solar absorber applications were characterized. For this purpose an amorphous and a semi-crystalline polymer (a polyphenylene ether polystyrene blend (PPE+PS) and a crosslinked polyethylene (PE-X1), respectively) were exposed to hot water at 80 °C and tested at room temperature under monotonic tensile test conditions. As to physical aging, modulus in the pre-yield regime and as to chemical aging, strain-to-break values in the post-yield regime were determined. In the small strain regime up to 3 % and over the entire deformation regime, a digital image correlation system (DIC) and a video extensometer, respectively were applied to record strains optically.

While excellent reproducibility of the DIC results were found for PPE+PS, PE-X1 indicated more significant scatter in the measurements probably due to local crosslinking density differences. In comparison with the crosshead displacement measurement, the DIC system delivered lower overall strain values for both polymer films due to partial specimen slippage. In the large strain regime, significant higher strain values were obtained optically compared to the crosshead displacement because of specimen slippage and the choice of the initial nominal gage length of the dumb-bell test specimens.

For PPE+PS no significant influence of immersion to hot water on the modulus was obtained. However, the DIC system indicated some increase within the first 2000 h of aging compared to the nominal crosshead measurement. Hence, for precise measurements optical measurement techniques are to be preferred.

Strain-to-break values of PPE+PS vs. aging time exhibited the same trend with the optical and the crosshead measurements, indicating massive chemical degradation already after 200 h of aging.

PE-X1 also showed similar dependencies in the small- and large-strain regime, when using the DIC system and the video extensometer, respectively. High strain variations were observed in the unaged and aged material (compare Fig. 2), not allowing for any precise determination of physical and chemical aging mechanisms. Thus, further analytical methods are needed to elucidate the precise mechanisms of physical and chemical aging. However, optical strain measurements (DIC system in the pre-yield and video extensometer in the post-yield regime) allow for a more precise strain determination than nominal crosshead measurements.

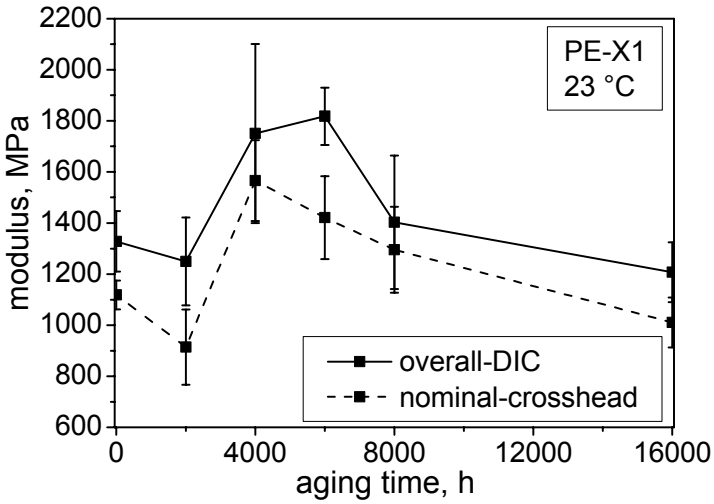

Fig. 2: Effect of aging time (water exposure at 80 °C) on modulus of PE-X1 at room temperature; comparison of modulus data based on strain measurements with the DIC system and the crosshead displacement method.

3.2 Aging Behavior of Polymeric Solar Absorber Materials – Part 1: Engineering Plastics (Paper 2)

The degradation behavior of 4 commercially available engineering plastics including 2 amorphous (polyphenylene ether polystyrene blend (PPE+PS) and polycarbonate (PC)) and 2 semi-crystalline (polyamide 12 (PA12-1 and PA12-2))

plastic grades for solar thermal applications was investigated. According to northern climate conditions and based on the experiences with the Solarnor® collector (Meir and Rekstad, 2003), maximum stagnation temperatures in air at 140 °C up to 500 h and maximum operation temperatures in water at 80 °C up to 16000 h were considered as aging conditions. To characterize the aging behavior, analytical tests including differential scanning calorimetry (DSC) and size exclusion chromatography (SEC) were performed and a tensile test was carried out. For the interpretation of physical aging effects, DSC measurements and modulus and yield stress values delivered the most sensitive parameters. While for the amorphous plastics physical aging was characterized as enthalpy relaxation around the glass transition, for the semi-crystalline plastics mainly changes in crystallinity were obtained. To interpret chemical degradation, changes in weight average molecular mass and in strain-to-break values turned out to be most appropriate.

Among the investigated materials, most significant degradation was obtained for PPE+PS after exposure to hot air already within the first 125 h in hot air and after 2000 h in hot water (see Fig. 3). While hot water aging led to physical and chemical aging for PC determined with mechanical properties, DSC and particularly M_w measurements did not show any indication for chemical aging after hot air exposure. Due to embrittlement and the strong scatter found with strain-to-break after aging in hot air, further investigations need to be carried out. In contrast to the results for PPE+PS and PC, hot water treatment was more severe to PA12 than hot air. Interestingly, significant degradation was obtained only for PA12-HT after hot water exposure. However, the significant drop in the oxidation temperature (T_{ox}) and physically detected aging by means of DSC of PA12-HI after hot water aging was presumably outbalanced by the various physical (post- and re-crystallization) and chemical aging effects (crosslinking, molecular degradation). Hence, the required performance as a black absorber material for northern climates seems to be met.

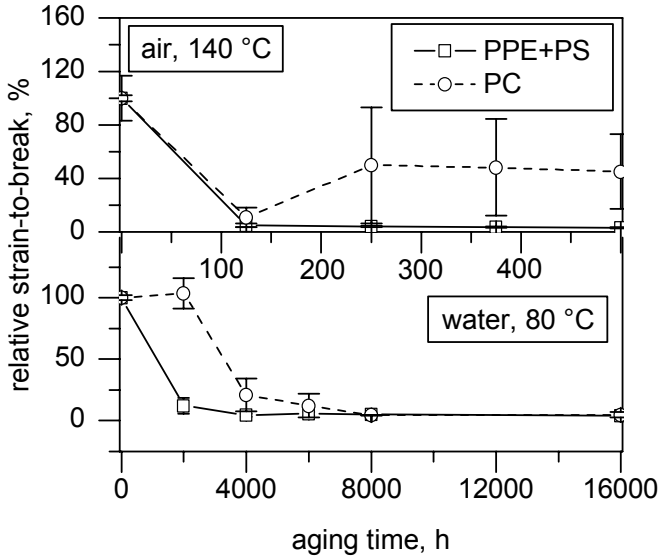

Fig. 3: Relative strain-to-break versus aging time in air at 140 °C and in water at 80 °C, respectively, for PPE+PS and PC.

3.3 Aging Behavior of Polymeric Solar Absorber Materials – Part 2: Commodity Plastics (Paper 3)

For this paper, 4 different commercially available so-called “commodity" polymers including 2 random copolymer polypropylenes (PP-1 and PP-2) and 2 silane crosslinked polyethylenes (PE-X1 and PE-X2) were investigated as to their aging behavior for the application as solar thermal absorber materials. Based on the experiences with northern climates, stagnation at 140 °C in air up to 500 h and operation at 80 °C in water up to 16000 h were considered as aging conditions. To study the aging behavior, differential scanning calorimetry (DSC), size exclusion chromatography (SEC) and tensile tests in the small and large strain regime were part of the experimental program.

The most significant degradation was obtained for PE-X1, indicated by a substantial decrease in strain-to-break within the first measurement interval in hot air and after 6000 h in hot water (see Fig. 4). While both PE-X types exhibited a decrease in crystallinity after exposure to air at 140 °C, probably caused by crosslinking, only PE-X2 revealed a decrease in crystallinity together with a strong decrease in the oxidation temperature (T_{ox}) (probably due to leaching of stabilizers) during hot water immersion also indicating crosslinking. The phenomena observed with DSC due to changes in the morphology and the

network were not reflected by mechanical properties such as modulus and yield stress, presumably due to competing effects of crosslinking and reduction in crystallinity. The two PP types, on the other hand both exhibited an increase in crystallinity after aging in hot air and hot water. For PP-1 also a decrease in M_w was found, enhancing the tendency for post- and re-crystallization. Moreover, for both PP types an increase in melting temperature due to re-crystallization was determined after hot air exposure. On the other hand, the broadening of the melting peak range after hot water exposure was related to post-crystallization. Nevertheless, mechanical properties in the small-strain and large-strain regime turned out to be nearly independent of the aging conditions, which implies that the aging mechanisms found by analytical methods may perhaps cancel each other out in terms of their effect on the mechanical performance parameters.

From the commodity type plastics, PE-X2 and PP-2 are the most promising candidates for solar black absorber materials. Due to the high stagnation temperatures for northern climates being in the range of the melting temperature for these plastics, suitable overheating protection devices are needed, however, to avoid dimensional instability.

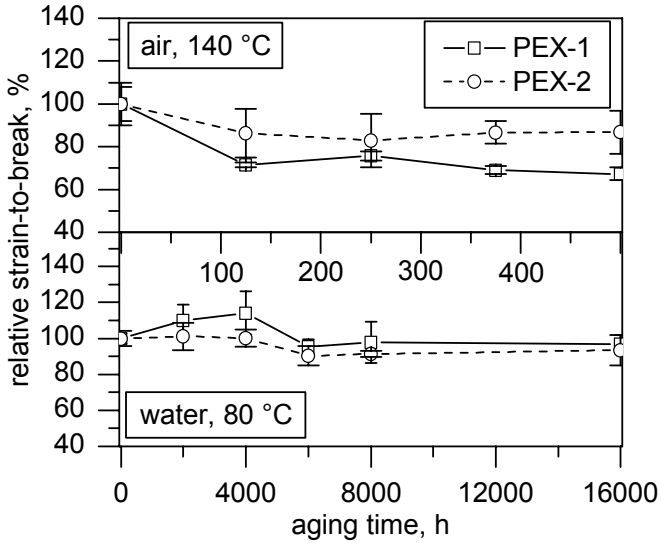

Fig. 4: Relative strain-to-break versus aging time in air at 140 °C and in water at 80 °C for PE-X1 and PE-X2.

3.4 Aging Behavior and Lifetime Modeling for Polymeric Solar Absorber Materials (Paper 4)

Different lifetime models for aging at different environmental conditions in air and water were evaluated for three different polymeric materials (PPE+PS, PC and PP-2). As to the temperatures, 120 to 140 °C in air and 70 to 90 °C in water were selected. As characteristic parameter for aging, strain-to-break values were determined on unnotched aged and unaged dumb-bell film specimens in monotonic tensile tests at ambient conditions. On the one hand, PPE+PS exhibited a significant drop in strain-to-break after a very short aging times and PP did not reveal any changes in strain-to-break after aging. On the other, for PC the effect of aging was found to strongly depend on the aging conditions. However, as pointed out in Section 3.2 (Paper 2), PC was not found to be a suitable candidate for solar absorber applications due to its limited performance in hot water. Nevertheless, three different lifetime models (according to ISO 2578, Gillen et al., 1997 and Hoang and Lowe, 2008) based on the Arrhenius equation were applied in order to illustrate the procedure of a reaction rate theory based lifetime prediction and the influence of the specific model chosen. For the determination of activation energies and endurance limits, two strain-to-break criteria were investigated, one being a decrease to 50 % and the other to 80 % of the unaged strain-to-break. For lifetime prediction, experimental data were fitted with a least square linear fit in air ranging from 90 to 110 °C and in water from 40 to 60 °C. Activation energies in water from 229 to 272 kJ/mol and in air from 65 to 118 kJ/mol were obtained, the latter being lower due to the susceptibility of PC against hot water exposure. While the activation energies did not exhibit high scatter, the endurance limits varied to a strong extent (for 90 °C in air from 17 to 204 h and for 40 °C in water from 5 to 58 years; compare Fig. 5) depending on the model chosen, presumably also due to the strong scatter in the strain-to-break values. These results raise the question as to the accuracy of the lifetime models applied and demand further investigations to define suitable lifetime models to predict reliable endurance limits.

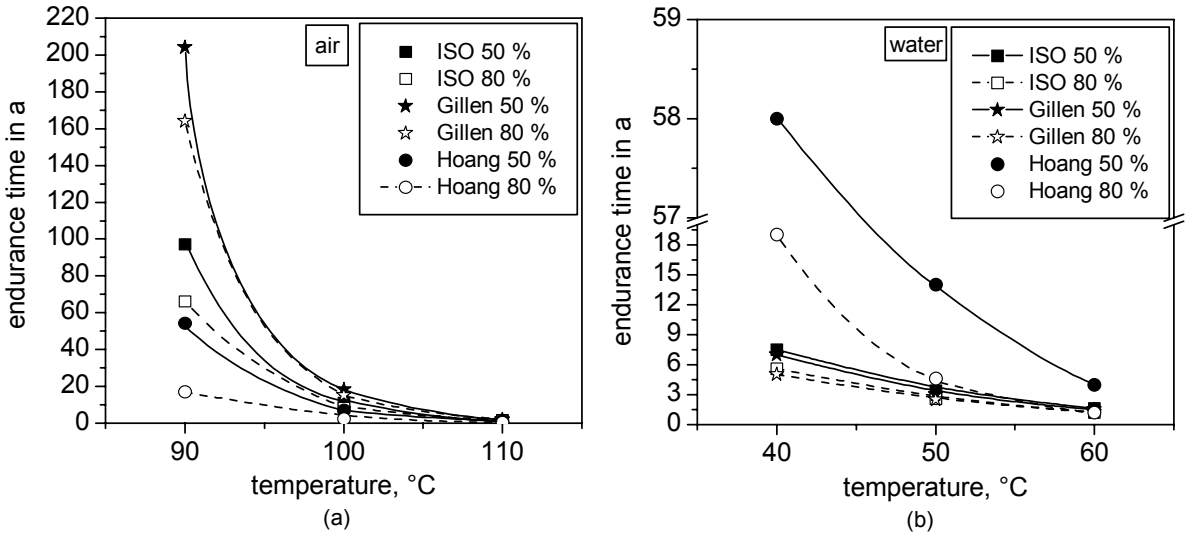

Fig. 5: Predicted lifetimes (endurance limits) for PC exposed to temperatures ranging (a) from 90 to 110 °C in air and (b) from 40 to 60 °C in water according to various models and assumptions (residual strain-to-break after aging).

3.5 Aging Behavior of Polymeric Solar Absorber Materials: Aging on Component Level (Paper 5)

The aging behavior of PPE+PS absorber sheets exposed to different aging conditions was investigated. As to laboratory aging, absorber sheets were exposed to 140 °C in air up to 500 h and in water at 80 °C up to 16000 h. Outdoor aging experiments were performed under service stagnation conditions at a test facility in Oslo (N). For the interpretation of the effects of aging on the mechanical performance of the absorber sheet, an indentation test developed by Olivares et al. (2008) was applied to determine the aging relevant parameters load of first transition (F_T) and ultimate indentation at break (I_B). Furthermore, analytical tests (differential scanning calorimetry (DSC) were performed to interpret the observed effects with the indentation test. While laboratory aging in hot air led to significant changes in F_T and I_B values, no influence of hot water exposure was obtained (see Fig. 6). By comparison, results on PPE+PS film specimens also indicated a dramatic decrease in ultimate elongation values after laboratory aging at the same temperatures in hot air and were interpreted as chemical aging (see Section 3.2,

Paper 2). Hence, the reduction in I_B and F_T values during laboratory aging in air on the component level mentioned above may also reflect chemical aging.

For the discussion of these results, the significant difference in deterioration during the extrusion process for the two different material states (5 % vs. 20 % for the sheets and the films, respectively) should be taken into account. Therefore, mechanical parameters of the PPE+PS sheets were probably only slightly affected by hot water exposure compared to the strong decrease observed for PPE+PS films. Outdoor experiments revealed the same behavior as laboratory aging experiments at 140 °C in air. Hence, indentation at break values were fitted with an exponential decay function for both aging conditions and a correlation between accumulated irradiation energy (E_{cum}) and laboratory aging time (t_L) was established being $E_{cum} \cong 0.229 * t_L$, when applying a strain-to-break criterion as proposed in Section 3.4 (Paper 4), 51 h and 159 h were obtained for a decrease to 80 % and 50 % indentation at break. Since a lifetime of 500 h (accumulated in 20 years of service) is aimed at for such a solar thermal collector, PPE+PS may not be the proper choice for this application.

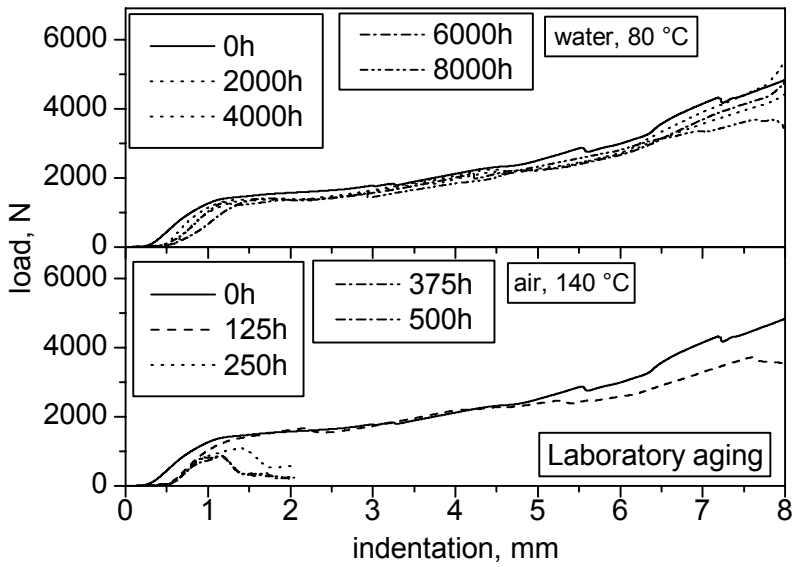

Fig. 6: Load-indentation curves for PPE+PS absorber segments after aging in air at 140 °C and in water at 80 °C.

4 SUMMARY AND CONCLUSIONS

In this dissertation a comprehensive characterization of commercially available polymers for their application as solar thermal absorber materials in terms of their aging behavior is described. Furthermore, aging studies on the component level were investigated to compare these results with the laboratory specimen level and to establish possible correlations between the different testing levels.

In Paper 1 the potential of mechanical properties to characterize physical and chemical aging of polymeric films for solar thermal absorber applications is described. Therefore film specimens of PPE+PS and PE-X1 were aged in water at 80 °C up to 16000 h and tested under monotonic tensile testing conditions at ambient temperature. With a digital image correlation (DIC) system and a video extensometer the modulus and strain-to-break values were determined and discussed as to the physical and chemical aging, respectively, and correlated with results obtained by crosshead measurements. At least for PPE+PS, a different trend in modulus values was obtained with the DIC system compared to the crosshead displacement, revealing the importance of an accurate measurement system to detect reliable mechanical properties. Specimen slippage in the small and a combined effect of specimen slippage and the choice of the initial gage length in the large strain region basically influence the different course in mechanical properties measured optically and with the crosshead. Future investigations are necessary and should focus on a single camera system to record both, the small and large strain regime with a sufficient high accuracy.

In the next two papers (Paper 2 and Paper 3) physical and chemical aging mechanisms of 8 plastics, 4 engineering (PPE+PS, PC and two types of PA12) and 4 commodity (two PP grades and two PE-X materials) plastics are investigated. Based on experiences with northern climate conditions, aging studies in air up to 500 h at 140 °C and in water up to 16000 h at 80 °C were performed. For the description of the aging behavior, different analytical methods including a differential scanning calorimetry (DSC) and a size exclusion chromatography (SEC) and a tensile test to determine the mechanical behavior optically as

described in Paper 1 in the small and large strain regime were investigated. Due to the changes found with analytical methods and by tensile testing, chemical aging was attributed to occur mainly in PPE+PS after hot air and hot water exposure at least partly caused by the deterioration of the PPE+PS raw material during the film extrusion process. While no clear trend was found for PC after hot air and hot water aging by mechanical and analytical measurements, in accordance with the behavior for PPE+PS, hot air exposure revealed to be more harmful. In contrast to the heat stabilized PA12-HT, the impact modified PA12-HI type turned out to be quite stable exhibiting mainly physical aging under the investigated environmental conditions. For both PE-X types, physical aging phenomena observed with DSC were not reflected by mechanical properties in the small strain regime. Moreover, T_{ox} values for PE-X2 decreased during hot water immersion, indicating enhanced stabilizer leaching in the less crystalline PE-X type. Also for PP-1 and PP-2 a discrepancy in the interpretation of the aging mechanisms was obtained in terms of competing effects of the results obtained with analytical and mechanical methods. Among the investigated materials, PA12-HI adequately modified and, PE-X2 and PP-2, with a proper stabilization and sufficient overheating protection to avoid dimensional instability are potential black absorber materials. Nevertheless and most importantly, a proper film extrusion process of PPE+PS has to be guaranteed to unambiguously characterize the aging behavior. Moreover, further investigations are needed to clearly classify the occurring aging mechanisms of the different plastics exhibiting inconsistencies in the above mentioned results.

In Paper 4 three selected polymer film specimens (PPE+PS, PC and PP-2) were further investigated as to their aging behavior under different temperatures in air (120 to 140 °C) and in water (70 to 90 °C). As characteristic property for aging, strain-to-break values of the aged film specimens tested at ambient conditions under monotonic tensile tests were selected. Moreover, with three different lifetime approaches based on the Arrhenius equation, endurance limits were determined. For lifetime modeling, only PC was further evaluated due to its continuous decrease after aging (however with a strong scatter in experimental data). Activation energies exhibited a rather strong scatter after hot air exposure, and endurance limits were very different depending on the model chosen. However,

these variations are probably also due to the strong scatter in strain-to-break data obtained for PC and emphasize the necessity of further aging tests at different temperatures in air and water but also raise the usefulness of such models for reliable lifetime predictions.

Absorber sheet specimens were exposed to laboratory and outdoor aging conditions and characterized mechanically and analytically (via DSC) as to their aging behavior in Paper 5. Laboratory aging was performed in air at 140 °C and in water at 80 °C and outdoor aging in northern climate under stagnation were carried out. As expected, a similar trend in mechanical properties by an indentation test was found for laboratory aged absorber sheet specimens in hot air and sheets exposed outdoors. However, while physical aging phenomena were confirmed with DSC, no clear evidence for chemical aging could be deduced. By applying an ultimate indentation criterion (based on a decrease in indentation at break to 80 % and 50 %, respectively), a service lifetime estimation was investigated. 51 h and 159 h were predicted for the 80 % and 50 % criterion, respectively, indicating that the absorber sheet would fail within the expected 500 h (accumulated over the 20 years lifetime). Hence, PPE+PS may not be suitable for black absorber applications for northern climates. However, further analytical tests are necessary to unambiguously define the aging phenomena of PPE+PS absorber sheet specimens. At the same time, future work should focus on the investigation of some of the other promising polymeric material candidates investigated in Paper 2 and 3 in terms of sub-component and component tests (e.g., PA12-HI, PE-X2, PP-2), and further potential material candidates should also be looked for.

REFERENCES

Davidson, J.H., Mantell, S.C., Jorgensen, G.J., 2003. Status of the Development of Polymeric Solar Water Heating Systems. Adv. in Sol. Energy 15, 149-186.

EIA, 2008. International Energy Outlook 2008. Chapter 1 – World Energy Demand and Economic Outlook, download from the website of the Energy Information Administration (EIA) http://www.eia.doe.gov.

Freeman, A., Mantell, S.C., Davidson, J.H., 2005. Mechanical performance of polysulfone, polybutylene, and polyamide 6/6 in hot chlorinated water. Sol. Energy 79, 624-637.

Gillen, K.T., Celina, M., Clough, R.L., Wise, J., 1997. Extrapolation of accelerated aging data – Arrhenius or Erroneous? Trends Polym. Sci. 5 (8), 250-257.

Hausner, R., 2009. Private communications. April, 2009.

Hoang, E.M., Lowe, D., 2008. Lifetime prediction of a blue PE100 water pipe. Polym. Degrad. Stab. 93, 1496-1503.

IEA, 2007. Trends in Photovoltaic Applications. Survey report of selected IEA countries between 1992 and 2006, download from www.iea-pvps.org.

IPCC, 2007. Climate Change Foruth Assessment Report – Mitigation, Chapter 4: Energy Supply, download from the website of the Intergovernmental Panel on Climate Change (IPCC) http://www.ipcc.ch.

ISO 2578, 1993 E. Plastics – Determination of time-temperature limits after prolonged exposure to heat.

Kahlen, S., Wallner, G.M., Lang, R.W., 2009a. Aging behavior of polymeric solar absorber materials. – part 1: engineering plastics. To be submitted in Sol. Energy.

Kahlen, S., Wallner, G.M., Lang, R.W., 2009b. Aging Behavior and Lifetime Modeling for Polymeric Solar Absorber Materials. To be submitted in Sol. Energy.

Kicker, H., 2009. Comparative life cycle assessment of solar thermal collectors. Bachelor Thesis. April, 2009. Institute of Materials Science and Testing of Plastics. University of Leoben, Austria.

Koehl, M., 2005. Concept paper for a Task fo the Solar Heating and Cooling Programme of the International Energy Agency ‘Polymeric Solar Materials’.

Lang, R.W., 1995. Einsatzmöglichkeiten von Kunststoffen bei der thermischen Energieversorgung von Niedrigenergie-Solarhäusern. Das Bauzentrum 9, 25-33.

Lang, R.W., 1999. Fortschritt durch Polymerwerkstoffe. Chemie Oktober 1999, 15.

Meir, M.G., Rekstad, J., 2003. Der Solanor Kunststoffkollektor - the development of a polymer collector with glazing. In: Wallner, G.M, Lang, R.W. (Eds.), Proceedings of 1st Leobener Symposium Polymeric Solar Materials, pp. II-1-II-8.

Meir, M., 2008. IEA-SHC Task 39: Polymeric solar thermal Collectors - State of the art. In: Wallner, G.M., Lang, R.W. (Eds.), Proceedings of 2nd Leobener Symposium Polymeric Solar Materials, pp. I-1-6.

Olivares, A., Rekstad, J., Meir, M., Kahlen, S., Wallner, G., 2008. A test procedure for extruded polymeric solar thermal absorbers. Sol. Energy Mater. Sol. Cells 92, 445-452.

Raman, R., Mantell, S., Davidson, J., Wu, C., Jorgenson, G., 2000. J. Sol.Energy Eng. 122, 92.

Resch, K., 2008. Polymeric Thermotropic Materials for Overheating Protection for Solar Collectors. PhD Thesis. November, 2008. Institute of Materials Science and Testing of Plastics. University of Leoben, Austria.

Rogner, H.H., 2000. Energy resources and technology options (Chapter 5). In: World Energy Assessment (WEA). UNDP, New York.

Sandnes, B., 2003. Exergy Efficient Production, Storage and Distribution of Solar Energy. PhD Thesis. University of Oslo, Norway.

Sayigh, A, 1999. Renewable Energy – the way forward. Appl. Energy 64, 15-30.

Streicher, W., 2005. Sonnenenergienutzung. Lecture at the Institute of Thermal Institute at the University of Graz, Austria.

Wallner, G.M., Lang, R.W., 2005. Guest editorial. Sol. Energy 79 (6), 571-572.

Wallner, G.M., Lang, R.W., 2006. Kunststoffe - Neue Möglichkeiten in der Solarthermie. Erneuerbare Energie 2-2006, AEE-Intec, Austria.

Wu, C, Mantell, S.C, Davidson, J.H, 2004. Long-term Performance of PB and Nylon 6,6 Tubing in Hot Water. J. Sol. Energy Eng. 126 (1), 581-586.

PART II:

COLLECTION OF PAPERS

PAPER 1°

Characterization of Physical and Chemical Aging of Polymeric Solar Materials by Mechanical Testing

S. Kahlen[a)]*, M. Jerabek[a)], G. M. Wallner[b)], R.W. Lang[b)]

[a)] Polymer Competence Center Leoben GmbH, Roseggerstrasse 12, Leoben, 8700, Austria

[b)] Institute of Materials Science and Testing of Plastics, University of Leoben, Franz-Josef Strasse 18, Leoben, 8700, Austria

ABSTRACT

In this paper the potential of mechanical tensile testing to characterize aspects of physical and chemical aging of polymeric solar materials as films is investigated. For this purpose, two types of polymer films, one being a multi-phase amorphous material (blend of polyphenylene ether and polystyrene (PPE+PS)) the other being a crosslinked semi-crystalline material (polyethylene (PE-X1)), were exposed to water at 80 °C for up to 16000 hours prior to being tested mechanically at room temperature. The properties deduced from mechanical tests to indicate aging were the modulus of the films, characteristic for the small-strain behavior, and the values for strain-to-break, characteristic for the post-yield behavior and ultimate failure at large strains. In both cases, two strain determination techniques were applied, one based on conventional crosshead displacement measurements, the other based on optical techniques (digital image correlation for the small-strain regime and video extensometry for the large-strain regime).

While significant chemical aging was detected for PPE+PS indicated by a significant drop in strain-to-break values even after 2000 hours of aging exposure, no clear conclusion could be drawn for PE-X1 partially due to the large data

---

° To be submitted to “Polymer Testing”.

* Corresponding author. Tel.: +43 (0) 3842 42962 50
Email address: kahlen@pccl.at

scatter observed for this material. In any case, when comparing strain values deduced from optical techniques and crosshead displacement measurements, the former are to be preferred due to the higher accuracy.

Keywords: Polymer films, solar thermal application, aging, mechanical testing.

1 INTRODUCTION

Due to improved performance profiles in combination with processing advantages, polymeric materials are becoming increasingly of interest for applications in glazed hot-water solar thermal collectors (Lang et al., 1997; Wallner and Lang, 2005; Wallner and Lang, 2006). While polymers have been used in such collector systems for casings, as sealing materials mainly made of ethylene propylene diene monomer (EPDM) (Wallner and Lang, 2006) and as glazing material (www.arcon.dk, www.solarventi.com) for quite some time, more recently polymers are also used to replace copper or aluminum as absorber material as Integrated/Collector storage type (ICS) system (Meir et al., 2008) and the Solarnor® collector (Meir and Rekstad, 2003). As such polymer based glazed collector absorber materials are exposed to elevated temperatures up to 80 °C under operating conditions and up to 140 °C under stagnation (Kahlen et al., 2009a), knowledge of the aging behavior of existing and potential polymeric absorber materials under the combined influence of heat and water or air is of utmost importance. While the subject of aging at elevated temperatures under water or air exposure has been investigated intensively for numerous polymers used in hot water piping systems and to a lesser extent in polymeric heat exchangers, these studies primarily focused on polyolefins (Gedde et al., 1994; Dörner and Lang, 1998a+b, Lang et al., 1997; Pinter et al., 2002), polysulfone and polyamide 6, 6 (Freeman et al., 2005) exposed to air, water or chlorinated water up to 105 °C and 80 C, respectively. Regarding the aging behavior under stagnation conditions (up to 140 °C), hardly any information is available.

In terms of aging characterization, the methodologies applied include mechanical experiments such as pressurized pipe tests (Gedde et al., 1994), and tensile and creep tests (Freeman et al., 2005; Dörner and Lang, 1998a+b; Lang et al., 1997;

Pinter et al., 2002), on the one hand, and various analytical characterization techniques such as the determination of the oxidation temperature and the oxidation induction time via differential thermal analysis (DTA) or differential scanning calorimetry (DSC), high pressure liquid chromatography (HPLC) and size exclusion chromatography (SEC). The applicability and the advantages of proper mechanical test methods in characterizing both, physical and chemical aging of polymers in solar applications have been addressed most recently by Oreski, 2008 and Wallner et al., 2004. In principle, both physical and chemical aging of polymers may affect the pre-yield, the yield and the post-yield regime. While modulus changes represent a proper measure for aging in the pre-yield regime (e.g., modulus dependence on free volume changes, post-crystallization and crosslinking), in the post-yield regime strain-to-break values are frequently used to characterize aging. However, a proper allocation of physical and/or chemical aging to observed alterations in properties generally also requires knowledge on the molecular and morphological structure of the polymer under investigation along with potential physical and chemical aging mechanisms and their effects on mechanical properties in both, the pre-yield and post-yield regime. In any case, an important prerequisite for the generation of adequate mechanical data is a rather precise strain measurement technique over the entire deformation range (pre-yield and post-yield).

In terms of strain determination, contactless optical strain measurement has become an important tool to characterize the tensile behavior of polymers offering advantages in the post-yield regime and when investigating polymer films which do not allow for the attachment of mechanical extensometers (Wallner et al., 2006; Buisson and Ravi-Chandar, 1990; G'Sell et al., 2002; Hiss et al., 1999; Fauster et al., 2005; Jerabek et al., 2009). In this context it is specifically pointed out in ISO 527-3, that film specimens shall not carry the weight of a contacting extensometer, and it is therefore suggested to measure the nominal strain via the crosshead displacement. As to the optical strain determination, two different measurement systems may be distinguished. When using video extensometer based systems (Fauster et al., 2005), the strain is measured between two fixed edges within a defined gage length. Alternately, full field strain analysis (FFSA) systems based on the principle of comparing speckle pattern structures of undeformed and deformed

surfaces allow for the determination of both, local and average global strain values (Jerabek et al., 2009). Despite the high potential of optical strain measurement systems in characterizing aging phenomena in plastics, only limited information on the application of such techniques for this purpose is available. For example, Wallner et al., 2006 investigated unnealed vs. annealed samples of double notched PVDF films by recording the global load displacement curves via the crosshead displacement and the local crack opening displacement (COD) curves via video extensometer. For the annealed samples, slight differences in the fracture parameters deduced from global and local strain measurements were obtained.

Hence, it is the purpose of this paper to establish a methodology for the characterization of physical and chemical aging of polymeric solar absorber materials by performing monotonic tensile tests of unaged and aged polymer films, making use of contactless optical strain measurement techniques. The materials investigated include polyphenylene ether polystyrene blend (PPE+PS), which is already in use for absorbers in glazed collectors (Solarnor AS, Oslo, N), and crosslinked polyethylene (PE-X), which may potentially be used as absorber materials particularly if certain requirements to prohibit excessive overheating are met (Resch, 2008).

2 EXPERIMENTAL

2.1 Methodology

As pointed out above, the main objective of this paper is to investigate the potential of tensile test results of unaged and pre-aged polymer films to characterize the aging behavior and the main aging mechanisms (physical aging vs. chemical aging) in these films by applying a contactless strain measurement technique. As also alluded to above, the use of such a technique allows for accurate strain measurements of specimens with reduced thickness (e.g., films) and offers numerous advantages both in the pre-yield and the yield and post-yield regime, thus perhaps allowing for an improved data analysis and interpretation in terms of physical and chemical aging mechanisms. Although a comprehensive

analysis of aging phenomena would require the application of other analytical and chemical techniques in addition to the knowledge on the molecular nature and architecture of the polymer/additive compound of interest, in this paper the focus is to relate physical aging to changes in the pre-yield regime (i.e., modulus) and chemical aging to changes in the post-yield regime (i.e., strain-to-break). Nevertheless, as some other techniques have been applied to the same materials investigated in this paper in other publications by the authors, in the discussion section reference will be made to these results published elsewhere.

In terms of the experimental program, polymer film specimens were aged in water at 80 °C up to 16000 hours. Following aging exposure, tensile tests were performed at room temperature. For comparison, tensile tests were also performed with unaged specimens, corresponding to the original state of the polymer films. Finally, the results of optical strain measurements and the nominal strain determination via the crosshead displacement are compared in terms of advantages and disadvantages.

2.2 Materials, Specimens and Conditioning

The materials investigated include two commercially available polymer compounds, one being amorphous, and the other semi-crystalline. The amorphous polymer of black color was a blend of polyphyenylene ether and polystyrene (designation: PPE+PS; trademark: Noryl EN 150SP; manufacturer: Sabic, Bergen op Zoom, NL). The translucent semi-crystalline polymer was a silane-crosslinked polyethylene (designation: PE-X1; trademark: Taborex; manufacturer: Silon, Brno, CZ).

The amorphous PPE+PS was supplied as granules and was extruded to films on a single screw extruder followed by a chill roll unit at Dr. Collin (Dr. Collin GmbH; Ebersberg; D). The film thickness of PPE+PS ranged from 420 to 480 µm. The semi-crystalline PE-X1 was directly supplied as film with a thickness of about 500 µm.

Tensile test specimens of the S2 type (DIN 53504) with an overall length of 75 mm were machined from the polymer films with a puncher. The tensile test specimens had an, respectively. The dumb-bell specimens were tested in the unaged and

pre-aged state. As to the aging conditions, specimens were exposed to distilled water at 80 °C for 2000, 4000, 6000, 8000 and 16000 hours. Aging was carried out using an air-circulating oven (type Kendro 6000; Kendro Laboratory Products GmbH; Langenselbold; D). The specimens were placed in a water filled glass jar covered by a screw top. The distilled water was changed in intervals of 2000 hours.

2.3 Monotonic Tensile Testing

Tensile tests were carried out according to ISO 527-3 using a screw driven universal testing machine (type: Instron 4505; Instron International Ltd.; High Wycombe, UK). The test temperature was 23 °C, the test speed was 10 mm/min. Clamping of the specimens in the grids was adjusted to obtain a gage length of about 40 mm (overall specimen length of 75 mm). Depending on the quality of the stress-strain data, 3 to 10 specimens were tested for each specimen condition.

To determine strain, three methods were applied simultaneously for each test performed. An optical strain measurement technique referred to as digital image correlation (DIC) technique was used for strain measurements in the pre-yield regime up to 3 % strain for modulus determination. For post-yield deformations and ultimate strain determination (strain-to-break), a video extensometer (VE) was applied. The measurement devices of the DIC system and the VE system were positioned on the same side of the specimen (see Fig. 1[*]). In addition, nominal strain measurements via the crosshead displacement were performed over the entire deformation regime (pre-yield and post-yield). While essential aspects of these techniques are briefly described below, more detailed information may be obtained elsewhere for the DIC technique (Hild and Roux, 2006; Jerabek et al., 2009) and the VE technique (Fauster, et. al, 2005), respectively.

2.3.1 Small-strain Measurement Using the DIC Technique

The DIC technique, consisting of two high-speed cameras (type: Nikkor 105 mm f/1.8; Nikon corporation; Tokyo; J) and allowing for a full field strain analysis (FFSA), was applied to accurately resolve the strains in the pre-yield regime (up to

[*] All figures of this paper are collected at the end of the text.

3 %) for precise modulus determination. While the system in principle may also be used in the post-yield regime at least with bulk specimens (Jerabek et al., 2009), it turned out in preliminary investigations that complications in strain resolution arise with thin films at strain levels beyond about 300 %, which complicates the measurement of ultimate strains. The high-speed cameras were mounted on a positioning frame directly connected to the testing machine frame. To optimize the strain resolution, a sampling rate of 20 Hz was chosen and the distance between the cameras and the specimen was set to cover the entire specimen gage length with the camera image up to 3 % strain. A calibration of the camera set-up was performed prior to the measurement.

Specimen Preparation

Strain determination applying the DIC system requires a finely distributed stochastic pattern painted onto the specimen, which must resolvable by the camera system. For optimal results, several requirements have to be met (Jerabek et al., 2009). To provide high contrast (preferably black-white), a white spray was first applied as base coat on the specimen surface. Subsequently, a black graphite spray was used to produce the pattern. The adhesion and the elasticity of the paint shall be high enough so that the pattern deforms with the specimen. In addition, any effects of solvents of the white color film on the film behavior should be excluded. This was assured by ascertaining that nominal ultimate strain values of unpainted and painted specimens measured via the crosshead displacement were identical. Examples of specimens to which such a stochastic paint pattern was applied are shown in Fig. 2 for PPE+PS (original black color) and PE-X (originally milky-white translucent).

Specimen Illumination

As with other optical systems, the illumination of the object is a crucial factor, which needs to be adopted for each new test set-up (i.e., depending on the optical appearance of the specimen). In the experimental set-up used here meeting optimal conditions for illumination was complicated by the use of two optical systems simultaneously (DIC and VE), each with its own illumination system along with specific requirements as to the illumination quality and potentially interfering with one another. For the DIC system illumination had to be uniform over the full

measurement area, and bright light was needed to allow a frame rate of 20 Hz (Jerabek et al., 2009). To avoid specimen heat-up, a cold light source (type: halogen cold-beam reflector; Conrad Electronics GmbH & Co KG; Vienna, A) was used, mounted on the horizontal bar between the two DIC cameras (Fig. 1).

Data Recording and Reduction

To process the pictures recorded by the DIC system during the tensile test, the strain measurement area of interest is covered with so-called subsets, from each of which a three-dimensional displacement vector is calculated to obtain strain values in lateral and axial direction (Jerabek et al., 2009). Quadratic subsets with a pixel size of 25 and a step of 19 overlapping pixels between two subsets were used. To obtain best results for this experimental set-up and the parameters chosen, the camera shutter time was set to approximately 15 ms.

The analogue force signal from the tensile testing machine was also acquired by the DIC system and saved with the corresponding camera images. Using mean thickness values determined for each sample, stress-strain curves were generated.

2.3.2 Large-strain Measurement Using a Video Extensometer

The video extensometer, consisting of an analog progressive scan camera of the type Sony XC-HR70 (Sony cooperation; Tokyo; J), was mounted on a tripod and positioned on the same side but below the DIC system (see Fig. 1). Specific features of this VE system are monochromic light, 1024 x 768 pixels, and a maximum frame rate of 30 Hz. Depending on the expected ultimate strain value of the sample, different optics with focal lengths between 25 mm and 50 mm were employed. Ductile samples with high strain-to-break values were recorded with 1.5 Hz for the first 500 seconds and 0.2 Hz thereafter. More brittle samples were measured with 3 Hz in the first 500 sec and then with 1 Hz to provide a sufficient time for the resolution of the yield point and the strain-to-break.

Specimen Preparation

Two parallel distance indicator marks to be traced by the VE system were painted on the specimen with a pen at a distance of approximately 21 mm within the straight specimen gage length. For transparent or translucent specimens (e.g.,

PE-X1; see Fig. 2), a white background surrounding the black marks needed to be painted on the surface to ensure a good contrast. Analogous to the procedure described above, it was ascertained by tests of specimens with and without paint application that the ultimate crosshead displacement was not affected by the paint.

Specimen Illumination

To provide for sufficient illumination at large deformations, a separate cold light source (type: polytec fiber-optic system; Polytec PT GmbH Polymere Technologien; Waldbronn, D) was applied for the video extensometer. Two line light sources were mounted along the vertical bar of the positioning frame, one at the height of the upper specimen clamp, the other at a position corresponding to the ultimate deformation position of the lower marker prior to specimen failure (see Fig. 2).

Data Recording and Reduction

The images recorded by the VE system were further processed on a personal computer to determine strain values. The programs used to acquire the images and to determine stress-strain curves are described in more detail in (Fauster et al., 2005).

It is worth mentioning, that in some cases the measurement markers faded after an elongation of approximately 600 to 700 %, thus impeding the contrast needed for the VE measurement. Corrections in illumination (e.g., by a change of the intensity or the angle of the light towards the specimen) helped to resolve this problem.

An example of a stress strain curve with the strains determined using the video extensometer is shown for PE-X1 in Fig. 5 along with photographs of the deformed specimens at various positions of deformation. These photographs illustrate the necking of the polymer film specimen and the position and deformation of the measurement markers as the specimen is stretched in the post-yield regime.

2.3.3 Nominal Strain Measurement with the Crosshead Displacement

In addition to the above optical strain measurement procedures, nominal strain values according to ISO 527-3 were determined over the entire deformation

regime via crosshead displacement measurements. In this case the specimen gage length was taken as the distance between the specimen grips at the start of the test. This distance was determined at the start of the test using a conventional caliper.

Referring to the above techniques of strain determination, the evaluation of the mechanical properties of interest (modulus in the pre-yield regime and strain-to-break in the post-yield regime) is shown schematically in Fig. 3. According to ISO 527-3, values for Young's Modulus were calculated in the range between 0.05 % and 0.25 % axial strain based on DIC strain data. To better compare the results with the nominal strain measurement via the crosshead displacement, a second modulus definition was used, calculating an elastic modulus for the strain range between 0.05 % and 0.9 % strain. In all modulus data reduction schemes, a linear fit between the limiting strain values (0.05 % and 0.25 %, and 0.05 % and 0.9 %, respectively) was performed for the stress-strain data, using the slope of this straight line to deduce modulus values. Finally, average values for modulus and strain-to-break were calculated for each testing series.

3 RESULTS

In the following sections, first the tensile behavior of unaged specimens in the small and large-strain regime will be described and discussed. Subsequently the tensile behavior of aged specimens, again for both deformation regimes, will be treated including a comparison of results of aged and unaged material behavior.

3.1 Tensile Behavior of Unaged Specimens

3.1.1 Small-strain Regime of Unaged Specimens

Axial strain distributions at different stages of overall strain in the small-strain regime ($\leq$ 3 %) are shown in Fig. 4 as color plots for PE-X1. Also indicated in the figure are the corresponding overall strain values and the local strain variations for each of the deformation stages. At an overall strain of 0.05 %, the local strain distribution varies from about 0.02 to 0.35 %, the red dots being artifacts associated with dust on the objective. The corresponding local strain variations at

overall strain values of 1.9 % and 3.0 % are in the range from 1.6 to 2.5 % and 2.4 to 3.5 %, respectively. While no indication for the position of subsequent yielding may be deduced from the strain distribution at the lowest overall strain level of 0.05 %, the illustrations for 1.9 and 3 % overall strain indicate at an early stage the position of necking of the specimens at subsequent higher overall strains (i.e., top section of the color plots in Fig. 4).

Representative stress-strain plots utilizing the overall strain values measured with the DIC system and illustrating the degree of reproducibility are shown in Fig. 6 and Fig. 7 for PPE+PS and PE-X1, respectively. While excellent reproducibility was achieved for the former material, more significant variations were obtained for the latter (i.e., ca. +/- 12 % in terms of stress for a given strain value). The origin of the noise in both stress strain curves can be related to oscillations in force measurement, which becomes evident in Fig. 8, where the actual strain values and the force values are plotted separately as a function of time. This effect may be associated with the comparatively low resolution of 12 bit of the analog digital converter of the DIC system when transforming the original force signal of the test machine. Why the reproducibility of the stress strain measurements in the small-strain regime apparently depends on the material investigated is not yet clear. Potential causes are local variations in crosslinking density of the silane-crosslinked PE-X1 material.

A comparison of stress strain curves based on overall strain measurements using the DIC system and the crosshead displacement for strain determination is shown for PPE+PS and PE-X1 in Fig. 9. In principle, for dumb-bell specimens at a given stress level, one would expect lower nominal strain values (based on crosshead displacement) than overall strain values (based on the DIC technique). However, some deviation in the opposite direction was obtained for both polymer films, which is due to some specimen slippage of the film specimens in the tensile grips. The more significant differences for PPE+PS are apparently caused by the stronger slippage of the rather smooth surface of these film specimens. In any case and although not shown here, when applying the video extensometer for strain determination in the small-strain regime, good agreement was found with the results obtained by the DIC system.

To characterize the small-strain regime for the materials investigated also in quantitative terms, modulus values were deduced for various strain limits (0.05 % to 0.25 % and 0.05 % to 0.9 % axial strain based on DIC strain data; 0.05 % to 0.9 % axial strain based on crosshead displacement nominal strain data) as described above. The results are summarized in Table 1.

Table 1: Comparison of modulus values (in MPa) at room temperature determined using the DIC system (2 strain ranges) and based on crosshead displacement measurements (1 strain range).

Material	**DIC** (0.05 – 0.25 %)	**DIC** (0.05 - 0.9 %)	**Crosshead displacement** (0.05 - 0.9 %)
PPE+PS	1960 ± 60	1980 ± 20	1510 ±30
PEX-1	1710 ± 180	1330 ± 120	1120 ± 40

In good agreement with expectations, while modulus values determined with the DIC system were found to be rather strain range independent for the amorphous polymer film of PPE+PS, they were found to decrease with increasing strain range for the semi-crystalline PE-X1, which at room temperature is above T_g thus exhibiting a higher degree of nonlinearity. Moreover, as a consequence of the slippage effects described above, modulus values determined via the crosshead displacement measurement are lower than those obtained using the DIC strain values. The difference amounts to about 24 % for PPE+PS and 16 % for PE-X1. Hence, the difference between “effective” overall strain values (DIC system) and nominal overall strain values (crosshead displacement measurement) clearly depends on the material. These results reinforce the importance of using both strain measurement techniques for aging investigations, as the unaged and aged materials of a given material type may also well be considered as different material states for which slippage effects may become more or less pronounced.

3.1.2 Large-strain Regime of Unaged Specimens

Stress strain curves for the entire deformation regime including the yield and post-yield regime up to specimen failure using the video extensometer for strain measurements are shown in Fig. 10 and Fig. 11. Also depicted are specimen dependent variations, indicating a good reproducibility of the experimental results.

A comparison of stress-strain curves using the video extensometer and the crosshead displacement for strain determination is provided in Fig. 12. A quantitative comparison of yield stress values and strain-to-break values using the two strain measurement techniques is listed in Table 2.

Table 2: Comparison of yield stress values and strain-to-break at room temperature determined using the video extensometer (VE) and based on crosshead displacement measurements.

	VE		**Crosshead displacement**	
Material	**Yield stress** in MPa	**Strain-to-break** in %	**Yield stress** in MPa	**Strain-to-break** in %
PPE+PS	45.6 ± 0.8	73 ± 12	44.9 ± 0.6	37 ± 4
PEX-1	26.1 ± 1.5	631 ± 50	28.2 ± 2.3	365 ± 38

As expected, the yield stress values with ca. 45 MPa for PPE+PS and ca. 27 MPa for PE-X1 are essentially independent of the strain measurement technique. Comparing the strain-to-break results for both techniques, the lower values for the crosshead displacement method are again a result of specimen slippage in the initial stages of the test and the nominal strain definition, which uses the entire specimen gage length as original reference length. Thus, the crosshead displacement measurement yielded strain-to-break values that were 40 to 50 % lower than those obtained with the video extensometer.

3.2 Tensile Behavior of Aged Specimens

3.2.1 Aging Effects on Mechanical Behavior of PPE+PS

The effect of aging time (i.e., exposure to hot water at 80 °C) on small-strain and large-strain mechanical behavior of PPE+PS is illustrated in Fig. 13 and Fig. 14, respectively. The figures contain a comparison of the characteristic properties modulus and strain-to-break derived from optical strain measurements (DIC system for modulus and video extensometer for strain-to-break), on the one hand, and from crosshead displacement measurements, on the other. For a given aging condition and as indicated in the diagrams, the data scatter in both properties is remarkably low. Over the entire aging exposure time and for reasons described

above, the modulus values derived from the DIC system are again lower. However, while the DIC system indicates no modulus change over the aging period, modulus values were found to increase initially and subsequently decrease again with aging time when using the crosshead displacement data reduction method. This indicates, that for precise measurements, the optical strain method is to be preferred. Although there are also quantitative differences in the strain-to-break values when comparing optical and crosshead displacement measurements, the trends as a function of aging time are at least identical. In terms of aging mechanisms, the results suggest that hardly any physical aging takes place for these aging conditions (i.e., modulus remains unchanged versus aging time), while significant chemical aging occurs within the first 2000 hours of aging (i.e., significant drop in strain-to-break). This general conclusion from mechanical experiments is supported by analytical investigations published in a separate paper (Kahlen et al., 2009b).

3.2.2 Aging Effects on Mechanical Behavior of PE-X1

Corresponding data for modulus and strain-to-break as a function of aging time are depicted in Fig. 14 and Fig. 15 for PE-X1. In good agreement with the findings for unaged specimens described above, there is a rather large scatter in the results over the entire aging regime. While there is some tendency for modulus values to first increase and then decrease with aging time, and for strain-to-break values to decrease with aging time, the large data scatter does not allow for any clear and unambiguous conclusions regarding physical and chemical aging mechanisms. Separately performed differential scanning calorimetry measurements also did not provide any strong indication for changes in crystallinity with aging time. Hence, for this material further investigations are necessary to provide more insight as to specific aging mechanisms.

4 SUMMARY AND CONCLUSIONS

The potential of small strain and large strain mechanical tensile properties to characterize aging of polymeric solar materials as films was investigated. The two types of polymer films selected included a multi-phase amorphous blend of

PPE+PS and a crosslinked semi-crystalline designated PE-X1. The films were exposed to water at 80 °C for up to 16000 hours and were then tested mechanically at room temperature. Using two types of strain measurement techniques (i.e., crosshead displacement measurements and optical strain determination via DIC (up to 3 %) and video extensometry (entire deformation regime up to failure), modulus values and strain-to-break values characterizing the small-strain and ultimate behavior, respectively, were chosen as indicators for aging.

While excellent reproducibility in the small strain values determined was obtained with the DIC system for PPE+PS, more significant variations were found for PE-X1, the latter probably originating from local variations in the crosslinking density. Comparing the optical and the crosshead displacement technique, due to some specimen slippage the DIC systems delivered lower overall strain values for both polymer film types. In the large-strain regime (i.e., yield and post-yield behavior) up to final failure, for both materials significant lower values in the crosshead displacement based strains were determined because of specimen slippage and the choice of the initial nominal gage length of the dumb-bell tensile specimens.

While modulus values of PPE+PS did not change significantly with the time of aging exposure when determined with the DIC system, the nominal strain measurement (crosshead displacement) indicated some increase within the first 2000 hours and a decrease thereafter. Hence, for precise measurements of modulus, optical systems are to be preferred. Strain-to-break values of PPE+PS vs. aging time exhibited the same trend when measured with the DIC and the crosshead displacement technique, indicating significant chemical degradation after 2000 hours of aging in hot water. For PE-X1 also similar dependencies of properties on aging time in the pre-yield and the post-yield regime were found, when using the DIC system and the video extensometer, respectively, compared to the crosshead displacement measurements. However, high strain variations were observed for the unaged and aged PE-X1 materials, thus not allowing for clear conclusions regarding any mechanisms of physical and/or chemical aging. Nevertheless, overall it could be shown that the optical strain measurement techniques (DIC system in the small-strain regime and video extensometer in the

large-strain regime) allow for more precise measurements of strain and should thus be preferred when performing aging investigations via mechanical tensile testing. However, in addition to mechanical testing, further analytical techniques are needed to elucidate the precise mechanisms of physical and chemical aging.

Acknowledgments

The research work of this paper was performed within the project S. 11 “Aging of polymers in solar-thermal applications” at the Polymer Competence Center Leoben GmbH within the framework of the K_{plus} Program of the Austrian Ministry of Traffic, Innovation and Technology with contributions by the University of Leoben, Graz University of Technology, Johannes Kepler University Linz, JOANNEUM RESEARCH ForschungsgmbH and Upper Austrian Research GmbH. The PCCL is funded by the Austrian Government and the State Governments of Styria and Upper Austria.

Literature

Buisson, G., Ravi-Chandar, K., 1990. On the constitutive behaviour of polycarbonate under large deformation. Polymer 31 (11), 2071-2076.

DIN 53504, 1994. Testing of rubber; determination of tensile strength at break, tensile stress at yield, elongation at break and stress values in a tensile test.

Dörner, G., Lang, R.W., 1998a. Influence of various stabilizer systems on the ageing behavior of PE-MD – I. Hot-water ageing of compression molded plaques. Polym. Degrad. Stab. 62, 421-430.

Dörner, G., Lang, R.W., 1998b. Influence of various stabilizer systems on the ageing behavior of PE-MD – II. Ageing of pipe specimens in air and water at elevated temperatures. Polym. Degrad. Stab. 62, 431-440.

Fauster, E., Schalk, P., O’Leary, P., 2005. Evaluation and Calibration Methods for the Application of a Video-Extensometer to Tensile Testing of Polymer Materials. In: Price, J.R., Meriaudeau, F. (Eds.), Proceedings of SPIE-IS&T Electronic Imaging, San Jose, pp.187-198.

Freeman, A., Mantell, S.C., Davidson, J.H., 2005. Mechanical performance of polysulfone, polybutylene, and polyamide 6/6 in hot chlorinated water. Sol. Energy 79, 624-637.

Gedde, U.W., Viebke, J., Leijtström, H., Ifwarson, M., 1994. Long-Term Properties of Hot-Water Polyolefin Pipes – A Review. Polym. Eng. Sci. 34 (24), 1773-1787.

G’Sell, C., Hiver, J.M., Dahoun, A., 2002. Experimental characterization of deformation damage in solid polymers under tension, and its interrelation with necking. Int J Solids Struct 39 (13-14), 38573872.

Hild, F., Roux, S., 2006. Digital Image Correlation: from Displacement Measurement to Identification of Elastic Properties - a Review. Strain, 42- 69.

Hiss, R., Hobeika, S., Lynn, C., Strobl, G., 1999. Network Stretching, Slip Processes and Fragmentation of Crystallites during Uniaxial Drawing of

Polyethylene and Related Copolymers. A Comparative Study. Macromolecules 32 (13), 4390-4403.

ISO 527-3, 2005. Plastics - Determination of tensile properties - Part 3: Test conditions for films and sheets.

Jerabek, M., Major, Z., Lang, R.W., 2009. Applicability and limitations of a digital image correlation system for monotonic testing of polymeric materials. To be submitted in Polym. Test.

Kahlen, S., Wallner, G.M., Lang, R.W., 2009a. Aging behavior of polymeric solar absorber materials, part 1: engineering plastics. To be submitted in Sol. Energy.

Kahlen, S., Wallner, G.M., Lang, R.W., 2009b. Aging behavior of polymeric solar absorber materials, part 2: commodity plastics. To be submitted in Sol. Energy.

Lang, R.W., Stern, A., Doerner, G., 1997. Applicability and limitations of current lifetime prediction models for thermoplastics pipes under thermal presure. Macromol. Mater. Eng. 247, 131-137.

Meir, M., Buchinger, J., Kahlen, S., Köhl, M., Papillon, P., Rekstad, J., Wallner, G., 2008. Polymeric solar collectors – state of the art. In Fernandes, E.O. (Ed.), Proceedings of the EuroSun 2008, Lisbon, Portugal, N° 409, pp. 1-10.

Meir, M.G., Rekstad, J., 2003. Der Solarnor® Kunststoffkollektor - the development of a polymer collector with glazing. In: Wallner, G.M, Lang, R.W. (Eds.), Proceeedings of 1st Leobener Symposium Polymeric Solar Materials, pp. II-1-II-8.

Oreski, G., 2008. Polar Ethylene Copolymer Films for Solar Applications – Optical Properties and Aging Behavior. PhD Thesis. November, 2008. Institute of Materials Science and Testing of Plastics. University of Leoben, Austria.

Pinter, G., Duretek, I., Aust, N., Lang, R.W., 2002. Characterization of the Thermo-Oxidative Degradation of Polyethylene Pipes by Chromatographical, Rheological and Thermo-Analytical Methods. Macromol. Symp. 181, 213-223.

Resch, K., 2008. Polymeric Thermotropic Materials for Overheating Protection for Solar Collectors. PhD Thesis. November, 2008. Institute of Materials Science and Testing of Plastics. University of Leoben, Austria.

Wallner, G.M., Lang, R.W., 2005. Guest editorial. Sol. Energy 79 (6), 571-572.

Wallner, G.M., Lang, R.W., 2006. Kunststoffe-Neue Möglichkeiten in der Solarthermie. Erneuerbare Energie 2-2006, AEE-Intec, Austria.

Wallner, G.M., Major, Z., Lang, R.W., 2006. Influence of annealing on the fracture behavior of 200 mm thick α-PVDF films. Adv. Eng. Mater. 8 (11), 1140-1145.

Wallner, G.M., Weigl, C., Leitgeb, R., Lang, R.W., 2004. Polymer films for solar energy applications – thermoanalytical and mechanical characterisation of ageing behaviour. Polym. Degrad. Stab. 85, 1065-1070.

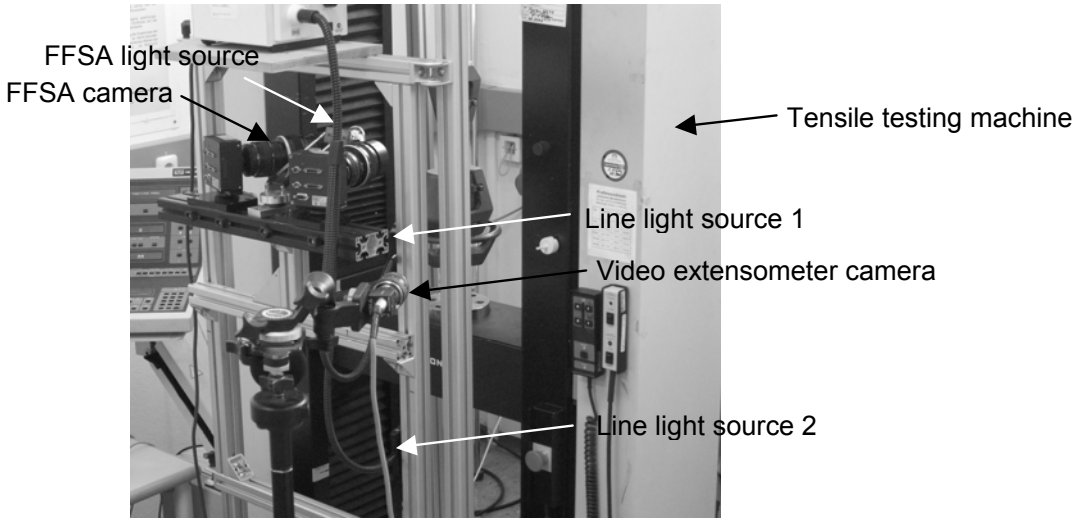

Fig. 1: Monotonic tensile test set-up for polymer films with the FFSA system in combination with the video extensometer for strain determination. The two FFSA cameras are mounted on a frame that is directly connected with the testing machine. The video extensometer camera is mounted on a tripod. Two line light sources for the video extensometer are also attached to the FFSA frame.

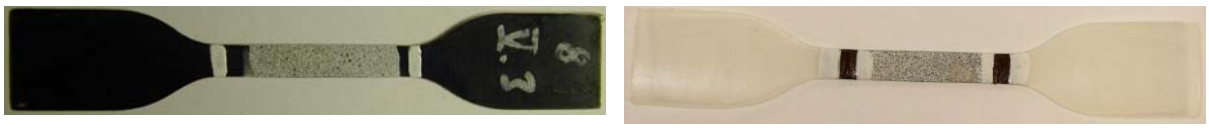

Fig. 2: PPE+PS sample (left image) and PEX-1 sample (right image) prepared for testing with the two black and white measurement line marks for the video extensometer and the speckle pattern for the FFSA system.

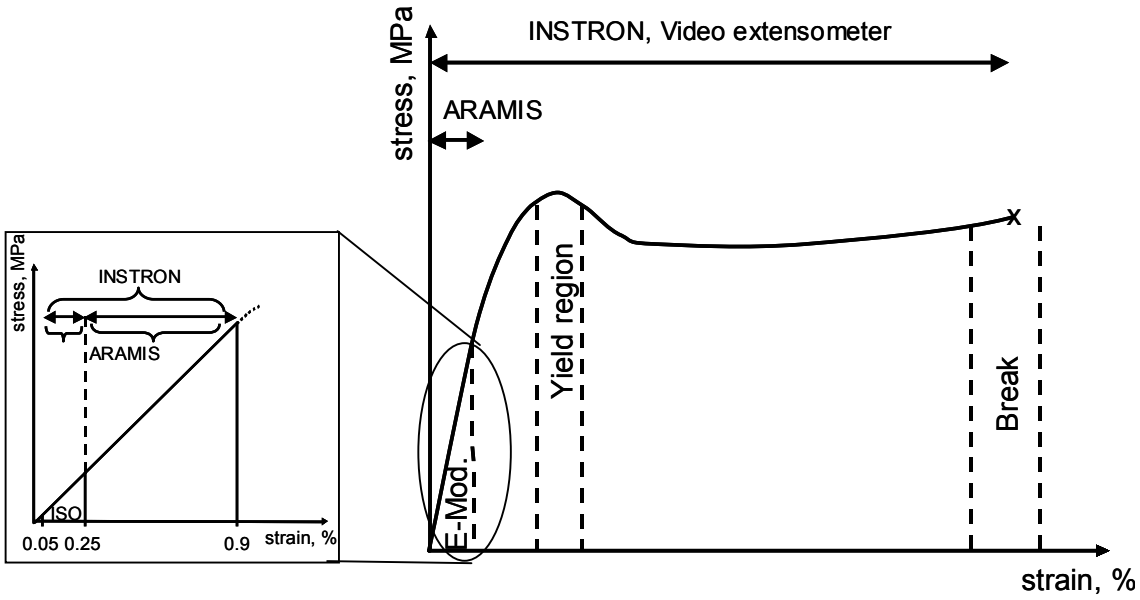

Fig. 3: Schematic illustration of evaluation of the mechanical properties indicating the regime of accurate strain determination by crosshead displacment measurements (Instron), by video extensometer and by the FFSA system (Aramis). The modulus E was evaluated in the range between 0.05 % and 0.9 % axial strain. The yield stress was determined as maximum stress in the yield region. Ultimate strain and stress values were calculated for specimen fracture (break).

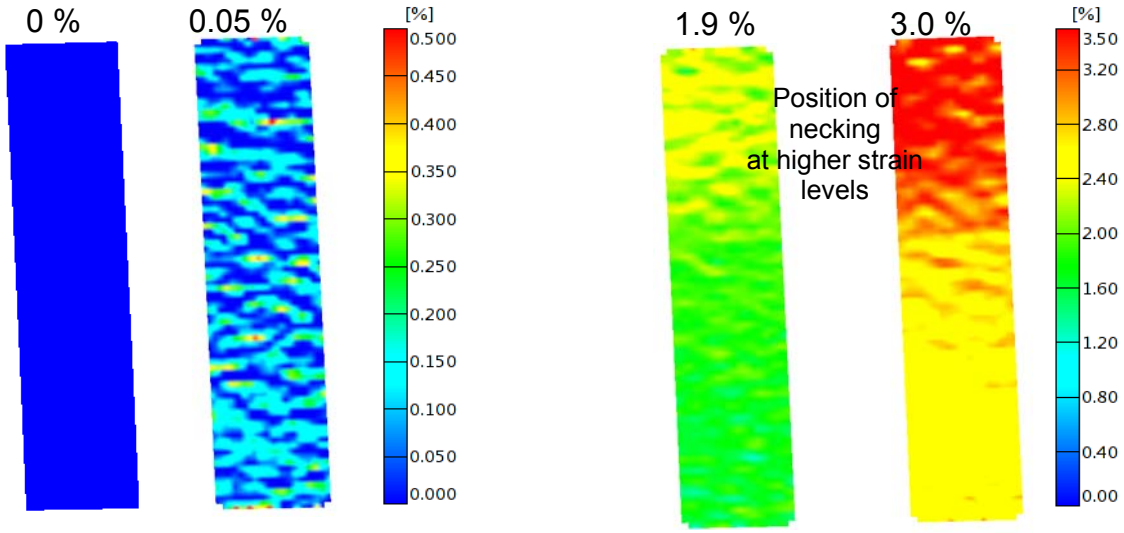

Fig. 4: Color plots of the axial strain distribution of a PE-X1 specimen (unaged at room temperature) in the small-strain regime (up to 3 % overall strain) using the DIC technique. Also indicated for each color plot is the associate range of local strains (color scale bar) and the overall strain (values above each color plot).

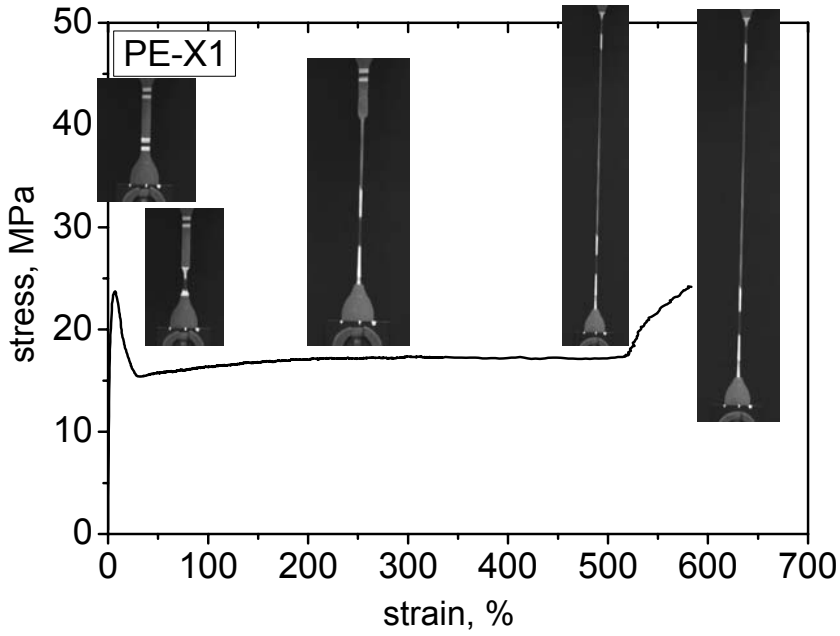

Fig. 5: Stress strain curve of PE-X1 generated at room temperature using the video extensometer for strain determination and illustrating various stages of deformations and stretching of the specimen.

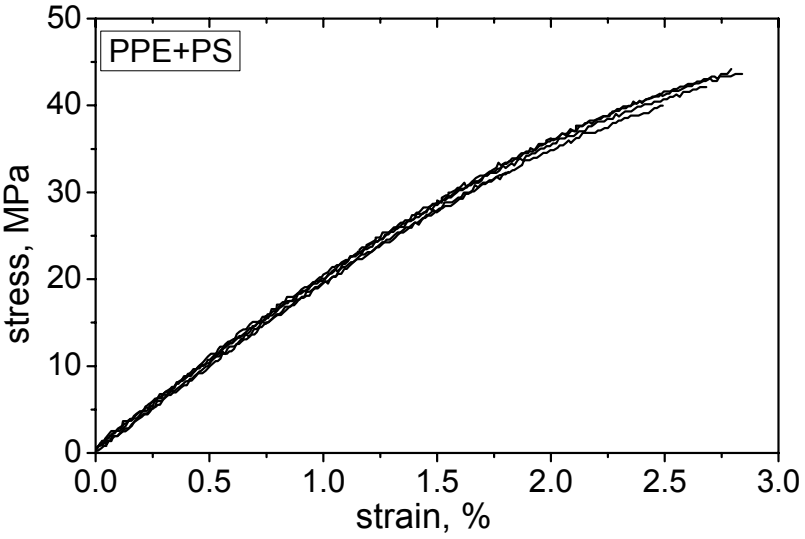

Fig. 6: Reproducibility of stress-strain curves of PPE+PS (unaged) at room temperature (total of 5 tests); strain measurement with the DIC system.

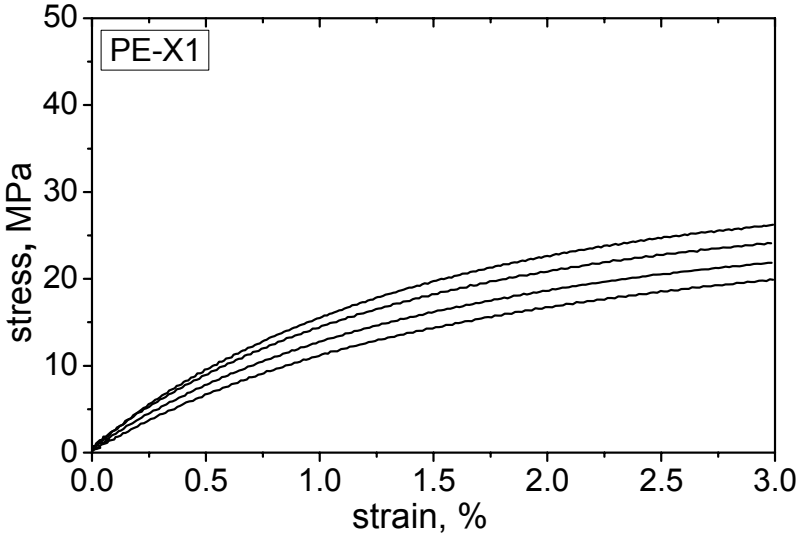

Fig. 7: Reproducibility of stress-strain curves of PE-X1 (unaged) at room temperature (total of 4 tests); strain measurement with the DIC system.

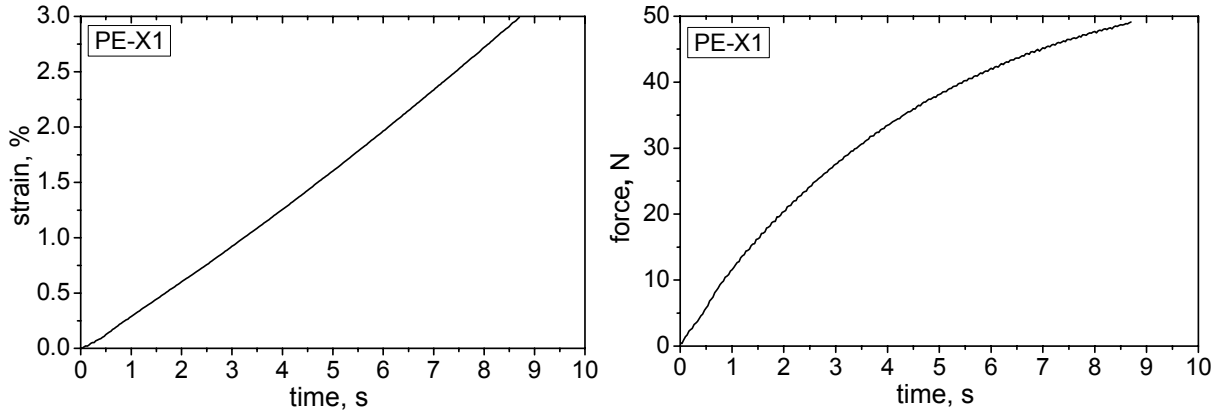

Fig. 8: Axial strain vs. time (left) and force vs. time (right) for a tensile test of PE-X1 (unaged) at room temperature; strain measurement with the DIC system.

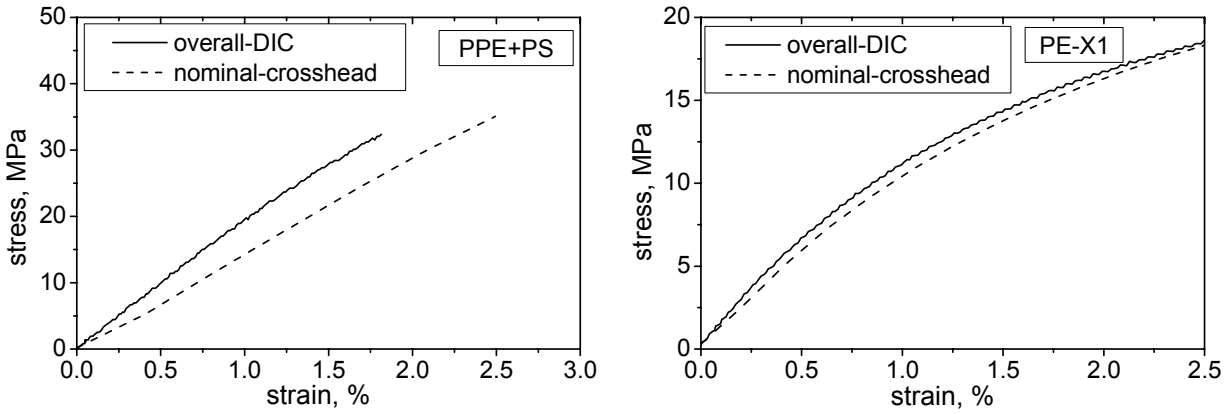

Fig. 9: Stress-strain curves for the small-strain regime of PPE+PS (left) and PE-X1 (right) at room temperature comparing the curves for strain measurement with the DIC system and the crosshead displacement method.

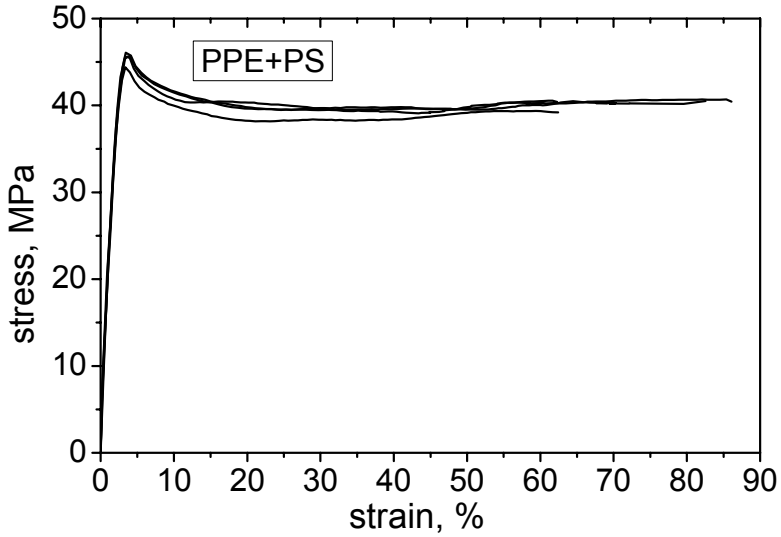

Fig.10: Reproducibility of stress-strain curves of PPE+PS (unaged) at room temperature (total of 5 tests); strain measurement with the video extensometer.

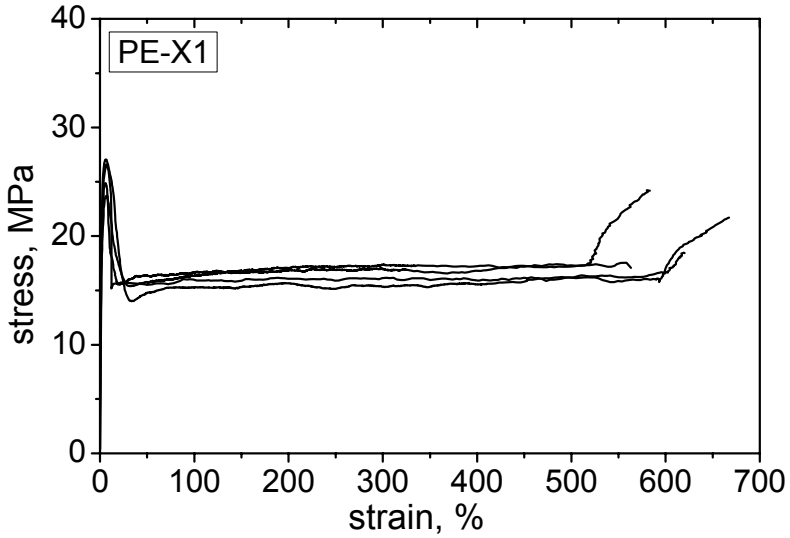

Fig.11: Reproducibility of stress-strain curves of PE-X1 (unaged) at room temperature (total of 4 tests); strain measurement with the video extensometer.

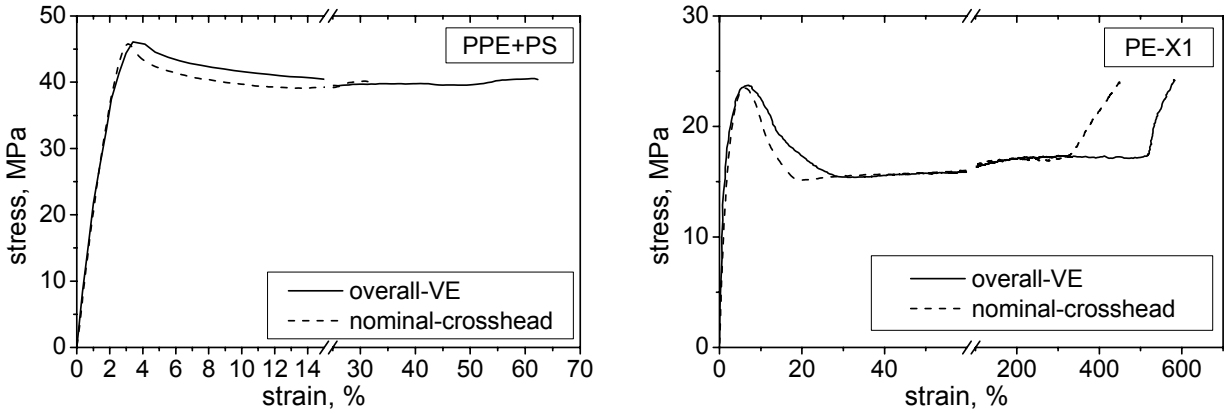

Fig. 12: Stress-strain curves for the entire deformation regime of PPE+PS (left) and PE-X1 (right) at room temperature comparing the curves for strain measurement with the video extensometer and the crosshead displacement method.

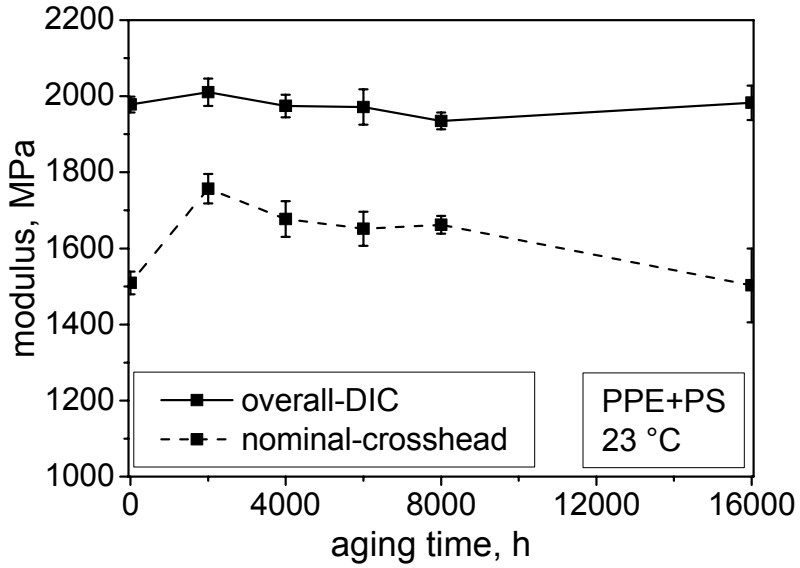

Fig. 13: Effect of aging time (water exposure at 80 °C) on modulus of PPE+PS at room temperature; comparison of modulus data based on strain measurements with the DIC system and the crosshead displacement method.

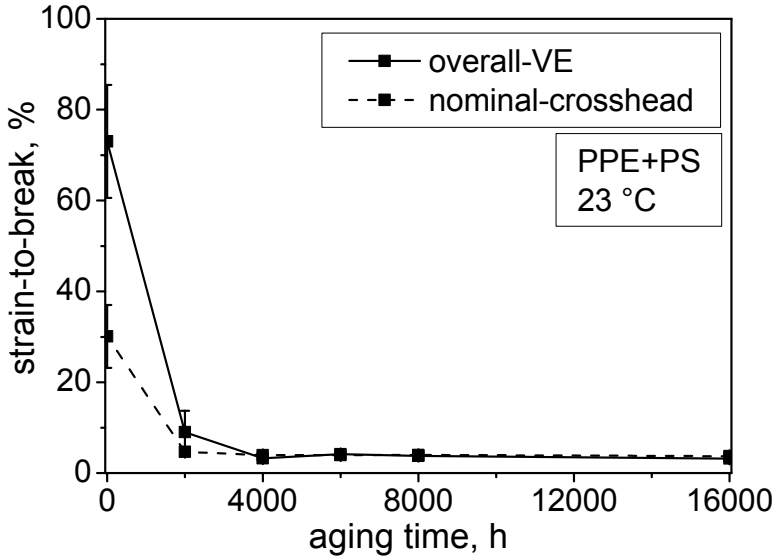

Fig. 14: Strain-to-break calculated with the video extensometer (VE) and via crosshead displacement measurement measured at room temperature for PPE+PS after aging in water at 80 °C.

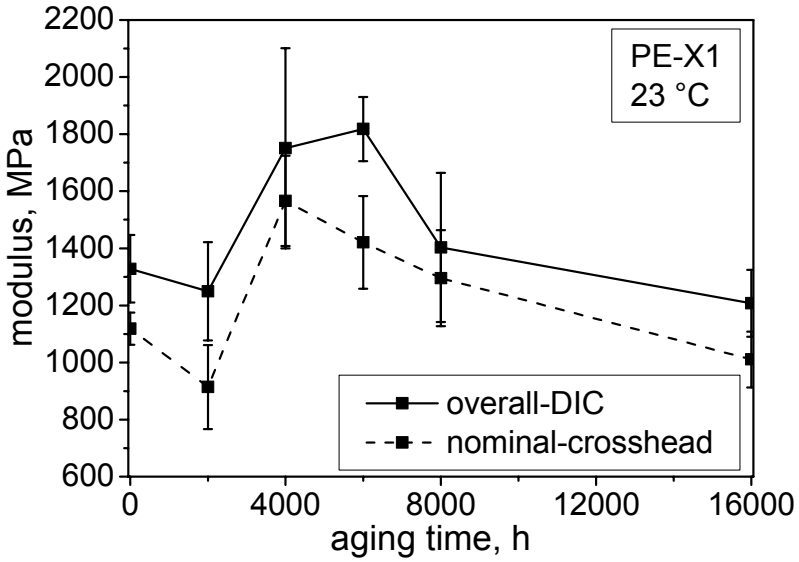

Fig. 15: Effect of aging time (water exposure at 80 °C) on modulus of PPE+PS at room temperature; comparison of modulus data based on strain measurements with the DIC system and the crosshead displacement method.

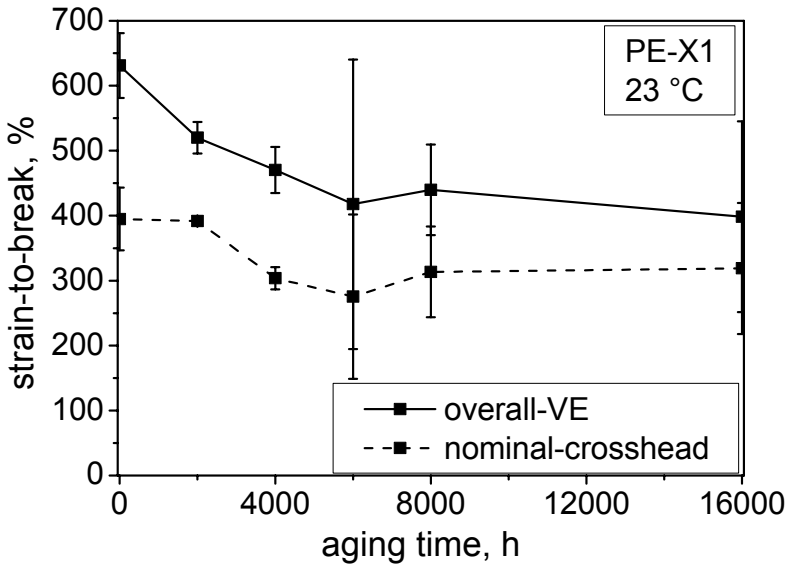

Fig. 16: Strain-to-break calculated with the video extensometer (VE) and via crosshead displacement measurement measured at room temperature for PPE+PS after aging in water at 80 °C.

PAPER 2°

Aging Behavior of Polymeric Solar Absorber Materials – Part 1: Engineering Plastics

S. Kahlen[a)*], G. M. Wallner[b)], R. W. Lang[b)]

[a)] Polymer Competence Center Leoben GmbH, Roseggerstrasse 12, Leoben, 8700, Austria

[b)] Institute of Materials Science and Testing of Plastics, University of Leoben, Franz-Josef Strasse 18, Leoben, 8700, Austria

ABSTRACT

In this series of two papers, various polymeric materials are investigated as to their potential applicability as absorber materials for solar thermal collectors. The focus of the investigation is to study the aging behavior of these materials under maximum operating conditions (80 °C in water up to 16000 h) and stagnation conditions (140 °C in air up to 500 h) typical for northern climate. The materials supplied or produced as polymer films were first characterized in the unaged state and then for different states of aging by differential scanning calorimetry (DSC), by size exclusion chromatography (SEC) and by mechanical tensile tests. Physical aging phenomena were studied by DSC, SEC analysis provided information on chemical degradation of the materials. In addition, physical and chemical aging were both analyzed via the small and large strain mechanical behavior. While the present Part 1 of this paper series deals with the aging behavior of engineering plastics, including two amorphous polymers (a polyphenylene ether polystyrene blend (PPE+PS) and polycarbonate (PC)) and two semi-crystalline polymers (2 types of polyamide 12 (PA12)), the aging behavior of so-called “commodity” plastics (PE and PP) is the subject of Part 2. Comparing the two aging conditions,

---

° To be submitted in “Solar Energy”.

* Corresponding author. Tel.: +43 (0) 3842 42962 50

Email address: kahlen@pccl.at

the amorphous materials (PPE+PS and PC) turned out to be more prone to physical and chemical aging at 140 °C in air. In contrast, the semi-crystalline PA12 materials were more strongly affected by exposure to water at 80 °C, although to different degrees, depending on the modification.

Keywords: engineering polymers, solar thermal application, physical and chemical aging.

1 INTRODUCTION

Nowadays there exist about 20 distinct groups of commercial plastics, each with numerous grades available to obtain an optimum property profile for the corresponding application (Plastics Europe, 2007a). An overview of the commercially significant polymers along with information on their molecular structure, the internationally standardized nomenclature and abbreviations are provided in ISO 1043. On the one hand, plastics grades consist of the polymer, on the other a variety of additives is used to tailor plastics grades for specific applications. Depending on their market share and their performance properties for structural applications, i.e. the mechanical properties and the temperature resistance, plastics are divided into so-called commodity type plastics (PE, PP, PVC and PS), engineering plastics (PMMA, PC, PA, PET, PBT, POM), and specialty plastics (PSU, PES, PEI, PI, PPA, PPS, PEEK) (Plastics Europe, 2007b). The material pyramid (see Fig. 1[*]) shows the three levels of plastics along with current material costs per kg (indicative cost values for 2007).

In the solar thermal market, major contributions of plastics have been reached mainly for unglazed thermal solar absorbers (Weiss, 2003). Main problems for polymers in glazed collectors are high stagnation temperatures, pressurized loops and glycol as heat carrier. With an integrated storage or a sufficient large storage on the system level or the use of thermotropic protection layers, the overheating problem can be solved (Resch et al., 2009). To avoid high pressure levels and glycol as heat carrier, drain-back systems are appropriate measures.

[*] All figures of this paper are collected at the end of the text.

Despite the high potential for plastics applications in solar thermal systems (Wallner and Lang, 2005; Wallner and Lang, 2006; Weiss et al., 2007) and according to a recent study, the use of plastics in solar thermal absorbers also offers ecological advantages (Kicker, 2009), so far only few glazed plastics collectors have been developed. Two plastics collector types that deserve special mentioning are the one referred to as integrated collector storage (ICS) (Meir et al., 2008) and the Solarnor® collector (Meir and Rekstad, 2003). In the ICS system, during stagnation hot water is drained and cold water provided from the mains to protect the system against overheating. As a frost protection, cold water is drained and replaced with warmer water from the mains. In contrast to the ICS system, where parts of the collector are made of non-plastics materials, in the Solarnor® collector all relevant components are made of plastics. The glazing consists of a twin-wall polycarbonate (PC) sheet. The absorber is made of a twin-wall sheet of a polyphenylene ether polystyrene blend (PPE+PS). The Solarnor® collector has been developed for northern climates. Furthermore, it is designed in drain back so that during stagnation and freezing water is drained back to the tank.

In a previous publication (Kahlen et al., 2005), 12 polymeric material candidates for potential use in thermal collectors were selected, and a basic characterization was carried out performing different analytical and a mechanical tests to evaluate and classify the materials in the unaged state. In another study, Davidson et al. (2002) describe and provide a classification of relevant polymers for solar thermal applications, however at this time without referring to any specific aging characteristics. In later studies by this research group, the aging behavior was investigated for polyamide 66 (PA66), polysulfone (PSU) and polybutylene (PB) (Freeman et al., 2005; Wu et al., 2004). The long-term effects on material behavior were restricted to the creep behavior of components made out of these plastics in potable hot chlorinated water at 60 and 80 °C. Thus, so far no comprehensive investigation is available describing and analyzing the effects of the exposure of various plastics to solar absorber service conditions in terms of physical and chemical aging mechanisms. A more profound knowledge on these aging mechanisms is, however, of utmost importance for a proper material selection for solar absorber applications to also ensure save service performance.

Hence, the overall objective of the research performed was to systematically investigate the aging behavior of potential plastics absorber materials and to elucidate the mechanisms of physical and chemical aging for service- and application-near conditions. Part 1 of this series of two papers covers the aging behavior of 4 engineering plastics, while Part 2 deals with the aging behavior of 4 commodity type plastics (polyolefins).

2 BACKGROUND AND METHODOLOGY

Based on experience with the Solarnor® collector developed by the Institute of Physics at the University of Oslo (Oslo; N), Solarnor (Solarnor AS; Oslo; N) and Sabic IP (SABIC Innovative Plastics Holding BV; Bergen op Zoom; The Netherlands), the selection of the polymers investigated in this study was based on the assumption that water is used as heat carrier under typical northern climate conditions. This assumption was also used to define the aging exposure parameters of this study to achieve service-near and application relevant conditions. During operation, such a collector experiences low-pressure levels of 0.1 - 0.5 bar with hot water as heat carrier. Hence, accumulated for a lifetime of 20 years, the “wet load” occurs for up to 16000 h at 80 °C. When in stagnation, the water is drained back into the storage tank, and an accumulated “dry load” of up to 500 h at 140 °C in air is deduced for the collector lifetime. Due to the relatively low mechanical stress of approximately 2.5 MPa acting in service (design stress of 5 MPa assuming a safety factor of 2) (Olivares et al., 2008), no superposition of mechanical stresses and environmental effects on aging of the materials is assumed. Hence, the aging of the materials selected and investigated was carried out by exposure to water or air at the above temperatures without any simultaneous application of a mechanical stress.

Considering the above service conditions, a market study was carried out to select in total 12 potential material grades for solar absorber applications. These were initially investigated in the unaged state (Kahlen et al., 2005) and based on these results, the number of materials for this aging study was reduced to 8 (4 engineering plastics and 4 commodity plastics). The 4 engineering plastics investigated in Part 1 of this paper series include 2 amorphous plastics

(polyphenylene ether polystyrene (PPE+PS), the currently used polymer in the Solarnor® collector, and polycarbonate (PC)) and 2 semi-crystalline polymers (2 types of polyamide 12 (PA12)). For methodological and experimental reasons, it was decided to investigate the aging behavior of these materials using thin films with a thickness of approximately 500 μm, which also corresponds to the minimum wall thickness of the Solarnor® absorber.

3 EXPERIMENTAL

3.1 Materials, Specimens and Conditioning

Information as to the 4 commercially available polymers chosen for this investigation is provided in Table 1. From the two types of PA12, one grade was impact modified (PA12-HI) using a functionalized olefinic copolymer, the other was modified for improved heat resistance (PA12-HT) using a specific heat stabilizer. Regarding stabilization, PA12-HI was also stabilized but using two different stabilizers, one for the PA12 matrix the other for the impact modifier (i.e., a polyolefinic elastomer).

Table 1: Material designation, polymer type and supplier of the materials investigated. M_w designates the weight average molecular mass in the unaged state (film samples).

Material designation	Polymer type	Commercial designation	Material supplier	M_w in g/mol[1)]
PPE+PS	Polyphenylene ether polystyrene blend	Noryl EN 150SP	Sabic Innovative Plastics Holding BV (Bergen op Zoom, The Netherlands)	-
PC	Polycarbonate	Makrolon 3103	Bayer MaterialScience AG (Leverkusen, D)	30,500
PA12-HI	Polyamide 12 (impact modified)	Grilamid L25ANZ	EMS-CHEMIE AG (Domat/Ems, CH)	48,000
PA12-HT	Polyamide 12 (heat resistant)	Grilamid L25H	EMS-CHEMIE AG (Domat/Ems, CH)	57,000

[1)] see section 3.2.2

While PC films with a thickness of 480 μm were directly provided by the supplier, PPE+PS, PA12-HI and PA12-HT were supplied as granules and extruded to 500 μm films on a single screw extruder followed by a chill roll unit at Dr. Collin (Dr. Collin GmbH; Ebersberg; D). Tensile test specimens of the S2 type (DIN 53504) with an overall length and a measuring length of 75 and 40 mm, respectively, were machined from the polymer films with a puncher. The dumb-bell specimens were tested in the unaged state and in various states of aging. As to the aging conditions, specimens were either heat aged in air at 140 °C for 125, 250, 375 and 500 h (simulating collector stagnation) or exposed to water at 80 °C for 2000, 4000, 6000, 8000 and 16000 h (simulating collector operation). Both aging conditions (air and water) were carried out using an air-circulating oven (type Kendro 6000; Kendro Laboratory Products GmbH; Langenselbold; D). The specimens exposed to hot air were placed on a metal grid, the specimens exposed to hot water were placed in a water filled glass jar covered by a screw top. The distilled water was changed in intervals of 2000 h to reduce and avoid saturation effects in the water by leaching out additives. Following the aging exposure and prior to testing, the samples were stored in a climatized room (23 °C, 50 % r.h.). No re-drying was carried out for the samples exposed to hot water.

3.2 Characterization and Testing

To characterize any molecular degradation and thus chemical aging, size exclusion chromatography (SEC) was used to determine the molecular mass distribution of the materials in various stages of aging. To detect any physical aging effects by analytical means, differential scanning calorimetry (DSC) was used. Moreover, tensile tests were performed on unaged films and films aged at various conditions to obtain additional information on the effects of aging particularly also with regard to any potential performance deterioration.

3.2.1 Size Exclusion Chromatography

The data for the molecular mass distribution determined by size exclusion chromatography (SEC) were provided by the respective material suppliers. To

indicate any molecular mass changes by aging, the weight average molecular mass (M_w) was taken as relevant parameter for this study.

In the SEC analysis of the PPE+PS, the blend was separated into PPE and PS by selective solution. For the calculation of the weight average molecular mass, a PS reference sample was taken. Due to the lack of experience with extruding the PPE+PS blend, an initial decrease in weight average molecular mass of the PS fraction of 20 % for the films compared to the granulate material was obtained. Non-disclosure agreements with the supplier of this material do not allow the authors to present absolute values for M_w of PPE+PS. Hence only relative changes in weight average molecular mass values are reported for this material. The relative changes after aging are referred to the initial molecular mass values of the film material. For the PC, PA12-HI and PA12-HT films, the initial M_w values were determined to 30500 g/mol, 48000 g/mol and 57000 g/mol, respectively (see also Table 1).

3.2.2 Differential Scanning Calorimetry (DSC)

Thermal analysis was carried out using a Mettler Toledo DSC 821e instrument (type: Mettler Toledo GmbH; Schwerzenbach, CH). Samples with a mass in the range between 8 and 12 mg were put in a 40 µl pan and closed with a perforated lid. The thermograms were recorded under static air applying a heating/cooling/heating cycle at a heating/cooling rate of 10 K/min. To analyze any effects of the aging exposure, only results of the initial (1^{st}) heat-up were considered. In other words, all diagrams shown in the section on results and discussion correspond to the 1^{st} heating scan.

The degree of crystallinity (α) of PA12 was calculated based on the relationship $\alpha = \Delta H_s/\Delta H_c$, with ΔH_s and ΔH_c representing the melting enthalpy of 100 % crystalline PA12 and of the measured sample, respectively. According to literature (Metha, 1999) for ΔH_s a value of 95 J/g was assumed. The oxidation temperature T_{ox} was determined with the tangent method by determining the intercept point of the baseline and the slope to the final exothermal ascent of the DSC curve.

3.2.3 Mechanical Testing

Tensile tests were carried out at 23 °C according to ISO 527-3 using a screw driven universal testing machine (type: Instron 4505; Instron International Ltd.; High Wycombe, UK). The test speed was 10 mm/min. The dumb-bell film specimens were tested in the unaged state and in various states of aging. A digital image correlation (DIC) system (Jerabek et al., 2009; Kahlen et al., 2009b) was utilized for small strain measurement below the yield point, and a video extensometer (Kahlen et al., 2009b) for strains up to final failure.

4 RESULTS

4.1 Size Exclusion Chromatography

In Fig. 2 and Fig. 3, the relative weight average molecular mass values are plotted as a function of aging time for the investigated materials after hot air and hot water exposure, respectively. As illustrated in Fig. 2, a decrease by 40 % was obtained for the PS constituent of the PPE+PS blend after 125 h aging in air at 140 °C. According to literature (Pospisil et al., 1999; Stack et al., 2003), this decrease can be attributed to chain scission of the PS molecules. The second constituent of the PPE+PS blend, that is PPE, reveals an increase in weight average molecular mass by 12 % after 125 h and by 85 % after 250 h compared to the unaged film material indicating cross-linking. This is in agreement with results by others (Kryszewki and Jachowicz, 1982) describing cross-linking and branching reactions of PPE after aging in air below 200 °C. In turn, exposure of PPE+PS to water at 80 °C results in a decrease of the relative M_w data for both components by 12 % and 25 % for PPE and PS, respectively, after 16000 h, again indicating chemical aging by molecular degradation.

Also shown in Fig. 2 is the effect of aging on the relative weight average molecular mass of PC. After aging in air at 140 °C, no change in the M_w values was detected. Conversely, when exposed to water at 80 °C, a relative drop in M_w by 23 % was observed after 16000 h. The higher sensitivity of polycarbonate to hot water aging compared to aging in hot air is presumably due to the nature of the chain formation process via polycondensation which is prone to hydrolysis in an

hot-wet environment. This mechanism of hydrolysis is in agreement with findings by others (Factor et al., 1998; Ram et al., 1985; Edge et al., 1994). For hot air exposure, a reduction in molar mass and significant thermal degradation of PC is mainly described at temperatures above 300 °C, accompanied by extensive random chain scission and formation of methyl, ketone, biphenyl and phenol end groups (Montaudo et al., 2002; Kovarskaya et al., 1963), which also corroborates the excellent stability in hot air at 140 °C found in our study.

Regarding PA12-HI and PA12-HT an increase in weight average molecular mass was determined for hot air exposure (Fig. 3), indicating some degree of cross-linking in the initial stages of exposure to 140 °C in air (up to 125 h). While the M_w values remain constant thereafter for PA12-HT, a subsequent decrease is observed for PA12-HI. Due to the lack of detailed information as to the chemistry of the stabilizers and the elastomer modifier used, these effects perhaps reflect the superposition of competitive effects related to further crosslinking and molecular degradation. After aging in hot water, only slight changes in M_w were observed for PA12-HI, while M_w of PA12-HT steadily decreases by up to 51 % after 16000 h. At this point, the precise mechanisms causing this different behavior for these two PA12 grades are not yet clear. However, at least for PA12-HT chain scission due to hydrolysis after hot water exposure is described in the literature (Chaupart et al., 1998), thus confirming our results. By comparison, PA12-HI is perhaps better stabilized or modified towards hydrolytic stability, an assumption which was confirmed by the material supplier.

4.2 Thermo-analytical Investigations

Typical DSC thermograms of the first heating run in the unaged state and after exposure to hot air and hot water for specific times are shown for the various materials in Fig. 4 to Fig. 7. The unaged PPE+PS films in Fig. 4 exhibit a glass transition temperatures of around 159 °C corresponding to the PPE phase and an oxidation temperature of about 289 °C. After 125 h of exposure to air at 140 °C, a small endothermic peak occurs for PPE+PS around the glass transition, indicating physical aging by free volume diffusion (Wallner et al., 2004; Hutchinson, 1995). Thus, within the first 125 hour interval, physical aging takes place. However, in contrast to others reporting a dependence of both, the peak temperature and the

enthalpy of the physical aging peak on the aging time and temperature (Chartoff, 1997), no such dependence of these parameters was detected in our investigations, at least up to 500 h. By comparison, no significant physical aging was obtained for PPE+PS when exposed to hot water at 80 °C. For both aging conditions (hot air and hot water), no clear indication of chemical aging can be deduced form the DSC thermograms as it is difficult to unambiguously define an oxidation temperature. As chemical aging was found for PPE+PS by SEC (chain scission in PPE and PS and crosslinking in PPE, compare Fig. 2), it follows that the DSC technique is not useful to detect molecular degradation in this material.

Analogous DSC thermograms are shown in Fig. 5 for PC. In the unaged state, this material exhibits an endothermic peak at around 152 °C followed by an exothermic peak at around 155 °C, the first peak being attributed to the glass transition temperature (150 °C), the second to entropy relaxation related to a reorientation of molecules from the frozen state caused by cool-down after extrusion, perhaps also associated with internal stress relaxation. This interpretation is in agreement with reports by others. Under both aging conditions, the exothermic peak vanishes after 125 h (air, 140 °C) and 2000 h (water, 80 °C) indicating changes in the state of orientation and/or internal stresses (physical aging). In terms of thermal degradation, an oxidation temperature can be identified at 376°C for the unaged PC, which essentially remains unchanged after aging at both conditions. This result corroborates the findings of the molecular mass determination for aging in air at 140 °C of the previous section, but does not reflect the molecular mass change by hydrolysis when exposed to water at 80 °C (compare Fig. 2).

In Fig. 6and Fig. 7 DSC thermograms of the first heating run of PA12-HI and PA12-HT after exposure to hot air and hot water are shown. The unaged PA12-HI and PA12-HT samples exhibit a melting peak temperature of 176 °C and 177 °C and an oxidation temperature of 257 °C and 280 °C, respectively. Furthermore, crystallinity values of 52 % and of 49 % were obtained for the unaged PA12-HI and PA12-HT.

In the unaged DSC traces of PA12-HI and PA12-HT samples, a small exotherm just before the melting peak appears, indicating some tendency for post- or re-crystallization. This phenomenon is a consequence of the high cooling rates during

film extrusion with chill-roll units where super-cooling occurs, leading to a frozen-in non-equilibrium crystalline morphology. During the DSC heating scan, post- or re-crystallization occurs before entering into the main melting peak. After aging in hot air the exotherm vanishes for PA12-HI and PA12-HT and aging induced post- or re-crystallization indicated by the secondary endothermic melting peak approximately 10 to 20 K above the aging temperature and below the main melting peak occurs. These secondary endothermic peaks presumably are related to the development of small instable crystals (Frick and Stern, 2004). Depending on the exposure time, the peak is moved towards higher temperatures approaching the main melting peak. Due to the lower exposure temperature, after aging in hot water this effect is not as pronounced as in air and even vanishes. The degree of crystallinity increases after 500 h of hot air treatment by 14 % and 16 % from 52 % and 49 % for PA12-HI and PA12-HT, respectively. The strongest increase in crystallinity was already found after 125 h. In accordance with the literature (Forsström and Terselius, 2000), a rapid increase in the degree of crystallinity during initial aging in hot air was also observed for polyamide 6, followed by a slower increase at longer exposure times.

Similar trends were observed after hot water treatment. After 2000 h of hot water exposure the crystallinity increases by 8 % and 14 % from 52 % and 49 % for PA12-HI and PA12-HT, respectively. After 16000 h an increase by 9 % and 17 % for PA12-HI and PA12-HT was detected. For PA12-HT slight chain scission was determined after hot water aging probably also enhancing the tendency for an increase in crystallinity.

For both PA12 grades pronounced oxidation exotherms were obtained above the melting peak. While the onset of oxidation is slightly reduced for PA12-HI after aging in hot air, no reduction in oxidation temperature was found for PA12-HT. This reflects the more effective stabilization of PA12-HT towards elevated temperature exposure, for which it was specifically developed and modified. On the other hand, hot water treatment causes a significant decrease of oxidation temperature of PA12-HI after 16000 h. In contrast, no decrease in oxidation temperature was found for PA12-HT after hot water aging. While these results were somewhat surprising when comparing the findings on M_w in Fig. 3, they can

perhaps be rationalized by assuming leaching of one or both stabilizers used in PA12-HI and the enhanced tendency for oxidation of the polyolefinic and/or the PA12 constituent, the former even being absent in PA12-HT. To summarize, based on the DSC investigations, physical aging by post- or re-crystallization occurs for both PA12 systems investigated when exposed to air at 140 °C. For water exposure at 80 °C, for PA12-HI a drop in the oxidation temperatures was observed, while no such effect was found for PA12-HT.

4.3 Mechanical Investigations

Typical stress-strain curves from tensile tests of the unaged and the fully aged specimens for both, hot air and hot water exposure are shown in Fig. 8 and Fig. 9. The mechanical properties of specific interest such as modulus, yield stress and strain-to-break are listed in Table 2.

Table 2: Characteristic mechanical properties in the unaged and fully aged condition (air at 140 °C for 500 h and water at 80 °C for 16000 h) for PPE+PS, PC, PA12-HI and PA12-HT.

Polymer	**Modulus** in MPa	**Yield stress** in MPa	**Strain-to-break** in %
PPS+PE			
unaged	1960 ± 60	46 ± 1	73 ± 12
air (500 h, 140 °C)	2050 ± 11	(49 ± 1)*	4 ± 1
water (16000 h, 80 °C)	0	47 ± 1	9 ± 5
	2040 ± 90		
PC			
unaged	2340 ± 80	56 ± 1	105 ± 2
air (500 h, 140 °C)	1560 ± 30	66 ± 1	11 ± 8
water (16000 h, 80 °C)	2390 ± 12	68 ± 2	22 ± 14
	0		
PA12-HI			
unaged	810 ± 70	24 ± 1	376 ± 8
air (500 h, 140 °C)	780 ± 110	27 ± 3	376 ± 48
water (16000 h, 80 °C)	830 ± 20	28 ± 1	347 ± 67
PA12-HT			
unaged	1190 ± 11	38 ± 1	310 ± 19
air (500 h, 140 °C)	0	40 ± 1	261 ± 21
water (16000 h, 80 °C)	1390 ± 30	42 ± 3	164 ± 179
	1090 ± 19		

*) Ultimate failure just below reaching the yield stress.

Analyzing the mechanical properties of PPE+PS, the modulus and the yield stress remain essentially unaffected by the aging procedure, implying that any physical

aging as detected by the DSC measurements turns out to be insignificant in terms of mechanical product performance. However, the strong drop in strain-to-break from 73 % to below 5 % for hot air and hot water aging, indicates massive chemical aging for both aging conditions and corroborates the findings on M_w described earlier. Moreover, these results are in good agreement on investigations published before on neat PPE (Kahlen et al., 2005).

In the case of PC modulus values remain unchanged by hot water aging at 80 °C but are strongly affected by air aging at 140 °C. For both fully aged conditions yield stress values increase whereas strain-to-break values significantly decrease (in both cases more so for aging in water at 80 °C). While the effects of hot water aging on the mechanical properties reflect the phenomena of both physical and chemical aging as described before based on the results of the M_w determination and by DSC, the effects found for aging in air on mechanical properties are somewhat unexpected, particularly since no chemical aging could be deduced based on the M_w measurements. At this point, reference is made to Fig. 10 on the effects of various aging times on relative strain-to-break values, to be discussed later.

For PA12-HI, where both chemical and physical aging mechanisms were deduced from the analytical investigations, surprisingly no significant effects of the aging conditions on the mechanical properties were detected. For example, modulus, yield stress and strain-to-break remain unchanged despite the fact that M_w values first increase and then decrease with aging time (compare Fig. 3). Thus, it may well be that these changes occur either in the plateau region of the dependence of mechanical properties on molecular mass, or the various physical (post- or re-crystallization) and chemical aging effects (crosslinking, molecular degradation) outbalance one another.

As somewhat different behavior was found for PA12-HT, which compared to PA12-HI exhibits significantly higher values for modulus (1190 vs. 810 MPa) and yield stress (38 vs. 24 MPa) and somewhat lower values for strain-to-break (310 vs. 376 %) in the unaged reference state due to the lack of the elastomeric impact modifier. Both, aging in hot air and in hot water result in an increase in modulus and yield stress, although to various degrees, which correlate with the previously

described effects on post- and re-crystallization (compare Fig. 5) accompanied by an increase in crystallinity. The increase in crystallinity due to aging in air at 140 °C, which is also accompanied by chemical crosslinking (compare Fig. 3), may also help to explain the somewhat reduced strain-to-break of 260 % compared to the value of the unaged reference state of 310 %. Conversely, the strong decrease of the strain-to-break values from 310 % to 5 % by aging in water at 80 °C for 16000 h, clearly reflects the decrease in M_w due to chemical aging (compare Fig. 3).

Finally, the development of the various aging phenomena as a function of exposure time to the aging conditions is shown in terms of relative strain-to-break values (defined as the ratio of strain-to-break values in the aged and the unaged reference state in %) in Fig. 10 and Fig. 11. As shown in Fig. 10, for PPE+PS dramatic reductions in strain-to-break are observed after 125 h and 2000 h of exposure to hot air (140 °C) and hot water (80 °C), respectively, indicative of significant molecular degradation. Similar reductions of strain-to-break values were found for PC after 125 h hot air exposure and 4000 h hot water exposure. While the effect of hot water agrees with the reduction in M_w shown in Fig. 2, the pronounced effect of hot air aging on relative strain-to-break values still remains unclear in light of the apparently unchanged molecular mass. Interestingly, the relative strain-to-break values tend to increase again after 125 h in hot air, although there is a rather high scatter in the data. This strong and varying tendency of embrittlement with exposure time needs further investigations to be understood in terms of the precise nature of the physical and chemical aging mechanisms.

Analogously, the effects of aging time on relative strain-to-break values are depicted for both PA12 types in Fig. 11. Although physical and chemical aging has been determined by analytical means for both materials under both aging conditions (compare Fig. 3 and Fig. 6), in terms of mechanical properties both materials are rather stable to hot air exposure and PA12-HI also to hot water exposure. As explained above, this may be due to competing effects of physical and chemical aging, which outbalance each other. Merely, aging exposure of PA12-HT to hot water exhibits a significant drop in relative strain-to-break values

right from the beginning with total embrittlement after 8000 h. This again reflects the significant drop in M_w of PA12-HT when exposed to hot water.

5 SUMMARY AND CONCLUSIONS

The degradation behavior of 4 engineering plastics including 2 amorphous (PPE+PS and PC) and 2 semi-crystalline (PA12-HI and PA12-HT) plastic grades for solar thermal applications was investigated. According to northern climate conditions and based on the experiences with the Solarnor® collector (Meir and Rekstad, 2003), hot air exposure at 140 °C up to 500 h and hot water exposure at 80 °C up to 16000 h were chosen as aging conditions.

To characterize the aging behavior, analytical techniques (DSC and SEC) and tensile testing were applied. While DSC measurements provided information on physical aging phenomena, SEC was used to detect chemical degradation processes. Tensile tests were carried out to evaluate any performance changes as a result of aging, and were interpreted in terms of physical and chemical aging mechanisms.

To detect physical aging effects, DSC measurements and mechanical properties in the pre- and yield-regime (modulus and yield stress) turned out to be the most sensitive parameters. While for the amorphous plastics, physical aging was related to enthalpy relaxation around the glass transition, for the semi-crystalline plastics mainly post- and/or re-crystallization in some instances associated with an increase in crystallinity were found to be main mechanisms. To detect chemical aging (molecular degradation and crosslinking), average molecular mass results and strain-to-break values proved to be the most appropriate parameters.

Among the investigated materials, the most significant chemical degradation was obtained for PPE+PS after aging in hot air and in hot water, indicated by massive reductions in M_w and strain-to-break. For PC, hot water and hot air aging led to physical and/or chemical aging as indicated by DSC and mechanical properties, although for hot air exposure, M_w measurements did not provide any indication for chemical aging. While the strong scatter in strain-to-break values in the embrittled state after hot air aging is perhaps a sign of inhomogeneous local aging, further

investigations need to be carried out to substantiate this hypothesis. Compared to PPE+PS and PC, in terms of aging, hot water exposure was more severe for both PA12 types and also turned out to be more detrimental than hot air aging. For PA12-HT the aging detected by analytical techniques (DSC and SEC) also resulted in a reduction in the ultimate mechanical performance (strain-to-break). Conversely, while both, physical and chemical aging were clearly found via the analytical tests no influence on strain-to-break were observed, most likely as a result of outbalancing effects by various physical (post- and re-crystallization) and chemical aging mechanisms (crosslinking, molecular degradation).

From the materials investigated, PA12-HI appears to be the most promising candidate for an application as a black absorber material for solar thermal collectors in northern climates. The use of PPE+PS for this purpose should be evaluated once more making sure that the film extrusion process of PPE+PS does not cause any significant chemical aging in the processing step.

Acknowledgments

The research work of this paper was performed within the project S. 11 “Aging of polymers in solar-thermal applications” at the Polymer Competence Center Leoben GmbH within the framework of the K_{plus} Program of the Austrian Ministry of Traffic, Innovation and Technology with contributions by the University of Leoben, Graz University of Technology, Johannes Kepler University Linz, JOANNEUM RESEARCH ForschungsgmbH and Upper Austrian Research GmbH. The PCCL is funded by the Austrian Government and the State Governments of Styria and Upper Austria.

Literature

Chartoff, R.P., 1997. Thermoplastic Polymers. In: Turi, E.A. (Ed.), Thermal Characterization of Polymeric Materials, p.548.

Chaupart, N., Serpe, G., Verdu, J., 1998. Molecular weight distribution and mass changes during polyamide hydrolysis. Polymer 39 (6-7), 1375-1380.

Davidson, J.H., Mantell, S.C., Jorgensen, G., 2002. Advances in Solar Energy, vol. 15. American Solar Energy Society, Boulder, CO, pp 149-186.

DIN 53504 (1994). Testing of rubber; determination of tensile strength at break, tensile stress at yield, elongation at break and stress values in a tensile test.

Edge, M., Allen, N.S., He, J.H., Derham M., 1994. Physical aspects of the thermal and hydrolytic ageing of polyester, polysulphone and polycarbonate films. Polym. Degrad. Stab. 44, 193-200.

Ehrenstein, G.W., private communications 2008.

Factor, A., 1995. Mechanisms of thermal and photodegradations of Bisphenol A Polycarbonate. In Clough, R.L., Billingham, N., Gillen, K. (Eds.), Polymer durability: Degradation, stabilization and lifetime prediction, American Chemical Society, Washington, DC, pp. 59-76.

Freeman, A., Mantell, S.C., Davidson, J.H., 2005. Mechanical performance of polysulfone, polybutylene, and polyamide 6/6 in hot chlorinated water. Sol. Energy 79, 624-637.

Forsström, D., Terselius, B., 2000. Thermo oxidative stability of polyamide 6 films I. Mechanical and chemical characterization. Polym. Degrad. Stab. 67, 69-78.

Frick, A., Stern, Cl., 2004. Qualitätssicherung von Kunststoffformteilen mittels DSC Teil 2: Fertigungskontrolle. Thermal Analysis Information for Users (UserCom) 2, 9-12.

Ho, C.H., Vu-Khanh, T., 2003. Effects of time and temperature on physical aging of polycarbonate. Theor. App.l Fract. Mec. 39, 107-116.

Hutchinson, J.M., 1995. Physical aging of polymers. Prog. Polym. Sci. 20, 703-760.

ISO 527-3 (2005). Plastics - Determination of tensile properties - Part 3: Test conditions for films and sheets.

ISO 10463-1:2001/DAM 1:2008. Plastics - Symbols and abbreviated terms - Part 1: Basic polymers and their special characteristics - Amendment 1; German version EN ISO 1043-1:2001/prA1: 2008.

Kahlen, S., Jerabek, M., Steinberger, R., Wallner, G.M., Lang, R.W., 2009. Characterization of Physical and Chemical Aging of Polymeric Solar Materials by Advanced Mechanical Testing. To be submitted in Polym. Test.

Kahlen, S., Wallner, G.M., Fischer, J., Meir, M.G., Rekstad, J., 2005. In: Židonis, V., Lapinskienė, A. (Eds.), Proceedings of NorthSun 2005, Vilinius, Lithuania, pp. 32-40.

Kicker, H., 2009. Comparative life cycle assessment of solar thermal collectors. Bachelor Thesis. April, 2009. Institute of Materials Science and Testing of Plastics. University of Leoben, Austria.

Kovarskaya, B.M., Akutin, M.S., Sindev, A.I., Yazvikova, M.P., Neiman, M.B., 1963. Thermal-oxidative degradation of a polycarbonate. Polym. Sci. USSR 5, 649-654.

Kryszewski, M., Jachowicz, J., 1982. Thermal Degradation of poly(phenylene oxides). In: Grassi, N. (Ed.), Developments in polymer degradation, vol. 4. Applied Science Publishers, London, pp. 1-25.

Kuzovleva, O.Y.E., Kabal'nova, L.Y.U., Yarysheva, L.M., Ashkinadze, L.D., Vinogradov, A.M., Ped', A.A., Kozlov, P.V., 1988. Ageing of polyamide film materials in response to the combined action of environmental factors-raised temperatures and moist air. Polym. Sci. USSR 30 (1), 60-66.

Meir, M.G., Rekstad, J., 2003. Der Solarnor® Kunststoffkollektor - the development of a polymer collector with glazing. In: Wallner, G.M, Lang, R.W.

(Eds.), Proceeedings of 1st Leobener Symposium Polymeric Solar Materials, pp. II-1-II-8.

Meir, M., Buchinger, J., Kahlen, S., Köhl, M., Papillon, P., Rekstad, J., Wallner, G., 2008. Polymeric solar collectors – state of the art. In Fernandes, E.O. (Ed.), Proceedings of the EuroSun 2008, Lisbon, Portugal, N° 409, pp. 1-10.

Metha, R.H., 1999. Physical constants of various polyamides: polyamide 6, polyamide 66, polyamide 610, polyamide 12. In Brandrup, J., Immergut, E.H., Grulke, E.A. (Eds.), Polymer handbook, 4th ed., John Wiley & Sons, Inc., New York, pp. 121-33.Olivares, A., Rekstad, J., Meir, M., Kahlen, S., Wallner, G., 2008. A test procedure for extruded polymeric solar thermal absorbers. Sol. Energy 92(4), 445-452.

Montaudo, G., Carroccio, S., Pulgisi, C., 2002. Thermal and thermoxidative degradation processes in poly(bisphenol a carbonate). J. Anal. Appl. Pyrolysis 64, 229-247.

Olivares, A., Rekstad, J., Meir, M., Kahlen, S., Wallner, G., 2008. A test procedure for extruded polymeric solar thermal absorbers. Sol. Energy Mater. Sol. Cells 92, 445-452.

Plastics Europe, 2007a. The compelling facts about plastics 2007. An analysis of plastics production, demand and recovery for 2007 in Europe. http://www.plasticseurope.org.

Plastics Europe, 2007b. Business Data and Charts 2007. Market Research Group (PEMRG). www.plasticseurope.org.

Posipisil, J., Horak, Z., Krulis, Z., Nespurek, S., Kuroda, S., 1999.

Degradation and aging of polymer blends I. Thermomechanical and thermal degradation. Polym. Degrad. Stab. 65 (3), 405-414.

Ram, A., Zilber, O., Kenig, S., 1985. Life expectation of Polycarbonate. Polym. Eng. Sci. 25 (9), 535-540.

Resch, K., Wallner, G.M., Lang, R.W., 2009. Thermotropic layers for flat-plate collectors – A review of various concepts for overheating protection with polymeric materials. Sol. Energy Mater. Sol. Cells 93 (1), 119-128.

Serpe, G., Chaupart, N., Verdu, J., 1997. Ageing of polyamide 11 in acid solutions. Polymer 38 (8), 1911-1917.

Stack, S., O`Donoghue, O., Birkinshaw, C., 2003. The thermal stability and thermal degradation of blends of syndiotactic polystyrene and polyphenylene ether. Polym. Degrad. Stab. 79, 29-36.

Wallner, G.M., Weigl, C., Leitgeb, R., Lang, R.W., 2004. Polymer films for solar energy applications-thermoanalytical and mechanical characterisation of ageing behaviour. Polym. Degrad. Stab. 85 (3), 1065-1070.

Wallner, G.M., Lang, R.W., 2005. Guest editorial. Sol. Energy 79 (6), 571-572.

Wallner, G.M., Lang, R.W., 2006. Kunststoffe-Neue Möglichkeiten in der Solarthermie. Erneuerbare Energie 2-2006, AEE-Intec, Austria.

Weiss, W., 2003. Solar Heating Systems for Houses. Wiley, New York, pp. 6-9.

Wallner, G.M., 2007. Positionspapier für ein österreichisches Solarforschungs- und Technologieprogramm, ASTTP Österreichische Solarthermie Technologie Plattform, Gleisdorf, A.

Weiss, W., Brunner, C., Fechner, H., Fink, C., Gottwald, D., Guggenberger, W., Hochreiter, E., Holter, C., Huemer, H., Jähnig, D., Lang, R.W., Podesser, E., Rabensteiner, G., Schnitzer, H., Slawitsch, B., Streicher, W., Steinmaurer, G.,

Wu, C, Mantell, S.C, Davidson, J.H, 2004. Long-term Performance of PB and Nylon 6,6 Tubing in Hot Water. J. Sol. Energy Eng. 126 (1), 581-586.

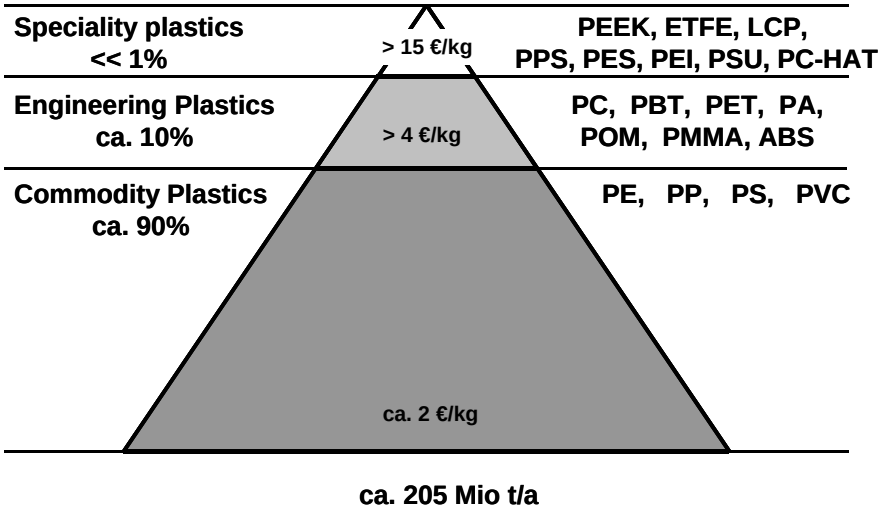

Fig. 1: Material pyramid for plastics; status September 2008 (Plastics Europe, 2008).

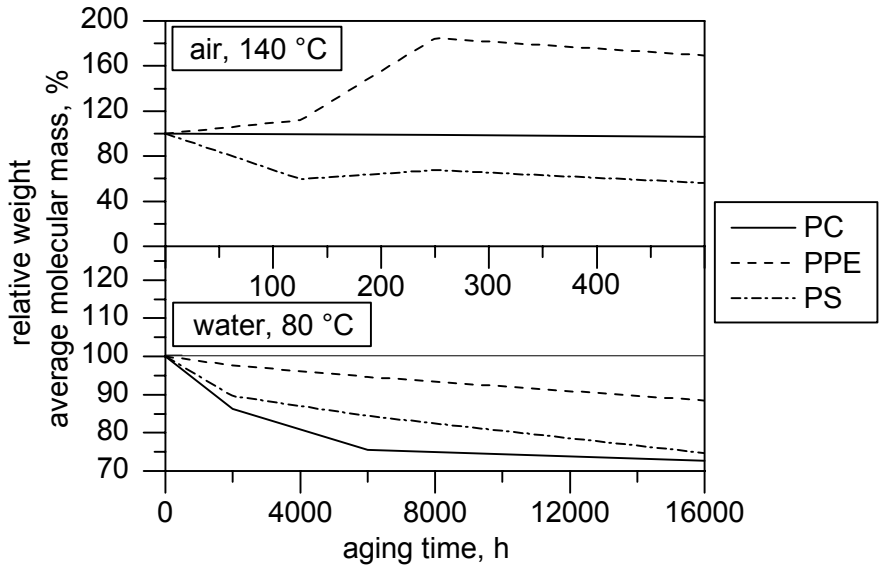

Fig. 2: Weight average molecular mass versus aging time in air at 140 °C and in water at 80 °C, respectively, for PPE+PS and PC.

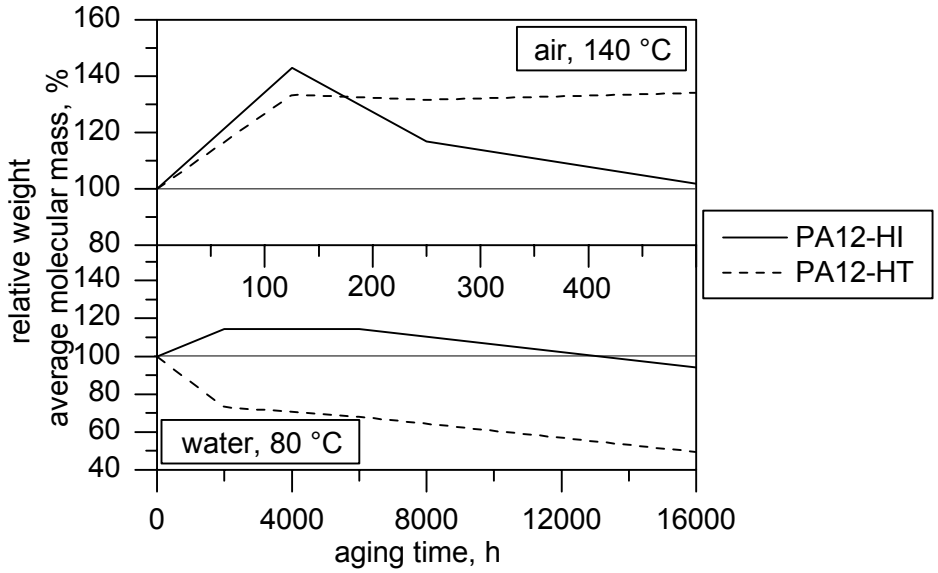

Fig. 3: Weight average molecular mass versus aging time in air at 140 °C and in water at 80 °C, respectively, for PA12-HI and PA12-HT.

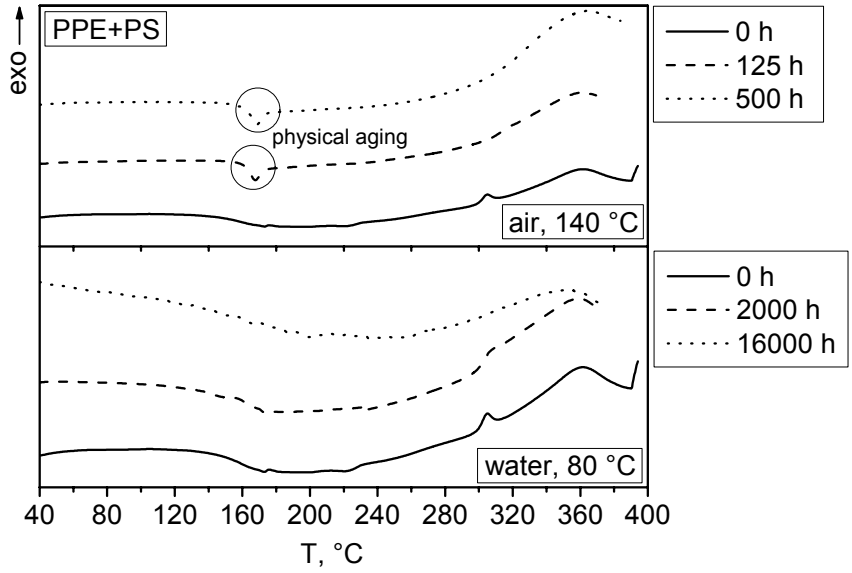

Fig. 4: DSC thermograms of PPE+PS films exposed to air at 140 °C (0, 125 and 500 h) and to water at 80 °C (0, 2000 and 16000 h).

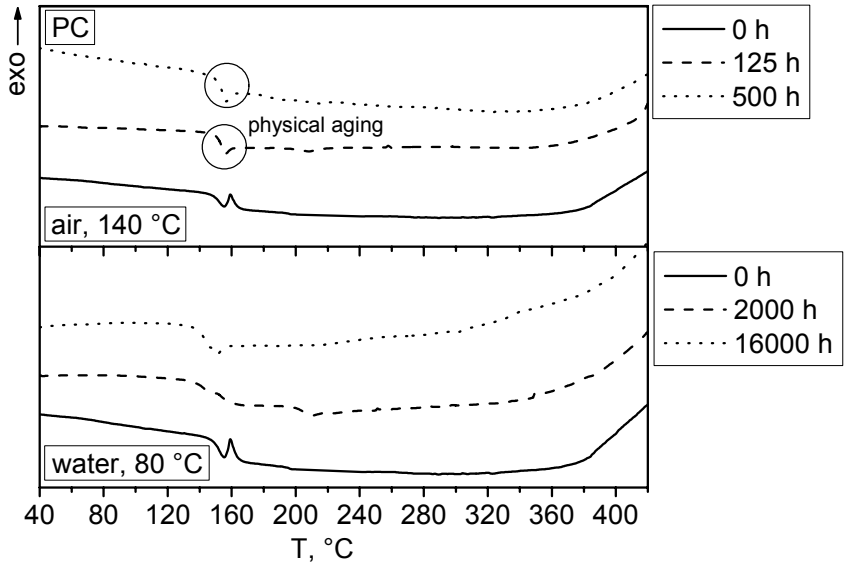

Fig. 5: DSC thermograms of PC films exposed to air at 140 °C (0, 125 and 500 h) and to water at 80 °C (0, 2000 and 16000 h).

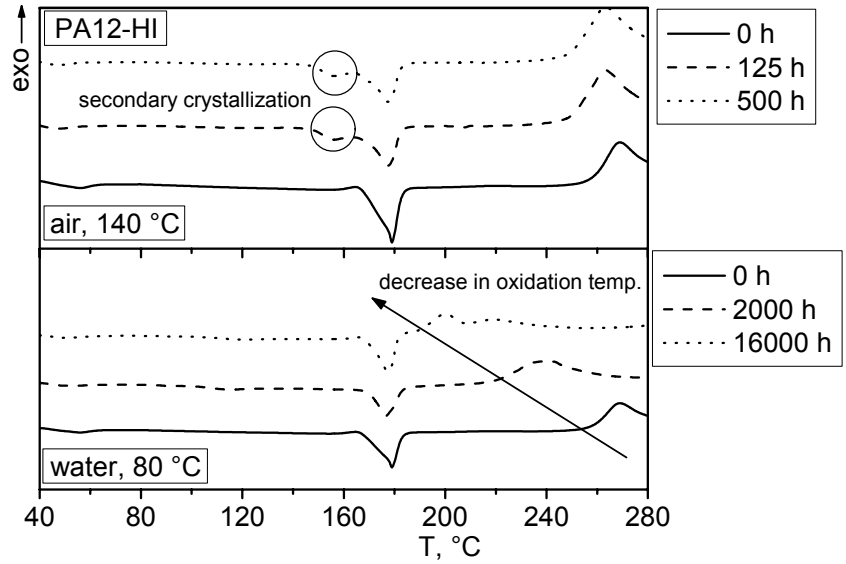

Fig. 6: DSC thermograms of PA12-HI films exposed to air at 140 °C (0, 125 and 500 h) and to water at 80 °C (0, 2000 and 16000 h).

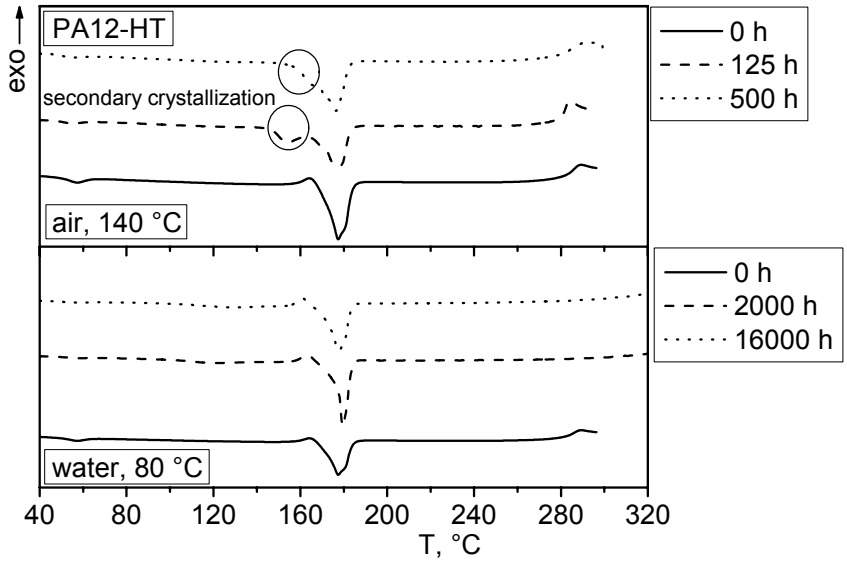

Fig. 7: DSC thermograms of PA12-HT films exposed to air at 140 °C (0, 125 and 500 h) and to water at 80 °C (0, 2000 and 16000 h).

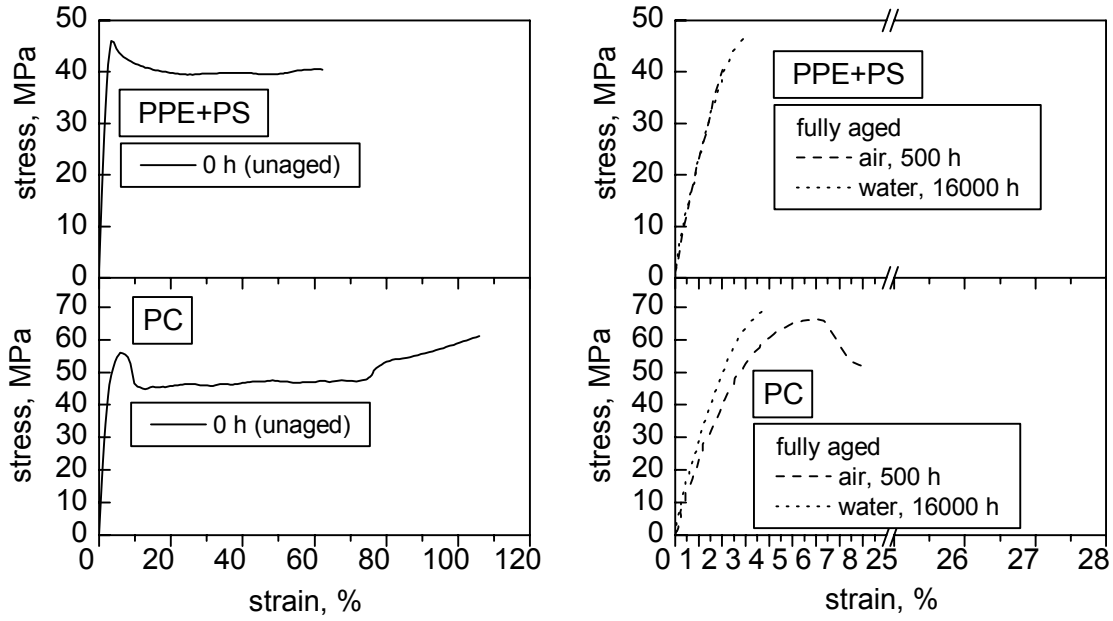

Fig. 8: Stress-strain curves for PPE+PS and PC comparing the behavior of the unaged reference state (0 h) and the fully aged state (500 h in air at 140 °C and 16000 h in water at 80 °C).

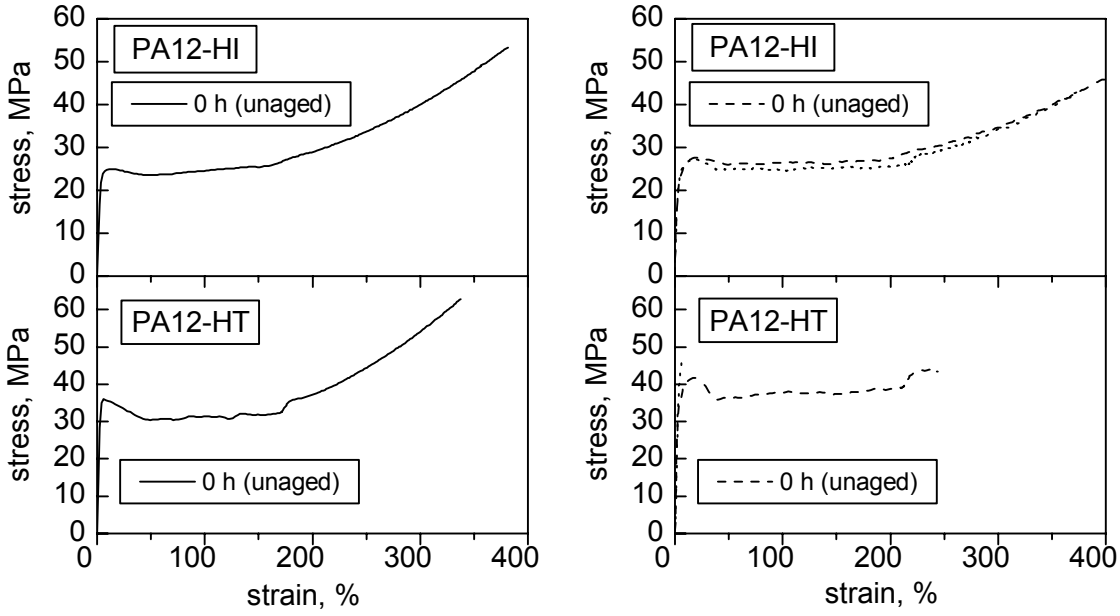

Fig. 9: Stress-strain curves for PA12-HI and PA12-HT comparing the behavior of the unaged reference state (0 h) and the fully aged state (500 h in air at 140 °C and 16000 h in water at 80 °C).

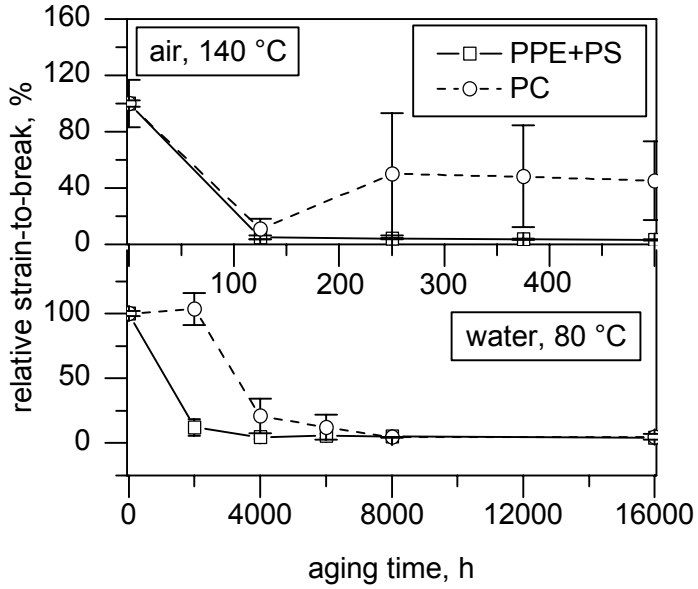

Fig. 10: Relative strain-to-break versus aging time in air at 140 °C and in water at 80 °C, respectively, for PPE+PS and PC.

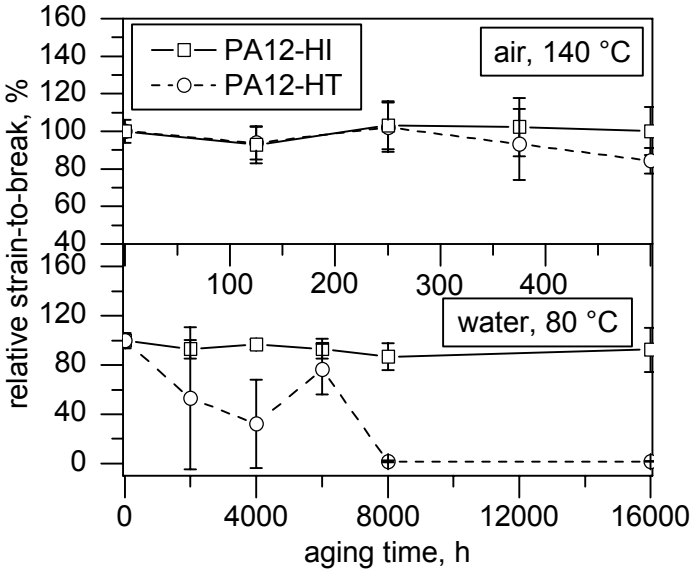

Fig. 11: Relative strain-to-break versus aging time in air at 140 °C and in water at 80 °C, respectively, for PA12-HI and PA12-HT.

PAPER 3°

Aging Behavior of Polymeric Solar Absorber Materials – Part 2: Commodity Plastics

S. Kahlen[a)*], G. M. Wallner[b)], R. W. Lang[b)]

[a)] Polymer Competence Center Leoben GmbH, Roseggerstrasse 12, Leoben, 8700, Austria

[b)] Institute of Materials Science and Testing of Plastics, University of Leoben, Franz-Josef Strasse 18, Leoben, 8700, Austria

ABSTRACT

In this series of two papers, various polymeric materials are investigated as to their potential applicability as absorber materials for solar thermal collectors. While Part 1 of this paper series deals with the aging behavior of engineering plastics, including two amorphous polymers (PPE+PS) and (PC) and two semi-crystalline polymers (2 types of PA12), the present Part 2 treats the aging behavior of semi-crystalline so-called “commodity” plastics (two types of crosslinked polyethylene (PE-X) and two types of polypropylene (PP)). As in Part 1, the focus of the investigation is to study the aging behavior of these materials under maximum operating conditions (80 °C in water up to 16000 h) and stagnation conditions (140 °C in air up to 500 h) typical for northern climate. The materials supplied or produced as polymer films were first characterized in the unaged state and then for different states of aging by differential scanning calorimetry (DSC), by size exclusion chromatography (SEC) and by mechanical tensile tests. DSC was applied primarily to obtain information on physical aging phenomena, whereas SEC analysis was used to characterize chemical degradation of the materials. In addition, physical and chemical aging were both analyzed via the small and large

---

° To be submitted in “Solar Energy”.

* Corresponding author. Tel.: +43 (0) 3842 42962 50

Email address: kahlen@pccl.at

strain mechanical behavior. Comparing the two aging conditions in hot air and hot water, a rather stable mechanical performance profile was found for both PP types over the investigated aging time, which was interpreted in terms of competing physical and chemical aging mechanisms. Analogously such competing mechanisms were also inferred for one of the PE-X materials, while the other exhibited substantial degradation in terms of strain-to-break values for both aging conditions. In principle, both PP and PE-X are promising candidates for black absorber applications in northern climates if proper measures against overheating are taken and when adequately modified.

Keywords: commodity polymers, solar thermal application, physical and chemical aging.

1 INTRODUCTION

While plastics offer an extraordinary potential for the use in solar thermal systems in general (Lang, 1995; Wallner and Lang, 2005; Wallner and Lang, 2006), their application in thermal collectors and particularly as absorber material is still rather limited (part 1). Part 1 of this paper briefly analyzes the situation in terms of the wide variety of existing polymeric material classes, and also describes the current state of technology of glazed plastics collectors. Nevertheless, despite the fact that plastics are already in use even for use in solar absorbers, the information as to the aging and degradation behavior of these materials under typical application conditions is still rather scarce. Hence, to ensure the proper performance of plastics already in use or to select novel grades of high potential for use, more knowledge on aging and degradation of these materials under all service conditions is clearly needed. While Part 1 of this paper series dealt with this subject by investigating various types of engineering plastics including a blend of polyphenylene ether polystyrene (PPE+PS), polycarbonate (PC) and two grades of polyamide 12 (PA12) (part 1 paper), this paper investigates the aging behavior of so-called “commodity” plastics including two types of crosslinked polyethylene (PE-X) and two types of polypropylene (PP).

The aging conditions defined for this study are based on the assumption that water is used as heat carrier under typical northern climate conditions and on experience with the Solarnor® collector (Meir and Rekstad, 2003), an all-polymeric collector developed by the Institute of Physics at the University of Oslo (Oslo; N), Solarnor (Solarnor AS; Oslo; N) and Sabic IP (SABIC Innovative Plastics Holding BV; Bergen op Zoom; The Netherlands). During operation, such a collector experiences low-pressure levels of 0.1 - 0.5 bar with hot water as heat carrier. Hence, accumulated for a lifetime of 20 years, the "wet load" occurs for up to 16000 h at 80 °C. When in stagnation, the water is drained back into the storage tank, and an accumulated "dry load" of up to 500 h at 140 °C in air is deduced for the collector lifetime. Due to the relatively low mechanical stress of approximately 2.5 MPa acting in service (design stress of 5 MPa assuming a safety factor of 2) (Olivares et al., 2008), no superposition of mechanical stresses and environmental effects on aging of the materials is assumed. Hence, the aging of the materials selected and investigated as part of the present study was carried out by exposure to water or air at the above temperatures without any simultaneous application of a mechanical stress.

In general, polyolefins such as PE-X and PP are rather insensitive to water exposure, at least when the temperature and the acting pressure are low. However, thermo-oxidative material degradation is usually observed under the combined influence of elevated temperatures and oxygen, the latter being of course present in air but also in water. As to the aging mechanisms and the course of material degradation, at least two stages must be discerned (see Fig. 1*; see also Zweifel, 2001). The duration of stage one, referred to as induction period, is controlled by the stabilizer type and content (or by the stabilizer system consisting of various thermo- and photo-active stabilizers). During this stage, the performance properties remain rather stable. Stage two is characterized by fast oxygen uptake and degradation of the polymeric material, leading to a rapid deterioration of performance properties. Superimposed to the various chemical degradation mechanisms (i.e., chemical aging) also physical aging (e.g., post-

* All figures of this paper are collected at the end of the text.

and/or re-crystallization, free volume change) may occur in polyolefins when exposed to elevated temperatures for prolonged times.

For methodological and experimental reasons, it was decided to investigate the aging behavior of the selected materials using thin films with a thickness of approximately 500 μm. This thickness also corresponds to the minimum wall thickness of the Solarnor® absorber. Analogous to Part 1 (Kahlen et al., 2009a), size exclusion chromatography (SEC) was used to determine the molecular mass distribution of the materials in various stages of aging and to characterize any molecular degradation and thus chemical aging. Moreover, to detect chemical and in particular any physical aging, differential scanning calorimetry (DSC) was applied. Furthermore, tensile tests were performed on unaged films and films aged at various conditions to obtain additional information on the effects of aging but particularly also with regard to any potential performance deterioration.

2 EXPERIMENTAL

2.1 Materials, Specimens and Conditioning

Table 1 provides information as to the 4 commercially available polymers chosen for this investigation. Both types of PE-X are silane-crosslinked, one was delivered in the crosslinked state, the other was delivered as uncrosslinked material and was crosslinked in our laboratory (see below). Moreover, both PE-X types are stabilized for the potential/intended application as solar absorbers. However, no information as to the stabilizer system and content used is available.

The two PP types are of the random copolymer type one being unnucleated and therefore crystallizes in the α-form, the other being β-nucleated. In the β-nucleated form PP usually exhibits enhanced toughness, higher drawability and better resistance against high stress levels at elevated temperatures, but at the cost of lower modulus and yield stress values. According to information by the material supplier, both PP types are stabilized with an identical stabilizer system consisting of a combination of phenolic and phosphitic antioxidants, with PP-2 containing a higher concentration of the stabilizer system.

Table 1: Material designation, polymer type and supplier of the materials investigated. M_w designates the weight average molecular mass in the unaged state (film samples).

Material designation	Polymer type	Commercial designation	Material supplier	M_w in g/mol[1)]
PE-X1	Silane-crosslinked polyethylene	Taborex	Silon International GmbH (Düsseldorf, D)	-
PE-X2	Silane-crosslinked polyethylene	Polidan T/A-HF	Solvay Padanaplast S.P.A. (Parma, IT)	-
PP-1	Polypropylene random copolymer	RA130E-8427[2)]	Borealis Polyolefine GmbH (Linz, A)	1.260,000
PP-2	Polypropylene random copolymer	Beta-PPR RA7050[3)]	Borealis Polyolefine GmbH (Linz, A)	1.170,000

[1)] see section 2.2.1

[2)] stabilized with phenolic antioxidants.

[3)] stabilized with phenolic antioxidants; containing 90 % ß-crystalline phase and 10 % α-crystalline phase (see section 2.2.2).

While PE-X1 films with a thickness of about 480 μm were directly provided by the supplier, PE-X2, PP-1 and PP-2 were supplied as granules and extruded to 500 μm films on a single screw extruder followed by a chill roll unit at Dr. Collin (Dr. Collin GmbH; Ebersberg; D). After the extrusion, the PE-X2 films were stored in distilled water at 60 °C for 10 h for crosslinking. Tensile test specimens of the S2 type (DIN 53504) with an overall length and a measuring length of 75 and 40 mm, respectively, were machined from the polymer films with a puncher. The dumbbell specimens were tested in the unaged state and in various states of aging. As to the aging conditions, specimens were either heat aged in air at 140 °C for 125, 250, 375 and 500 h or exposed to water at 80 °C for 2000, 4000, 6000, 8000 and 16000 h. Both aging conditions (air and water) were carried out using an air-circulating oven (type Kendro 6000; Kendro Laboratory Products GmbH; Langenselbold; D). The specimens exposed to hot air were placed on a metal grid, the specimens exposed to hot water were placed in a water filled glass jar covered by a screw top. The distilled water was changed in intervals of 2000 h to reduce and avoid saturation effects in the water by leaching out additives. Following the aging exposure and prior to testing, the samples were stored in a

climatized room (23 °C, 50 % r.h.). No re-drying was carried out for the samples exposed to hot water.

2.2 Characterization and Testing

To characterize any molecular degradation and thus chemical aging, size exclusion chromatography (SEC) was used to determine the molecular mass distribution of the materials in various stages of aging. To detect any physical aging effects by analytical means, differential scanning calorimetry (DSC) was used. Moreover, tensile tests were performed on unaged films and films aged at various conditions to obtain additional information on the effects of aging particularly also with regard to any potential performance deterioration.

2.2.1 Size Exclusion Chromatography

For the two PP compounds, the molecular mass distribution was characterized in the unaged state and for various stages of aging by size exclusion chromatography (SEC). The experiments were performed in the laboratory of the company supplying the materials. Initial weight average molecular mass (M_w) values of PP-1 and PP-2 films are 1.260,000 g/mol and 1.170,000 g/mol, respectively. The change in weight average molecular mass was chosen to indicate any chemical degradation effects.

For the crosslinked materials PE-X1 and PE-X2, no SEC analysis was performed.

2.2.2 Differential Scanning Calorimetry (DSC)

Thermal analysis was carried out using a Mettler Toledo DSC 821e instrument (type: Mettler Toledo GmbH; Schwerzenbach, CH). Samples with a mass in the range between 8 and 12 mg were put in a 40 µl pan and closed with a perforated lid. The thermograms were recorded under static air applying a heating/cooling/heating cycle at a heating/cooling rate of 10 K/min. To analyze any effects of the aging exposure, only results of the initial (1^{st}) heat-up were considered. In other words, all diagrams shown in the section on results and discussion correspond to the 1^{st} heating scan. For each aging condition, up to 5 samples were tested and the characteristic values deduced are reported as mean values with standard deviations.

The degree of crystallinity for the PE-X materials and the α-crystallized PP-1 was calculated based on the relationship $\alpha = \Delta H_s/\Delta H_c$, ΔH_s and ΔH_c representing the melting enthalpy of the 100 % crystalline polymer and of the measured sample, respectively. According to ATHAS database (1994) and Varga and Ehrenstein (1999), values of 293 J/g and 148 J/g, respectively, were assumed for ΔH_c of PE-X and PP-1. While PP-1 crystallizes nearly exclusively in the α-form, PP-2 also contains β-crystals amounting to about 10 % of the crystalline phase. Thus, for PP-2 only the position of the two endothermic peaks associated with the α- and β-crystalline phase at around 132 °C and 143 °C, respectively, was chosen as an indicator for morphology related physical aging. Due to the two crystal structures, no quantitative estimation of the degree of crystallinity was performed for this material. Instead, the melting enthalpy was determined in the range of two pre-defined temperatures, that is from 80 °C to 170 °C. To obtain an indication for stabilizer consumption during aging exposure, the oxidation temperature T_{ox} was determined applying the tangent method (intercept point of the baseline and the slope to the final exothermal ascent of the DSC curve).

2.2.3 Mechanical Testing

Tensile tests were carried out at 23 °C according to ISO 527-3 using a screw driven universal testing machine (type: Instron 4505; Instron International Ltd.; High Wycombe, UK). The test speed was 10 mm/min. The dumb-bell film specimens were tested in the unaged state and in various states of aging. A digital image correlation (DIC) system (Jerabek et al., 2009; Kahlen et al., 2009b) was utilized for small strain measurement below the yield point, and a video extensometer (Kahlen et al., 2009b) for strains up to final failure.

3 RESULTS

3.1 Size Exclusion Chromatography

The changes in the weight average molecular mass for the two PP materials are illustrated in Fig. 2 as a function of aging time for both aging conditions. While PP-1 exhibits a measurable molecular mass decrease after an exposure time of 125 h

at 140 °C in air, and 2000 h at 80 °C in water, PP-2 appears to be less sensitive to aging exposure, most likely due to the higher stabilization. In fact, in the latter case virtually no change in molecular mass was found for aging conditions up to 16000 h in hot water and up to about 300 h in hot air. The reduction in M_w for the 500 h exposure to air at 140 °C amounts to 23 % and 16 % for PP-1 and PP-2, respectively. This difference again reflects the differing stabilizer content. For PP-1 exposure to hot water for 16000 h leads to a reduction in M_w by about 20 %.

As to the details of potential chemical aging mechanisms on the polymer molecular scale, chain scission and branching may play a role. In this context it has been proposed that degradation of semi-crystalline polymers takes place by chain scission predominantly in the amorphous fraction and also at the lamellar folds (Rabello et al., 1997), and in PP stabilized with phenolic antioxidants also through depolymerisation by end chain scission (Kausch, 2005). Nonetheless, while PP-2 in terms of aging stability is clearly superior due to the higher stabilizer concentration, both PP types appear to be properly stabilized considering the harsh aging conditions.

3.2 Thermo-analytical Investigations

Typical DSC thermograms of the first heating run in the unaged state and after exposure to hot air and hot water for specific times are shown for the various materials in Fig. 3 to Fig. 6. In the unexposed reference state, PE-X1 and PE-X2 (Fig. 3 and Fig. 4) exhibit melting peak temperatures of 132 °C and 125 °C and oxidation temperatures of 271 °C and 256 °C, respectively. Furthermore, crystallinity values of 60 % and 51 % were determined for the reference state of PE-X1 and PE-X2, indicating that PE-X1 may be less cross-linked than PE-X2. An overview of the influence of both aging conditions on characteristic values such as the degree of crystallinity α, the melting temperature T_m and the oxidation temperature T_{ox} for the unaged and the fully aged state is shown in Table 1.

Table 2: Characteristic thermo-analytical properties in the unaged and fully aged condition (air at 140 °C for 500 h and water at 80 °C for 16000 h) for PE-X1, PE-X2, PP-1 and PP-2.

Polymer	Crystallinity α	T_m in °C	T_{ox} in °C
PE-X1	in %		
unaged	60 ± 3	132 ± 3	271 ± 1
air (500 h, 140 °C)	48±2	130 ± 1	257 ± 1
water (16000 h, 80 °C)	58 ± 1	132 ± 2	266 ± 2
PE-X2	in %		
unaged	51 ± 1	125 ± 2	256 ± 3
air (500 h, 140 °C)	40	124 ± 1	247 ± 3
water (16000 h, 80 °C)	42 ± 1	126 ± 1	226 ± 1
PP-1	in %		
unaged	43 ± 2	144 ± 3	264 ± 3
air (500 h, 140 °C)	50 ± 5	158 ± 3	253 ± 1
water (16000 h, 80 °C)	53 ± 2	143 ± 1	200 ± 2
PP-2	in J/g		
unaged	65 ± 1	142 ± 3	264 ± 1
air (500 h, 140 °C)	76 ± 3	159 ± 2	259 ± 1
water (16000 h, 80 °C)	79 ± 1	142 ± 1	260 ± 1

After aging in hot air, the crystallinity of both PE-X types decreases with aging time, indicating further cross-linking. The most significant decrease occurs during the first 125 h (PE-X1: from 60 % to 50 % and PE-X2: from 51 % to 40 %). The conclusion of further crosslinking by aging is in accordance with findings by Amato et al. (2005a), who showed that during aging above the melting temperature further carbonyl groups and crosslinks are caused by oxidation, thus disrupting chain regularity with a reduced tendency for crystallization.

Upon hot water aging, no significant effect on crystallinity and melting peak temperature was observed for PE-X1. In terms of the polymer network, there is no indication for physical and/or chemical aging to be deduced from these data. On the other hand, a somewhat different behavior was found for PE-X2 when aged in hot water. First, while the melting peak temperature also remained rather constant (at around 125 °C), the degree of crystallinity of this material decreased from 51 % (unaged state) to 42 % (80 °C/16000 h). Thus, it seems that PE-X2 experiences at

least some tendency for chemical aging and crosslinking which acts to reduce the degree of crystallinity even during hot water exposure.

The above conclusions based on the changes in crystallinity are also supported by the concomitant changes in the oxidation temperatures. For hot air exposure, the T_{ox} values for both materials are reduced by about the same amount, which corresponds to the roughly equivalent reductions in the degree of crystallinity, having been related above to chemical aging and crosslinking. Conversely, for hot water exposure, a significant reduction in T_{ox} values was determined for PE-X2, while PE-X1 shows a rather slight decrease only. This difference in behavior again corroborates the above conclusions based on the effect of hot water aging on the degree of crystallinity particularly of PE-X2. It must be emphasized, however, that changes in T_{ox} values per se do not provide clear and unambiguous evidence for chemical degradation of the polymer network, but rather are related to the remaining “effective” stabilizer concentration in the polymeric material. In this context it is well documented that reductions in T_{ox} values may also be related to stabilizer loss by leaching particularly upon water exposure (Dörner and Lang, 1998a+b; Amato et al., 2005b). Whether and to what extent such leaching effects play a role in the differences observed for PE-X1 and PE-X2, remains a topic for further investigations.

Turning to the data for PP in Table 1, both unaged PP types exhibit a melting peak temperature of around 143 °C and an oxidation temperature of 264 °C. As mentioned above, PP-2 crystallizes partly also in the β-form so that two melting peaks were detected (see Fig. 6). Hence, for this material, for T_m the second peak was chosen as characteristic value and the degree of crystallinity is reported in J/g rather than in % crystallinity.

For both PP types, a significant increase in the degree of crystallinity was observed upon both aging conditions (hot air and hot water) after the shortest intervals of exposure for which measurements were performed (125 h in hot air, 2000 h in hot water). Depending on the exposure conditions, this increase in crystallinity is clearly related to post- and/or re-crystallization, perhaps enhanced by simultaneous molecular degradation at least for PP-1 (compare Fig. 2).

Furthermore, the increase in the melting temperature for hot air aging from around 143 °C to about 159 °C indicates re-crystallization in terms of a better crystal perfection. On the other hand, for hot water exposure, the melting temperatures remain rather constant with a simultaneous broadening of the melting peak towards lower temperatures, thus implying post-crystallization.

The most pronounced shifts in melting peak temperature in hot air at 140 °C take place already after 125 h of exposure. This is in agreement with reports by Alberola et al. (1995a) and Groff et al., (1996) who also attribute this shift to partial melting combined with post- or re-crystallization. Moreover, due to the vicinity of the aging temperature to the melting temperature, for PP-2 also β-to-α re-crystallization may occur (Kotek et al., 2004; Scudla et al., 2003). Finally, an enhanced tendency for post- or re-crystallization caused by prior chain scission was also reported for PE by Dörner and Lang (1998a+b).

Surprisingly, hardly any reduction in T_{ox} was found for PP-2 upon hot water exposure. While this result is in good agreement with the SEC results in Fig. 2, it is somewhat surprising in light of the significant reduction in the T_{ox} values for PP-1 when exposed to hot water. Considering that both PP types contain the same stabilizer system just in different concentrations, it may be hypothesized that the different crystal structure of PP-1 (α-form only) and PP-2 (some β-form) may perhaps affect the leaching tendency of these stabilizers with the β-form being less prone to leaching. Of course, further investigations will be needed to corroborate or disregard this hypothesis.

A summary of the above conclusions on the aging phenomena observed for the materials investigated is provided in Table 2. Overall, one may conclude that some chemical aging occurs for both PE-X materials when exposed to hot air. Due to the exposure to a temperature above the melting temperature, any interpretation as to physical aging for these aging conditions in a true sense is of course meaningless. Nevertheless, for reasons of presentability, this term has been chosen to indicate the underlying physical and morphological changes of these materials when exposed to air at 140 °C. Hot water exposure, on the other hand, has a very different aging influence on the polymer network structure of the two PE-X materials. While there are no indications for physical and/or chemical aging for the

PE-X1 polymer network, significant chemical aging (further crosslinking) can be assumed for PE-X2. Under all aging conditions T_{ox} values were reduced by either stabilizer consumption in hot air and hot water and/or stabilizer leaching in hot water. For PP, both physical and chemical aging mechanisms were found to occur under the investigated aging conditions. The most pronounced difference in the two PP types was related to the higher concentration of the stabilizer system in PP-2, combined with the fact that PP-2 was nucleated to also crystallize in the β-form whereas PP-1 was unnucleated crystallizing in the α-form. In terms of aging stability, PP-2 turned out to be superior.

Table 3: Physical and chemical aging determined with analytical methods for the materials investigated.

Polymer and aging conditions	**"Physical aging"**	**"Chemical aging"**
PE-X1		
Hot air (140 °C)	(Reduction in α)	Crosslinking, leading to a reduction in α; Decrease in T_{ox}
Hot water (80 °C)	-	Slight decrease in T_{ox}
PE-X2		
Hot air (140 °C)	(Reduction in α)	Crosslinking, leading to a reduction in α; Decrease in T_{ox}
Hot water (80 °C)	(Reduction in α)	Crosslinking, leading to a reduction in α; Significant decrease in T_{ox}
PP-1		
Hot air (140 °C)	Increase in α; Increase in T_m	Slight decrease in M_w (enhances tendency for post- and re-crystallization); Decrease in T_{ox}
Hot water (80 °C)	Increase in α	Slight decrease in M_w (enhances tendency for post-crystallization); Significant decrease in T_{ox}
PP-2		
Hot air (140 °C)	Increase in α (β-to-α re-crystallization); Increase in T_m	Slight decrease in M_w (enhances tendency for post- and re-crystallization); Virtually no decrease in T_{ox}
Hot water (80 °C)	Increase in α	No change in M_w; Virtually no decrease in T_{ox}

3.3 Mechanical Investigations

Typical stress-strain curves from tensile tests are shown in Fig. 7 and Fig. 8 for the unaged and fully aged specimens (both, hot air and hot water aging) of the PE-X and PP materials. The mechanical properties of specific interest such as modulus, yield stress and strain-to-break are listed quantitatively in Table 3. Moreover, the development of aging effects as a function of exposure time to the aging conditions is shown in terms of relative strain-to-break values (defined as the ratio of strain-to-break values in the aged and the unaged reference state in %) in Fig. 9 and Fig. 10. These characteristics have been selected as they may be correlated to the underlying physical and chemical aging mechanisms as determined by analytical methods before.

Table 4: Characteristic mechanical properties in the unaged and fully aged condition (air at 140 °C for 500 h and water at 80 °C for 16000 h) determined for the materials investigated.

Polymer and aging conditions	**Modulus** in MPa	**Yield stress** in MPa	**Strain-to-break** in %
PE-X1			
unaged	1710 ± 180	26 ± 1	631 ± 50
air (500 h, 140 °C)	-*	20 ± 4	425 ± 19
water (16000 h, 80 °C)	1560 ± 160	24 ± 2	398 ± 147
PE-X2			
unaged	730 ± 60	17 ± 0.2	342 ± 34
air (500 h, 140 °C)	610 ± 50	14 ± 1	297 ± 34
water (16000 h, 80 °C)	840 ± 160	18 ± 1	318 ± 13
PP-1			
unaged	890 ± 30	20 ± 0.4	810 ± 24
air (500 h, 140 °C)	930 ± 80	21 ± 0.6	671 ± 164
water (16000 h, 80 °C)	970 ± 40	24 ± 0.2	785 ± 39
PP-2			
unaged	1100 ± 45	24 ± 0.4	883 ± 37
air (500 h, 140 °C)	1460 ± 60	25 ± 1	790 ± 114
water (16000 h, 80 °C)	1050 ± 60	26 ± 1	824 ± 74

*) No determination of modulus possible due to strong warpage of the specimens after hot air exposure.

Starting the discussion with the PE-X materials and comparing the mechanical characteristics for PE-X1 and PE-X2 in Table 3, the former exhibits higher modulus and yield stress values in the unaged and aged states, which is in good

agreement with the DSC results also indicating a higher degree of crystallinity for PE-X1 in all material states. On the other hand, looking at the fully aged conditions in Table 3, there is no clear tendency with regard to changes in modulus and yield stress due the aging exposure. While this is partly related to the rather high data scatter in the mechanical values, it may also be a result of the competing effect of crosslinking and the reduction in crystallinity, which would affect these values in an opposite direction. For hot air aging, there seems to be at least a tendential agreement with results by Amato et al. (2005a), who also reported a decrease in yield stress for PE-X after hot air aging (above 150°C) relating this change to additional crosslinking when the material is heated above the melting temperature. When aged in hot water, no effect on the yield stress was observed for PE-X2, while PE-X1 first exhibited an increase in yield stress by 36 % after 4000 h, which was then again reduced to about the original unaged value after 16000 h. These changes were accompanied by the changes in strain-to-break described below.

Interestingly, and although the data scatter partly is also rather high, strain-to-break values under both aging conditions decrease only slightly for PE-X2, whereas a significant reduction due to aging was observed for PE-X1. This is in contrast to the more significant decrease in T_{ox} values for PE-X2 particularly under hot water exposure (compare Fig. 4), which may perhaps indicate that the T_{ox} reduction may be more related to the enhanced tendency for stabilizer leaching in this less crystalline material. The effect of aging time on relative strain-to-break values shown in Fig. 9 for PE-X1 illustrates that the most pronounced effects of aging are observed in the short aging time regime (125 h at 140 °C in air; 6000 h at 80 °C in water) and with strain-to-break values remaining rather constant thereafter.

Turning to the data of the PP materials in Table 1, apart from the increase in modulus of PP-2 when aged in air, the other modulus values seem to be rather unaffected by the aging conditions. The same is essentially the case for yield stress and strain-to-break values. The rather stable mechanical performance of the two PP materials under both aging conditions over the time period investigated is also confirmed by the development of the relative strain-to-break values shown in Fig. 10. This is somewhat surprising, as a significant increase in crystallinity and

to some degree also a decrease in molecular mass, and for PP-2 also in T_{ox} values were found in the analytical investigations. Hence, overall this finding must again be interpreted in terms of competing effects of the changes in morphological and molecular structure with the net result of a rather constant mechanical performance. In other words, the mechanisms of physical aging and chemical aging, which were clearly determined by analytical means (compare Table 2), apparently cancel each other out in terms of the effects on mechanical properties. Unfortunately, hardly any literature is available for these types of materials that could help to further elucidate the observed trends. And yet, comparing the two material types in Fig. 10, PP-2 is still perhaps to be preferred due to the somewhat better stability in the fully aged state in hot air at 140 °C, which is also in line with the rather stable T_{ox} values for this material in Table 2.

4 SUMMARY AND CONCLUSIONS

The aging behavior of 4 semi-crystalline plastics including two PE-X and two PP types was investigated by exposing polymer film specimens to hot water (80°C up to 16000 h) and hot air (140 °C up to 500 h). These aging conditions were chosen as relevant for northern climates in accordance with previous investigations. To characterize the aging mechanisms and the effect of aging on properties, analytical methods (DSC and SEC) and tensile testing were applied.

The most significant property degradation in terms of a significant decrease in strain-to-break values in the shorter aging time regime (125 h in air at 140 °C and 6000 h in water at 80 °C) was found for PE-X1, which exhibited a higher degree of crystallinity compared to PE-X2. Furthermore, after hot air aging both PE-X types revealed a reduction in crystallinity, probably caused by crosslinking. Upon hot water exposure, only PE-X2 revealed a decrease in T_{ox} (probably indicative of an enhanced tendency for stabilizer leaching in this less crystalline material) along with a simultaneous reduction in crystallinity, again probably being caused by chemical aging and crosslinking. Interestingly, for both PE-X types modulus and yield stress values characteristic for the smaller strain regime did not reflect the molecular network and morphological changes observed by DSC, presumably as a result of the competing effects of crosslinking and the reduction in crystallinity.

Among the two PP types investigated, for PP-1 an increase in crystallinity accompanied by a decrease in M_w to enhance the tendency for post- and re-crystallization was found after exposure to elevated temperatures in air and water. Moreover, for both PP types an increase in melting temperature was determined after hot air aging, indicating re-crystallization. On the other hand, the broadening of the melting peak range after hot water exposure was related to post-crystallization. Nevertheless, mechanical properties in the small strain and large strain regime turned out to be nearly independent of the aging conditions, which implies that the aging mechanisms found by analytical methods may perhaps cancel each other out in terms of their effect on the mechanical performance parameters.

From the commodity type plastics investigated, PP-2 and PE-X2 appear to be the most promising candidates for an application as a black absorber material for solar thermal collectors in northern climates. However, to avoid any problems with dimensional instability, for both materials overheating protection measures are needed to ensure that the temperature under collector stagnation conditions remains substantially below the melting temperature of these materials (142 °C for PP-2 and 125 °C for PE-X2).

Acknowledgments

The research work of this paper was performed within the project S. 11 “Aging of polymers in solar-thermal applications” at the Polymer Competence Center Leoben GmbH within the framework of the K_{plus} Program of the Austrian Ministry of Traffic, Innovation and Technology with contributions by the University of Leoben, Graz University of Technology, Johannes Kepler University Linz, JOANNEUM RESEARCH ForschungsgmbH and Upper Austrian Research GmbH. The PCCL is funded by the Austrian Government and the State Governments of Styria and Upper Austria.

Literature

Alberola, N., Fugier, M., Petit, D., Fillon, B., 1995. Microstructure of quenched and annealed films of isotactic polypropylene. Part I. J. Mater. Sci. 30, 1187-1195.

Amato, L., Gilbert, M., Caswell, A., 2005a. Degradation studies of crosslinked polyethylene. I Aged in air. Plast. Rubber Compos. 34 (4), 171-178.

Amato, L., Gilbert, M., Caswell, A., 2005b. Degradation studies of crosslinked polyethylene. II Aged in water. Plast Rubber Compos 34 (4), 179-187.

ATHAS database, http:web.utk.edu/~athas/databank/ Ed. M. Pyda (1994).

Davidson, J.H., Mantell, S.C., Jorgensen, G., 2002. Advances in Solar Energy, vol. 15. American Solar Energy Society, Boulder, CO, pp 149-186.

DIN 53504 (1994). Testing of rubber; determination of tensile strength at break, tensile stress at yield, elongation at break and stress values in a tensile test.

Dörner, G., Lang, R.W., 1998a. Influence of various stabilizer systems on the ageing behaviour of PE-MD –I. Hot-water ageing of compression and molded plaques. Polym. Degrad. Stab. 62, 421-430.

Dörner, G., Lang, R.W., 1998b. Influence of various stabilizer systems on the ageing behaviour of PE-MD – II. Ageing of pipe specimens in air and water at elevated temperatures. Polym. Degrad. Stab. 62, 431-440.

Freeman, A., Mantell, S.C., Davidson, J.H., 2005. Mechanical performance of polysulfone, polybutylene, and polyamide 6/6 in hot chlorinated water. Sol. Energy 79, 624-637.

Groff, I., Franzese, R., Landro, L.D., Pagano, M.R., Genoni, M., 1996. Characterization of polypropylene pipes during accelerated aging in air and water. Polym. Test. 15, 347-361.

ISO 527-3 (2005). Plastics - Determination of tensile properties - Part 3: Test conditions for films and sheets.

Jerabek, M., Major, Z., Lang, R.W., 2009. Applicability and limitations of a digital image correlation system for monotonic testing of polymeric materials. To be submitted in Polym. Test.

Kahlen, S., Jerabek, M., Steinberger, R., Wallner, G.M., Lang, R.W., 2009b. Characterization of Physical and Chemical Aging of Polymeric Solar Materials by Advanced Mechanical Testing. To be submitted in Polym. Test.

Kahlen, S., Wallner, G.M., Fischer, J., Meir, M.G., Rekstad, J., 2005. In: Židonis, V., Lapinskienė, A. (Eds.), Proceedings of NorthSun 2005, Vilinius, Lithuania, pp. 32-40.

Kahlen, S., Wallner, G.M., Lang, R.W., 2009a. Aging behavior of polymeric solar absorber materials. – part 1: engineering plastics. To be submitted in Sol. Energy.

Kausch, H.H., 2005. The Effect of Degradation and Stabilization on the Mechanical Properties of Polymers Using Polypropylene Blends as the Main Example. Macromo. Symp. 225, 165-178.

Kotek, J., Kelnar, I., Baldrian, J., Raab, M., 2004. Structural transformations of isotactiv polypropylene induced by heating and UV light. Eur. Polym. J., 40, 2731-2738.

Lang, R.W., 1995. Einsatzmöglichkeiten von Kunststoffen bei der thermischen Energieversorgung von Niedrigenergie-Solarhäusern. Das Bauzentrum 9, 25-33.

Meir, M.G., Rekstad, J., 2003. Der Solarnor® Kunststoffkollektor - the development of a polymer collector with glazing. In: Wallner, G.M, Lang, R.W. (Eds.), Proceedings of 1st Leobener Symposium Polymeric Solar Materials, pp. II-1-II-8.

Meir, M., Rekstad, J., 2004. Personal communications.

Meir, M., Buchinger, J., Kahlen, S., Köhl, M., Papillon, P., Rekstad, J., Wallner, G., 2008. Polymeric solar collectors – state of the art. In Fernandes, E.O. (Ed.), Proceedings of the EuroSun 2008, Lisbon, Portugal, N° 409, pp. 1-10.

Olivares, A., Rekstad, J., Meir, M., Kahlen, S., Wallner, G., 2008. A test procedure for extruded polymeric solar thermal absorbers. Sol. Energy Mater. Sol. Cells 92, 445-452.

Plastics Europe, 2007. The compelling facts about plastics 2007. An analysis of plastics production, demand and recovery for 2007 in Europe. www.plasticseurope.org.

Rabello, M.S., White, J.R., 1997. The role of physical structure and morphology in the photodegradation behaviour of polypropylene. Polym. Degrad. Stab. 56, 55-73.

Ščudla, J., Raab, M., Eichhorn, K.-J., Strachota, A., 2003. Formation and transformation of hierachical structure of β-nucleated polypropylene characterized by X-ray diffraction, differential scanning calorimetry and scanning electron microscopy. Polymer 44, 4655-4664.

Varga, J., Ehrenstein, G.W., 1999. Beta-modification of isotactic polypropylene. In: Karger-Kocsis, J. (Ed.), Polypropylen an A-Z reference. Polypropylene from A-Z. Kluwer Academic publishers, Dordrecht, p. 57.

Wallner, G.M., Lang, R.W., 2005. Guest editorial. Sol. Energy 79 (6), 571-572.

Wallner, G.M., Lang, R.W., 2006. Kunststoffe-Neue Möglichkeiten in der Solarthermie. Erneuerbare Energie 2-2006, AEE-Intec, Austria.

Weiss, W., 2003. Solar Heating Systems for Houses. Wiley, New York, pp. 6-9.

Wu, C, Mantell, S.C, Davidson, J.H, 2004. Long-term Performance of PB and Nylon 6,6 Tubing in Hot Water. J. Sol. Energy Eng. 126 (1), 581-586.

Zweifel, H., Amos, S.E., 2000. Plastics Additives Handbook, fifth ed. Hanser, Munich.

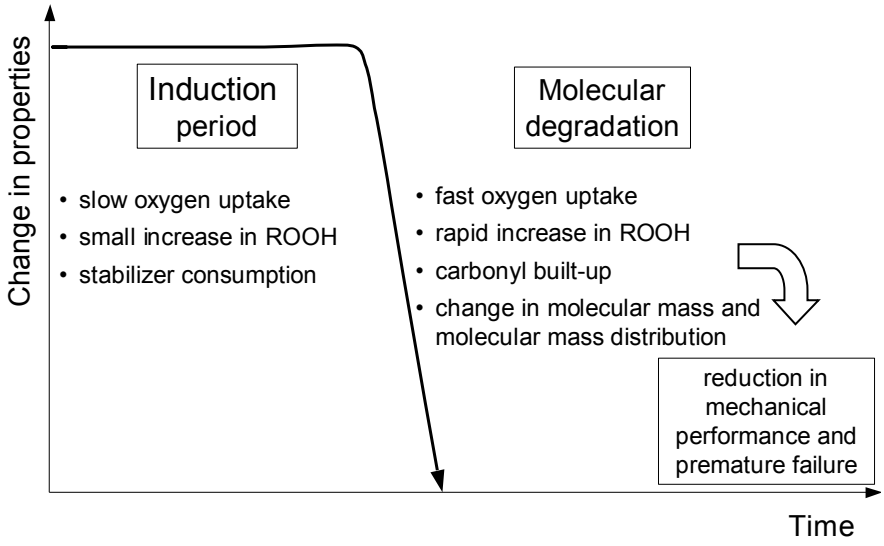

Fig. 1: Changes in material properties during aging of plastics based on polyolefins.

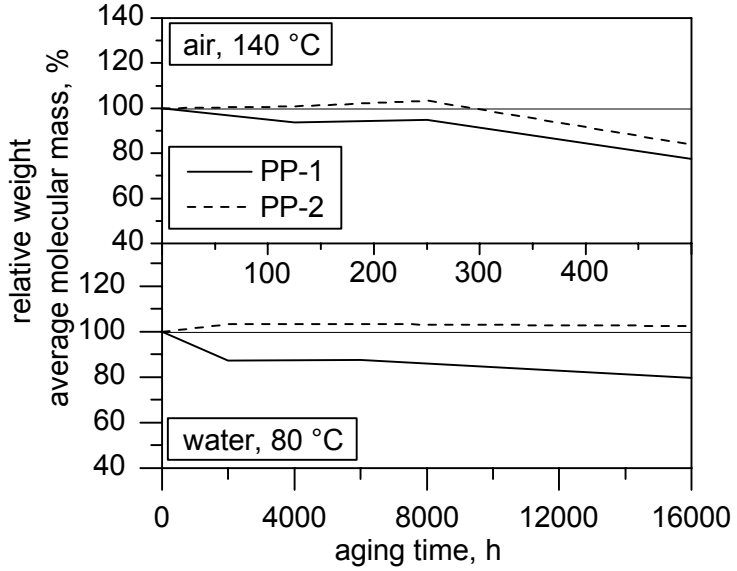

Fig. 2: Weight average molecular mass versus aging time in air at 140 °C and in water at 80 °C, respectively, for PP-1 and PP-2.

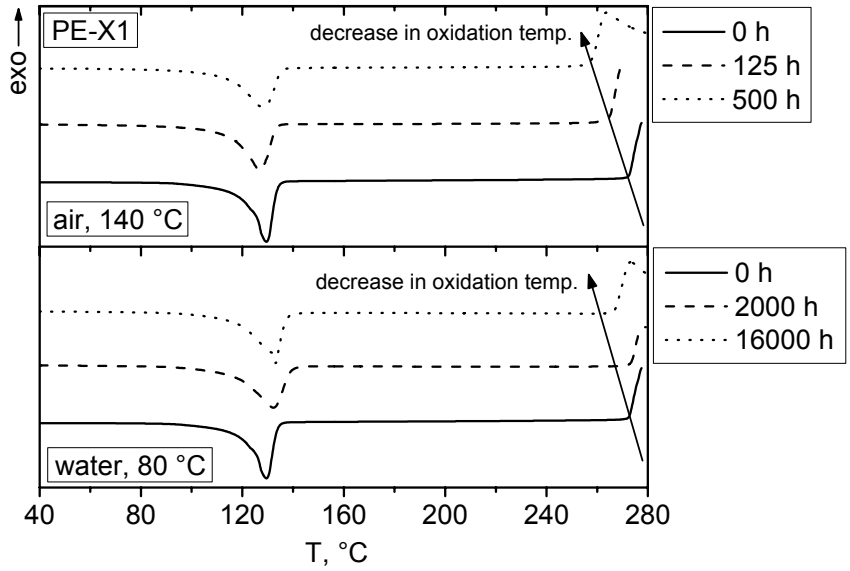

Fig. 3: DSC thermograms of PE-X1 films exposed to air at 140 °C (0, 125 and 500 h) and to water at 80 °C (0, 2000 and 16000 h).

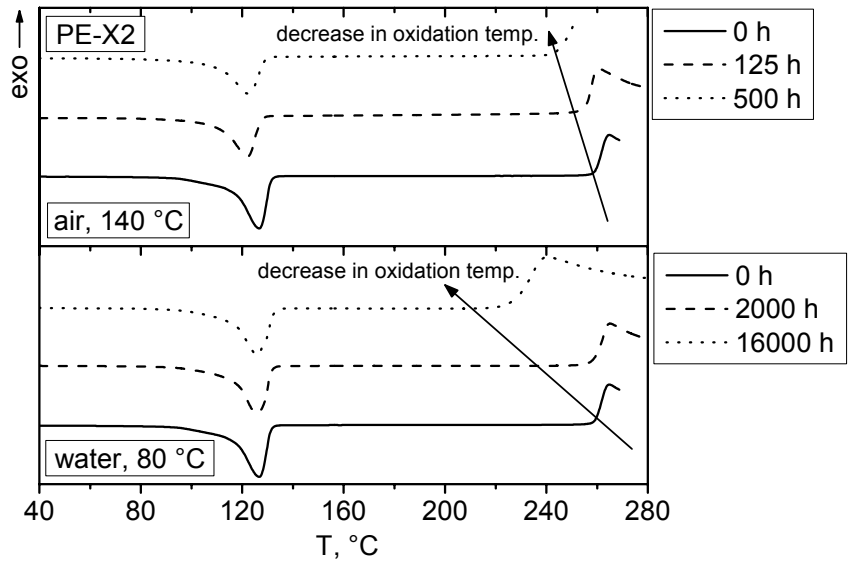

Fig. 4: DSC thermograms of PE-X2 films exposed to air at 140 °C (0, 125 and 500 h) and to water at 80 °C (0, 2000 and 16000 h).

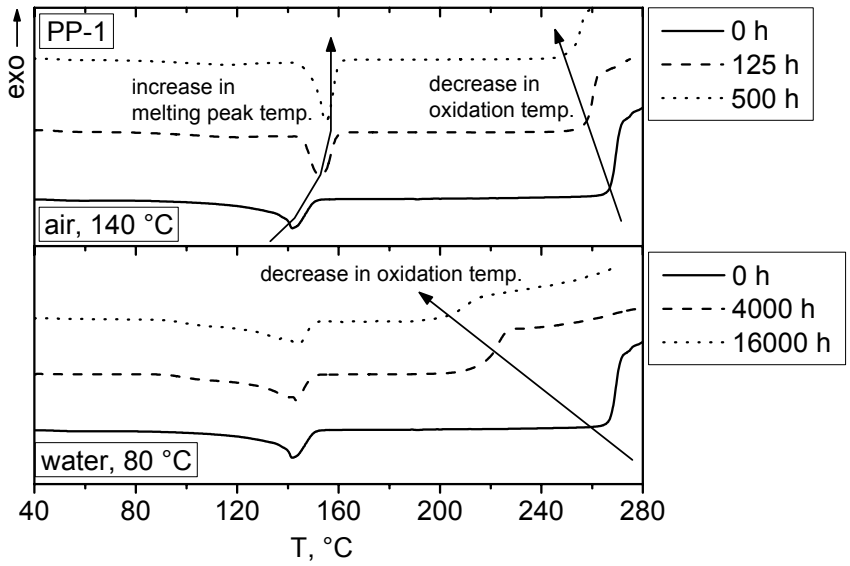

Fig. 5: DSC thermograms of PP-1 films exposed to air at 140 °C (0, and 500 h) and to water at 80 °C (0, 4000 and 16000 h.

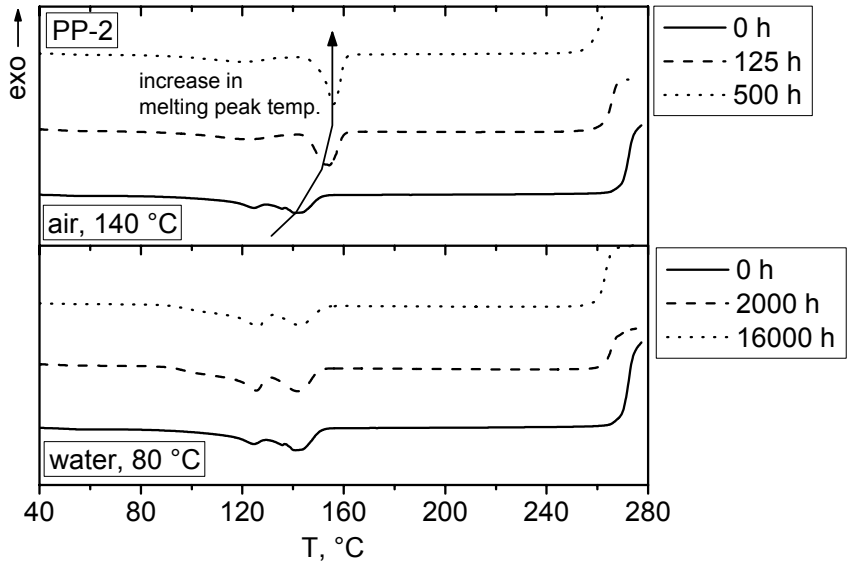

Fig. 6: DSC thermograms of PP-2 films exposed to air at 140 °C (0, 125 and 500 h) and to water at 80 °C (0, 2000 and 16000 h).

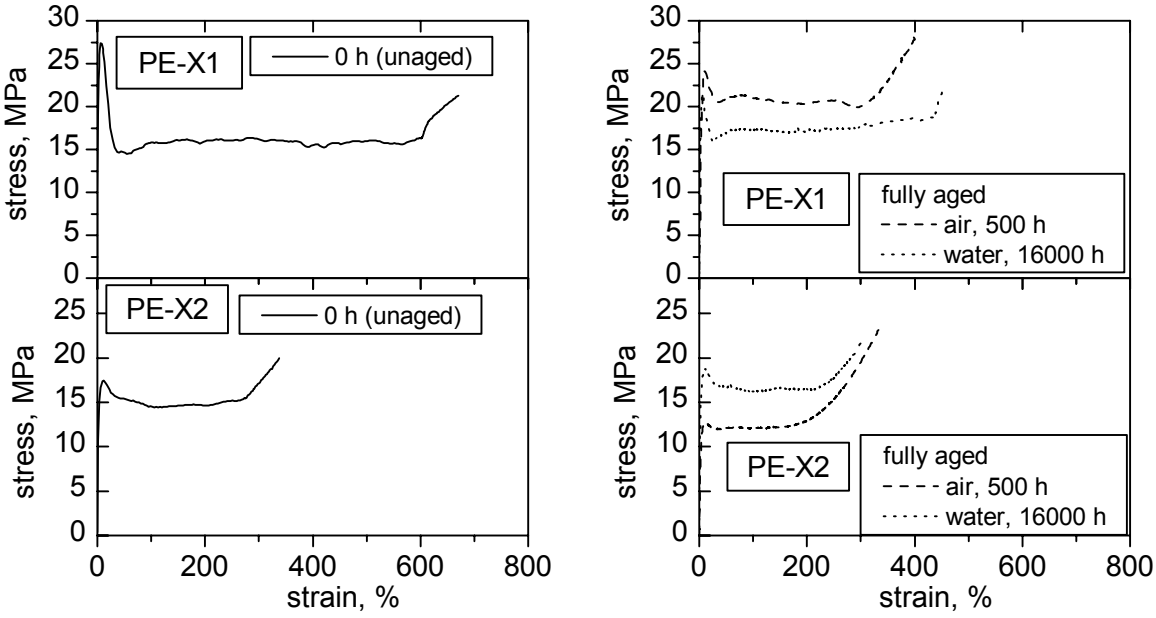

Fig. 7: Stress-strain curves for PE-X1 and PE-X2 comparing the behavior of the unaged reference state (0 h) and the fully aged state (500 h in air at 140 °C and 16000 h in water at 80 °C, respectively).

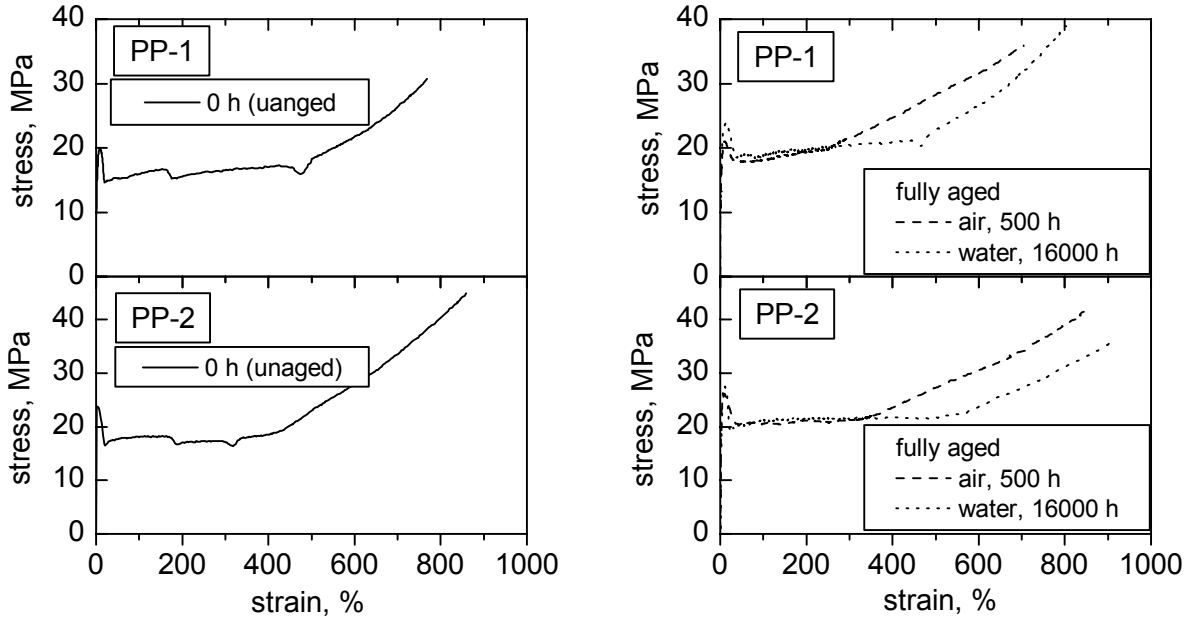

Fig. 8: Stress-strain curves for PP-1 and PP-2 comparing the behavior of the unaged reference state (0 h) and the fully aged state (500 h in air at 140 °C and 16000 h in water at 80 °C, respectively).

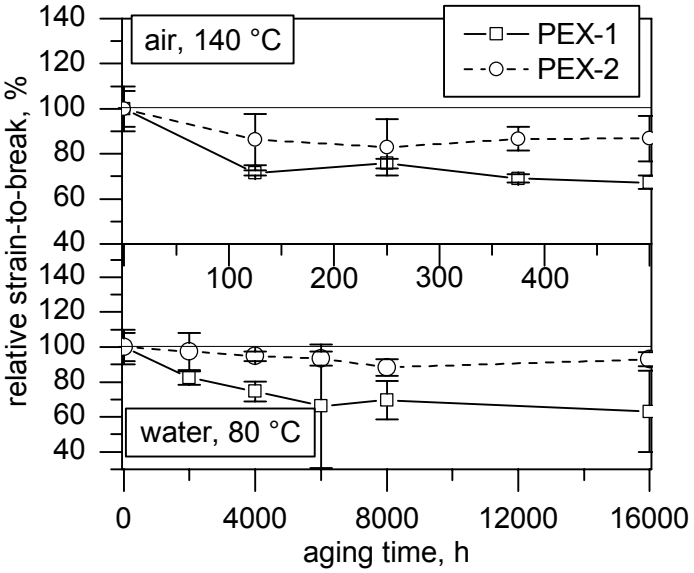

Fig. 9: Relative strain-to-break for PE-X1 and PE-X2 versus aging time in air at 140 °C and in water at 80 °C.

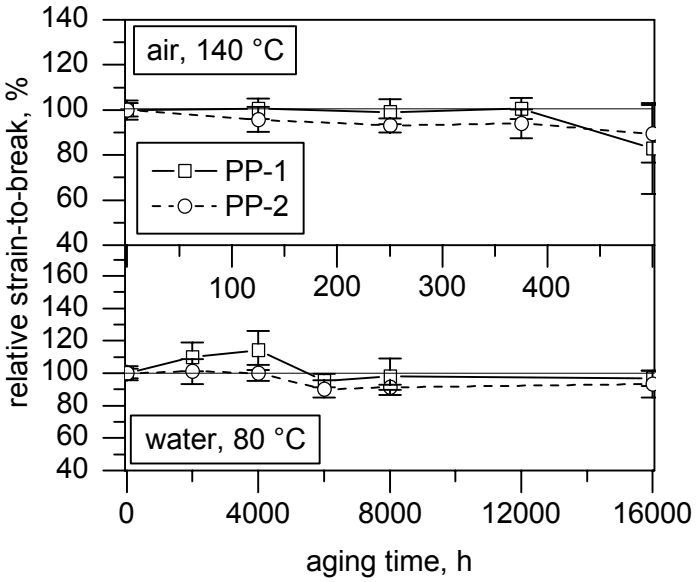

Fig. 10: Relative strain-to-break for PP-1 and PP-2 versus aging time in air at 140 °C and in water at 80 °C.

PAPER 4°

Aging Behavior and Lifetime Modeling for Polymeric Solar Absorber Materials

S. Kahlen[a)*], G. M. Wallner[b)], R. W. Lang[b)]

[a)] Polymer Competence Center Leoben GmbH, Roseggerstrasse 12, Leoben, 8700, Austria

[b)] Institute of Materials Science and Testing of Plastics, University of Leoben, Franz-Josef Strasse 18, Leoben, 8700, Austria

ABSTRACT

In this paper, three different polymeric material candidates for solar absorber applications are investigated as to their aging behavior at different temperatures in air and water. The materials supplied or produced as polymer films include the amorphous polymers polycarbonate (PC) and a blend of polyphenylene ether and polystyrene (PPE+PS), and the semi-crystalline polymer polypropylene (PP). The aging conditioning was performed in air in the temperature range from 120 to 140 °C and in water between 70 and 95 °C. Tensile tests were performed on unaged and aged film specimens at ambient temperature using strain-to-break values as a performance indicator for the degree of aging. While PP showed no significant aging under the investigated aging conditions, PPE+PS exhibited pronounced aging right from the beginning of aging exposure. For PC the effect of aging was found to strongly depend on the aging conditions. Hence, for this material only, activation energy based lifetime prediction models according to various methods described in the literature were applied. The activation energies and corresponding lifetime predictions for the temperature range from 40 to 60 °C in water and from 90 to 110 °C in air derived from these models are compared and interpreted in terms of other investigations and as to their practical relevance.

° To be published in “Solar Energy”.

* Corresponding author. Tel.: +43 (0) 3842 42962 50
Email address: kahlen@pccl.at

Keywords: polymers, solar thermal application, lifetime modeling.

1 INTRODUCTION

When applying polymer in solar thermal applications, they are usually exposed to elevated temperatures in an air and/or water environment for an extended period of time. For solar thermal collectors, a service life of at least 20 years is required (Köhl et al., 2005). Polymeric solar thermal collectors using liquids (i.e., mixture of water and glycol) as heat carrier are frequently designed as drain-back systems to avoid high pressure levels. Analogously, solar thermal air collectors operate without any significant pressure so that the mechanical stresses in the absorber remain low. Nevertheless, while several glazed thermal collectors with liquids as heat carrier and using plastics as absorber material exist commercially and are described in the literature (Meir et al., 2008; Meir et al., 2003), the problem of sufficiently accurate lifetime predictions for the practical service conditions of these polymeric absorbers is still unresolved. Based on experience described elsewhere (Meir et al., 2003; Kahlen et al., 2009a), such a polymeric absorber is usually operated at low-pressure levels of 0.1 - 0.5 bar with hot water as heat carrier. During the service life of 20 years under northern climate conditions, the absorber experiences an accumulated exposure time for up to16000 h at 80 °C in water (“wet load”) and up to 500 h at 140 °C in air (“dry load”) when in stagnation while the water is drained back into the storage tank. While the temperatures in solar thermal air collectors are generally lower and overheating is perhaps less important, the problem of proper lifetime assessments under service conditions exits here as well.

Aging of polymeric materials which are potential candidates for solar absorber applications has been a subject of several studies, both in terms of physical and chemical aging effects. Davidson et al. (2002) describe and provide a classification of relevant polymers for solar thermal applications in terms of aging, however in this paper without referring to any specific aging characteristics. In later studies by these authors, the aging behavior was investigated for polyamide 66 (PA66), polysulfone (PSU) and polybutylene (PB) (Freeman et al., 2005; Wu et al., 2004). The long-term effects on material behavior were restricted to the creep behavior of

components made out of these plastics in potable hot chlorinated water at 60 and 80 °C and thus do not allow any prediction of the service life under the harsher conditions described above. More recently, Kahlen et al. (2009a+b) studied the aging behavior of several amorphous and semi-crystalline plastics upon exposure to hot water (80 °C up to 16000 h) and to hot air (140 °C up to 500 h), relating the observed changes in mechanical tensile properties to the underlying physical and chemical aging mechanisms. While several material candidates appeared to be quite stable in terms of mechanical performance properties even when exposed to the temperatures and environments for the times indicated, others exhibited a significant performance loss.

At this point, to our knowledge no information is available on lifetime predictions or assessments for polymeric materials under practical absorber operating conditions using activation energy based models of polymer physics as they are frequently used in other fields of application. For example, to predict the lifetimes of pressurized thermoplastics pipes internal pressure tests are conducted at various temperatures, then applying the Ree-Eyring model to the experimental results (ISO 9080; Lang et al., 1997). Also widely recognized on a specimen level is the procedure according to ISO 2578, according to which a thermal index (TI) is defined which characterizes the maximum temperature below which the material retains a sufficient property level.

A sound science based prediction of lifetimes of plastics for solar absorber applications under service relevant conditions is undoubtedly of high importance. Thus, the main objectives of this paper are to investigate the aging behavior of three potential plastics absorber materials under service-near conditions, and to use the results in various activation energy based models to predict the lifetimes for these materials when exposed to air or water at elevated temperatures. The materials investigated include the amorphous polymers polycarbonate (PC) and a blend of polyphenylene ether and polystyrene (PPE+PS), and the semi-crystalline polymer polypropylene (PP). The aging conditioning was performed in air at 120 to 140 °C and in water at 70 to 95 °C without any simultaneous application of a mechanical stress. Subsequently, tensile tests at ambient temperature were performed using unaged specimens and specimens aged at various aging

conditions. To apply the activation energy based methods, strain-to-break values were used as a performance indicator for the degree of aging. This procedure is justified by the relatively low mechanical stress of approximately 2.5 MPa acting in service (design stress of 5 MPa assuming a safety factor of 2) (Olivares et al., 2008), so that no superposition of mechanical stresses and environmental effects on aging of the materials is assumed.

2 EXPERIMENTAL

2.1 Materials, Specimens and Conditioning

Table 1 provides information on the three commercially available polymers chosen for this investigation, two of which being amorphous (PPE+PS and PC) and one being semi-crystalline (PP-2). All three materials were investigated previously with regard to their aging behavior at specific conditions characteristic for northern climate (80 °C in water up to 16000 h and 140 °C in air up to 500 h). The results of these studies have been published elsewhere (Kahlen et al., 2009a+b) along with further details on the materials in terms of molecular mass, stabilization and nucleation.

While PC was directly supplied as film with a thickness of 480 μm, PPE+PS and PP were supplied as granules and extruded to 500 μm films on a single screw extruder followed by a chill roll unit at Dr. Collin (Dr. Collin GmbH; Ebersberg; D). Tensile test specimens of the S2 type (DIN 53504) with an overall length and a measuring length of 75 and 40 mm, respectively, were machined from the polymer films with a puncher.

Based on the above described temperature requirements for the exposure of glazed plastics absorbers in northern climate and on the experience of our previous aging studies with these materials (Kahlen et al., 2009a+b), the following aging conditions were defined for the purpose of this study:

For PPE+PS and PC: 70 °C, 80 °C and 90 °C up to 16000 h in water 120 °C, 130 °C and 140 °C up to 4500 For PP-2: 80 °C, 90 °C and 95 °C up to 16000 h in water

120 °C, 130 °C and 140 °C up to 4500

Table 1: Material designation, polymer type and supplier of the materials investigated.

Material designation	Polymer type	Commercial designation	Material supplier
PPE+PS	Blend of polyphenylene ether and polystyrene	Noryl EN 150SP	Sabic Innovative Plastics Holding BV (Bergen op Zoom, The Netherlands)
PC	Polycarbonate	Makrolon 3103	Bayer MaterialScience AG (Leverkusen, D)
PP-2	Polypropylene random copolymer	Beta-PPR RA7050[1)]	Borealis Polyolefine GmbH (Linz, A)

[1)] Crystalline phase containing 90 % ß-crystallites and 10 % α-crystallites; stabilized with a combination of phenolic and phosphitic antioxidants

Three aging temperatures were chosen for each of the environments, as this is the minimum required for the activation energy based lifetime prediction approaches described below. Aging in both environments (air and water) was carried out using an air-circulating oven (type Kendro 6000; Kendro Laboratory Products GmbH; Langenselbold; D). The specimens exposed to hot air were placed on a metal grid, the specimens exposed to hot water were placed in a water filled glass jar covered by a screw top. The distilled water was changed in intervals of 2000 h to reduce and avoid saturation effects in the water by leaching out additives. Following the aging exposure and prior to testing, the samples were stored in a climatized room (23 °C, 50 % r.h.). No re-drying was carried out for the samples exposed to hot water.

2.2 Testing and Lifetime Modeling

2.2.1 Mechanical Testing

Tensile tests were carried out at 23 °C according to ISO 527-3 using a screw driven universal testing machine (type: Instron 4505; Instron International Ltd.; High Wycombe, UK). The test speed was 10 mm/min. The dumb-bell film specimens were tested in the unaged state and in various states of aging. For the purpose of this paper, only strain-to-break values are of relevance. These were determined using a video extensometer. Further details as to the test procedure and the applied measurement techniques are described elsewhere (Kahlen et al., 2009c).

2.2.2 Lifetime Modeling Methods

For lifetime modeling and the evaluation of time-temperature limits ("apparent" endurance limit), three different methods, all being based on the Arrhenius activation energy relationship, were applied. In a strict sense, the Arrhenius approach assumes that degradation is controlled by a single thermally activated chemical process, with the rate of deterioration being proportional to exp ($-E_a/RT$), where E_a is the activation energy, R the gas constant and T the absolute temperature. So long as the degradation mechanism in a given temperature range remains the same, the approach may be used for lifetime prediction within this temperature range into realms not empirically accessible.

However, as polymers exhibit various aging and degradation mechanisms when investigated over a wide temperature range, procedures have been proposed to also deal with this phenomenon by defining a "cross-over" temperature at which a change in mechanism and thus in the activation energy occurs (Celina et al., 2005). In such cases, the Arrhenius plots are often separated into two individual processes, each with a specific activation energy, and the lower activation energy obtained in the lower temperature range (Celina et al., 2005; Gillen et al., 1997). For example, for PP aged in air, crossover temperatures of 70 °C and 83 °C were determined along with activation energies of 101 kJ/mol and 72 kJ/mol below and above the crossover temperature (Richters, 1970; Celina et al., 2005; Achimsky et al., 1997). Unfortunately, no such temperatures have been reported so far for

PPE+PS and PC, probably due to the lack of investigations over a sufficient wide temperature range.

For the present analysis, the activation energy for each of the two environments (air and water) is assumed to remain constant within the investigated temperature range. This is justified by the fact that the relevant temperatures for the above defined “wet load” and “dry load” service conditions have been predefined, with only minor alterations for the given climate conditions to be expected.

Another important aspect when applying an Arrhenius type rate approach to predict lifetimes is related to the choice of a proper lifetime limiting criterion. A criterion used for aging of polymers by several authors is oriented on the change in strain-to-break due to aging relative to values of the unaged state (Guseva et al., 2005). Frequently, a reduction in strain-to-break to 50 % of the unaged value is used. As such a reduction in the opinion of the present authors implies a significant degradation of the polymer, two criteria were selected for this study, also to analyze the associated effects. The one criterion corresponds to this reduction in strain-to-break to 50 % of the unaged value, the other uses a reduction in strain-to-break to only 80 % of the unaged value, being perhaps more indicative of the onset stage of aging rather than a fully aged state.

From the three models applied within this study, the first corresponds to ISO 2578, which aims at the determination of thermal endurance limits of plastics in general, and is based on a direct application of the strain-to-break criterion to the Arrhenius relationship. The advantage of this approach is that it is rather simple and straight forward and easy to apply to the experimental data directly, thus allowing for a fast lifetime estimation. The second method proposed by Gillen et al. (1997) and is based on the superposition of aging curves at different temperatures to a master curve by an empirical horizontal shifting procedure. The shift factors obtained are then analyzed in terms of the Arrhenius relationship. The third method according to Hoang and Lowe (2008) derives endurance limits by fitting of aging curves at different temperatures to a power law and then uses the exponent of this relationship (i.e., the slope of a semi-log linear plot) in the Arrhenius equation. While ISO 2578 has been applied successfully for different types of polymers, the latter two methods were developed mainly for polyolefins. Further details as to

these models in particular with regard to the data processing and reduction scheme are described below in the discussion section, when applying these models to our experimental results.

3 RESULTS

3.2 Effect of Aging on Strain-to-Break

Strain-to-break values for PPE+PS, PC and PP-2 after aging at the various temperatures in hot air and hot water for maximum time of exposure and in the unaged reference state are listed quantitatively in Table 2. Moreover, the development of aging effects as a function of exposure time to the various aging conditions (temperature and environment) is shown in terms of relative strain-to-break values (defined as the ratio of strain-to-break values in the aged and the unaged reference state in %) in Fig. 1* to Fig. 3.

Table 2: Strain-to-break values of the materials investigated in the unaged condition and for the various aged conditions for the maximum time of exposure.

Material	Strain-to-break in %							
	Unaged	Aged in air			Aged in water			
		120 °C, 4500	130 °C, 1500 h	140 °C, 500 h	70 °C, 6000 h	80 °C, 16000 h	90 °C, 2000 h	95 °C, 4000 h
PPE+PS	73 ± 12	1.6	1.8	4 ± 1	7 ± 1	9 ± 5	6 ± 1	-
PC	105 ± 2	21 ± 14	5	(11 ± 8)[1)] 47 ± 29	74 ± 33	22 ± 14	40 ± 38	-
PP-2	883 ± 37	845 ± 26	830 ± 32	790 ± 114	-	824 ± 74	879 ± 82	845 ± 15

[1)] A mean value for strain-to-break of 11 % was observed as lowest value after 125 h of aging at 140 °C in air. With increasing in aging time up to 500 h, strain-to-break values were again found to increase up to 47 % although with a rather high scatter of ± 29 %.

As shown in Fig. 1 for PPE+PS, a significant reduction in relative strain-to-break values occurs already at very short times under all aging conditions (less than a

* All figures of this paper are collected at the end of the text.

few hundred hours in air and water at all temperatures investigated). This may perhaps be due to the fact that problems were encountered in processing this material leading to some degradation already in the film processing stage (Kahlen et al., 2009a). In terms of the objective of the present paper, the rapid drop in properties of the strain-to-break values makes any application of a lifetime prediction model obsolete so that the data are not discussed further.

For PC, on the other hand, and although the overall scatter of the data is rather high, a continuous decrease of strain-to-break was found for all aging conditions in hot water (see Fig. 2). In hot air, the values of relative strain-to-break initially decreased down to 11 % and were then found to increase again up to nearly 47 % for an aging time of 500 h, however, with a relatively large scatter range of ± 29 % (see also Table 2). As expected, and apart from the just described phenomenon, in both environments aging is accelerated at higher temperatures. Also indicated in the figure are the limit lines for a reduction of the relative strain-to-break values to 80 % and 50 %. The corresponding quantitative values for the 80 % and 50 % reduction limit in terms of duration were determined graphically from the diagrams and are listed in Table 3. Depending on the criterion chosen (80 % or 50 % limit), these durations correspond to the “apparent” endurance limit or in this case to the empirically determined lifetime for this material under the respective aging conditions. In the case of aging in hot air at 140 °C, these “apparent” endurance limits were based on the initial drop-off in relative strain-to-break down to 11 % after 125 h. Moreover, as was pointed out in the previous paper, PC is not really a suitable candidate for black absorber applications since the lifetime at elevated temperatures in water is also very limited. On the other hand, PC when modified accordingly for UV resistance and weatherability may well be a candidate for solar thermal air collectors or for solar glazings. Thus the results for this material are used in the next section for lifetime modeling purposes in order to illustrate the procedure of a reaction rate theory based lifetime prediction and the influence of the specific model chosen.

Table 3: Empirically determined lifetimes or “apparent” endurance limit for PC under various aging conditions.

Relative strain-to-break criterion	**Aged in air** in years (in hours)		**Aged in water** in years (in hours)			
	120 °C	**130 °C**	**140 °C**	**70 °C**	**80 °C**	**90 °C**
Decrease to 80 %	0.19 (1670)	0.019 (170)	0.006 (50)	0.79 (6900)	0.37 (3240)	0.21 (1860)
Decrease to 50 %	0.25 (2150)	0.025 (220)	0.006 (60)	0.62 (5450)	0.3 (2670)	0.17 (1520)

The relative strain-to-break values for PP-2 under various aging conditions are shown in Fig. 3. Apart from the rather extreme exposure condition at 140 °C in air for 2300 h, at which the material was totally degraded, the strain-to-break values for all other conditions remained relatively stable with only minor or even negligible alterations relative to the unaged state. Analogous to the above results for PPE+PS, but this time for the opposite reason, the results generated for this material are also not suitable for being used in the reaction rate based lifetime modeling concept.

3.3 Lifetime modeling and endurance limits for PC

To exemplify the lifetime modeling procedures according to the various models proposed, the essential aspects of these models are first described briefly before the experimental results for PC are introduced into the models and the predictions obtained are compared.

3.3.1 Procedure according to ISO 2578

For the establishment of so-called time/temperature limits according to ISO 2578, the aging time causing a pre-defined reduction in the value for strain-to-break is proposed as a measure to define the endurance limit. As pointed out above, for this study two criteria were chosen as relevant, one being related to a reduction of relative strain-to-break values to 80 %, the other to 50 %. The former corresponds, of course, to a more conservative lifetime estimate. Based on an Arrhenius type relationship, the endurance limit (or endurance time) in terms of a virtual or projected time-to-failure may be described as follows:

$$\ln t_{endurance} = \ln A + 1/T * E_a \quad (1)$$

where $t_{endurance}$ represents the endurance time, A is a material constant, T is the absolute temperature in K, and E_a is the activation energy in J/mol. For data analysis and extrapolation, ISO 2578 recommends to apply the method of least squares to the experimental data. The graphical application of the above relationship and the ISO procedure to the existing experimental data generated for PC after hot air aging (120, 130, 140 °C) and hot water aging (70, 80, 90 °C) along with extrapolations to lower temperatures for both aging conditions and the two criteria for strain-to-break reduction is shown in Fig. 4. Also indicated in the figures is the quality of the linear fit in terms of the obtained regression coefficients ranging from 0.950 to 0.995.

3.3.2 Procedure according to Gillen et al.

The approach according to Gillen et al. (1997) is based on the application of the time temperature equivalency principle. The advantage of this procedure that it does not a priori require the definition of a failure criterion, as is the case in the ISO procedure above. Much rather it defines the extension or reduction of lifetimes at temperatures other than the reference temperature, as multiplicative factors to the lifetime at a given temperature, which may be based on any type of failure criterion.

An important prerequisite for the applicability of this approach is the fulfillment of the self-similarity criterion, that is, that the shape of the characteristic aging curves (i.e., strain-to-break vs. time) is similar for different temperatures. A superposition of data generated for various aging temperatures is obtained by shifting the various aging curves horizontally along the time axes, so that one single mastercurve is obtained. The shift factor a_T for the aging curves is defined by the following relationship:

$$\ln a_T = \ln\left(\frac{t_{T_1}}{t_{T_2}}\right) = \frac{E_a}{R} * \left(\frac{1}{T_1} - \frac{1}{T_2}\right) \quad (2)$$

where t_{T1} and t_{T2} are the respective aging times at the temperatures T_1 and T_2, respectively, E_a is the activation energy for a specific temperature window, R the gas constant and T the absolute temperature in K.

As shown in Fig. 5(a), the prerequisite of self-similar aging curves is reasonably fulfilled for the investigated PC grade for both aging conditions. The superposition of the aging curves to a mastercurves for a reference temperature of 120 °C in air and of 70 °C in water is depicted in Fig. 5(b) along with the shift factors applied.

Following the procedure proposed by Gillen et al. (1997), the logarithmic values of the empirically determined shift factors and the extrapolated shift factors for aging in air (90 °C, 100 °C and 110 °C) and for aging in water (40 °C, 50 °C and 60 °C) are plotted as a function of reciprocal temperature in Fig. 6. Again, the data reasonably fit the relationship of equation (2) above, with values for R^2 ranging from 0.980 to 0.998 for the least square linear fit of the experimental data.

3.3.3 Procedure according to Hoang and Lowe

The evaluation method of Hoang and Lowe (2008) is based on fitting the experimental strain-to-break data of aged samples to the following empirical equation:

$$\ln(\varepsilon_t) = \ln(\varepsilon_0) + S_T * t \tag{3}$$

where ε_t is the strain-to-break value of the material exposed over the time t (t being the aging time) to a specific environment (temperature T, medium), ε_0 corresponds to the strain-to-break of the unaged reference material, and S_T represents the reaction rate. The latter parameter is equivalent to the slope of a linear regression line of the experimental data, and is then used in an Arrhenius relationship as follows:

$$\ln(S_T) = \ln C - \frac{E_a}{R} * \frac{1}{T} \tag{4}$$

where C is a temperature independent constant, E_a is the activation energy in J/mol, R is the gas constant, and T is the absolute temperature in K.

The experimental data obtained for PC after aging in air and water are plotted according to equation (3) in Fig. 7. The best fit values for S_T based on these diagrams were then transformed into the Arrhenius diagram in Fig. 8, here again a

linear least square fit procedure was applied to the experimental data, with R^2 values ranging from 0.861 to 0.959. The projected data for water and air are also depicted.

3.3.4 Comparison of Activation Energies and Lifetime Predictions

A comparison of the activation energies derived from applying the various models described above is provided in Table 4. As expected, according to all models, the activation energy for aging in hot air is significantly higher than the one for aging in hot water, reflecting the rather high sensitivity of PC to hot water exposure. Depending on the procedure used, activation energies for air aging were found to range from 229 to 272 kJ/mol, and for water aging from 65 to 118 kJ/mol. Moreover, when comparing the values according to ISO 2578, for the criterion of a reduction in strain-to-break to 80 vs. 50 %, the activation energies are rather similar, although slightly higher for the latter criterion. More significant are the differences in the activation energies derived from the different approaches with the methods of Gillen et al. and Hoang and Lowe yielding the highest value for air aging and for water aging, respectively.

There are only few data available in the literature to which the above results can be compared. Dobkowski and Rudnik (1997) and Zhou and Yang (2007) performed aging studies with PC in the temperature range from 326 to 437 °C in air, using mass loss experiments for their characterization and applying different methods to their data analysis. The activation energies reported are quite different and correspond to 83 kJ/mol (Dobkowski and Rudnik, 1997) and 162 kJ/mol (Zhou and Yang, 2007). These values are substantially lower than those found in our study for air aging. It must be emphasized, however, that the aging temperature in our case was below T_g and thus corresponded to solid state aging, whereas the aging temperature in the studies cited was significantly above T_g in the molten material state.

Table 4: Activation energies with standard deviations for PC exposed to temperatures ranging from 120 to 140 °C in air and from 70 to 90 °C in water according to various models and assumptions (residual strain-to-break after aging).

	Activation energies in kJ/mol		
	ISO 2578 50 % (80 %)	**Gillen et al. (1997)**	**Hoang and Lowe (2008)**
Air	242 ± 47 (237 ± 38)	272 ± 39	229 ± 47
Water	68 ± 5 (66 ± 3)	65 ± 3	118 ± 47

Using the above activation energies, the criterion of a reduction in strain-to-break to 50 % and 80 %, respectively, was applied to all three models used to calculate the endurance limits for temperatures ranging from 90 to 110 °C in air and from 40 to 60 °C in water. The results are depicted in Fig. 9 and listed in Table 5, indicating the rather significant variations in lifetime predictions by the various models. For example, while for 90 °C in air the Hoang and Lowe procedure predicts lifetimes between 17 and 54 years, depending on the residual strain-to-break criterion used, the procedure according to Gillen et al. projects 164 to 204 years. Similarly, for hot water aging, at 40 °C, the lifetime predictions range from 5 to 58 years and thus vary by an order of magnitude depending on the model selected and the failure criterion chosen. While these discrepancies may perhaps be due to the general high scatter in the raw data of the strain-to-break values and the limited temperature range investigated experimentally, the numbers also raise the question as to the meaningfulness of such predictions and provide an indication for the importance of the proper choice of a model. Most importantly, it becomes quite evident that solar thermal applications of plastics further research on the theoretical and experimental side is needed to improve lifetime prediction procedures of increased reliability.

Table 5: Predicted lifetimes (endurance limits) for PC exposed to temperatures ranging from 90 to 110 °C in air and from 40 to 60 °C in water according to various models and assumptions (residual strain-to-break after aging).

Temperature in °C	**Predicted lifetimes** in years		
Air	**ISO 2578** 50 % (80 %)	**Gillen et al., 1997** 50 % (80 %)	**Hoang and Lowe, 2008** 50 % (80 %)
110	1.5 (1.1)	1.8 (1.5)	1 (0.33)
100	11 (8)	18 (15)	7 (2.3)
90	96 (66)	204 (164)	54 (17)
Water			
60	1.6 (1.2)	1.5 (1.2)	4 (1.2)
50	3.4 (2.6)	3 (2.5)	14 (4.6)
40	7.5 (5.6)	7 (5)	58 (19)

4 SUMMARY AND CONCLUSIONS

Three different polymers including a blend of PPE+PS, PC and PP-2 were investigated as to their aging behavior at different temperatures in hot air and hot water. Tensile tests were carried out on unaged and aged film specimens at ambient temperature, and the change in strain-to-break values was chosen as characteristic indicator for aging. While for PPE+PS strain-to-break values dropped dramatically after very short aging times, probably due to the prior degradation imposed on the material already in the processing step, PP-2 was found to be remarkably stable for the aging conditions investigated. Hence, the data generated for these two materials were not suitable for lifetime modeling purposes.

For PC, on the other hand, a continuous decrease in strain-to-break was observed, allowing for a reasonable application of various lifetime models, although the scatter of the data after exposure to the various temperatures in air

and water was rather high. Also, and as described in a previous study (Kahlen et al., 2009a), PC was found to be rather susceptible to hot water exposure so that it is essentially a candidate for hot air collectors and glazings only. Three models according to ISO 2578, to Gillen et al. (1997) and to Hoang and Lowe (2008) were applied to determine apparent endurance limits in terms of a virtual or time-to-failure after aging in hot air and hot water and compare the results. As a measure for the endurance limit the decrease in strain-to-break to 50 % and to 80 %, respectively, of the value of the unaged reference state was applied. Experimentally determined endurance limits in hot air from 120 to 140 °C and in hot water from 70 to 90 °C were extrapolated to lower temperatures according to the various models and applying a least square linear fit method. As expected, activation energies for hot water exposure turned out to be lower than those for hot air exposure, reflecting the sensitivity of PC to hot water. For hot air aging and hot water aging, respectively, activation energies were found to be in the range from 229 to 272 kJ/mol and from 65 to 118 kJ/mol, depending on the model applied. While the activation energies determined by the three models do not vary significantly, much higher deviations in the predicted endurance limits were deduced, ranging for example from 17 to 204 years for 90 °C in air and from 5 to 58 years for 40 °C in water. These results raise the question of the reasonability of the various models when applied to PC, so that further studies to improve the accuracy and reliability of lifetime prediction methods are needed.

Acknowledgments

The research work of this paper was performed within the project S. 11 “Aging of polymers in solar-thermal applications” at the Polymer Competence Center Leoben GmbH within the framework of the K_{plus} Program of the Austrian Ministry of Traffic, Innovation and Technology with contributions by the University of Leoben, Graz University of Technology, Johannes Kepler University Linz, JOANNEUM RESEARCH ForschungsgmbH and Upper Austrian Research GmbH. The PCCL is funded by the Austrian Government and the State Governments of Styria and Upper Austria.

Literature

Achimsky, L., Audouin, L., Verdu, J., Rychly, J., Matisova-Rychla, L, 1997. On a transition at 80 °C in polypropylene oxidation kinetics. Polym. Degrad. Stab. 58, 283-289.

DIN 53504, 1994. Testing of rubber; determination of tensile strength at break, tensile stress at yield, elongation at break and stress values in a tensile test.

Dobkowski, Z., Rudnik, E., 1997. Thermal analysis techniques for characterization of polymer materials. Polym. Degrad. Stab. 91, 488-493.

Celina, M., Gillen, K.T., Assink, R.A., 2005. Accelerated aging and lifetime prediction: Review of non-Arrhenius behaviour due to two competing processes. Polym. Degrad. Stab. 90, 395-404.

Gillen, K.T., Bernstein, R., Celina, M., 2005. Non-Arrhenius behavior for oxidative degradation of chlorosulfonated polyethylene materials. Polym. Degrad. Stab. 87, 335-346.

Gillen, K.T., Celina, M., Bernstein, R., Shedd, M., 2006. Lifetime predictions of EPR materials using the Wear-out approach. Polym. Degrad. Stab. 9, 3197-3207.

Gillen, K.T., Celina, M., Clough, R.L., Wise, J., 1997. Extrapolation of accelerated aging data – Arrhenius or Erroneous? Trends Polym. Sci. 5 (8), 250-257.

Guseva, O., Lichtblau, A., 2005. Application of smoothing methods for estimation of service life for polymers from tensile testing. Polym. Test. 24, 718-727.

Hoang, E.M., Lowe, D., 2008. Lifetime prediction of a blue PE100 water pipe. Polym. Degrad. Stab. 93, 1496-1503.

ISO 1167, 2007. Thermoplastic pipes, fittings and assemblies for the conveyance of fluids – Determination of the resistance to internal pressure.

ISO 2578, 1993 E. Plastics – Determination of time-temperature limits after prolonged exposure to heat.

ISO 527-3, 2005. Plastics - Determination of tensile properties - Part 3: Test conditions for films and sheets.

ISO 9080, 2003. Plastics piping and ducting systems - the determination of the long-term hydrostatic strength of thermoplastics materials in pipe form by extrapolation.

Kahlen, S., Wallner, G.M., Lang, R.W., 2009a. Aging behavior of polymeric solar absorber materials – part 1: engineering plastics. To be submitted in Sol. Energy.

Kahlen, S., Wallner, G.M., Lang, R.W., 2009b. Aging behavior of polymeric solar absorber materials – part 2: commodity plastics. To be submitted in Sol. Energy.

Kahlen, S., Jerabek, M., Steinberger, R., Wallner, G.M., Lang, R.W., 2009c. To be submitted in Polymer Testing.

Köhl, M., Jorgenson, G., Brunold, S., Carlsson, B., Heck, M., Möller, K., 2005. Durability of polymeric glazing materials for solar applications. Sol. Energy 79, 618-623.

Lang, R.W., Stern, A., Doerner, G., 1997. Applicability and limitations of current lifetime prediction models for thermoplastics pipes under thermal presure. Macromol. Mater. Eng. 247, 131-137.

Langlois, V., Audouin, L., Verdu, J., Courtois, P., 1993. Thermooxidative aging of crosslinked linear polyethylene: Stabilizer consumption and lifetime prediction. Polym. Degrad. Stab. 40, 399-409.

Meir, M.G., Rekstad, J., 2003. Der Solarnor® Kunststoffkollektor - the development of a polymer collector with glazing. In: Wallner, G.M, Lang, R.W. (Eds.), Proceedings of 1st Leobener Symposium Polymeric Solar Materials, pp. II-1-II-8.

Meir, M., Buchinger, J., Kahlen, S., Köhl, M., Papillon, P., Rekstad, J., Wallner, G., 2008. Polymeric solar collectors – state of the art. In Fernandes, E.O. (Ed.), Proceedings of the EuroSun 2008, Lisbon, Portugal, N° 409, pp. 1-10.

Olivares, A., Rekstad, J., Meir, M., Kahlen, S., Wallner, G., 2008. A test procedure for extruded polymeric solar thermal absorbers. Sol. Energy Mater. Sol. Cells 92, 445-452.

Olivares, A., Rekstad, J., Meir, M., Kahlen, S., Wallner, G., 2009. Degradation model for an extruded polymeric solar thermal absorber. To be submitted in Sol. Energy Mater. Sol. Cells.

Pinter, G., Duretek, I., Austi, N., Lang, R.W., 2002. Characterization of the thermo-oxidative degradation of polyethylene pipes by chromatographical, rheological and thermo-analytical methods. Macromol. Symp. 181, 213-223.

Richters, R., 1970. Initiation process in the oxidation of polypropylene. Macromolecules 3 (2), 262-264.

Zhou, W., Yang, H., 2007. Flame retarding mechanism of polycarbonate containing methylphenyl-silicone. Thermochim. Acta 452, 43-48.

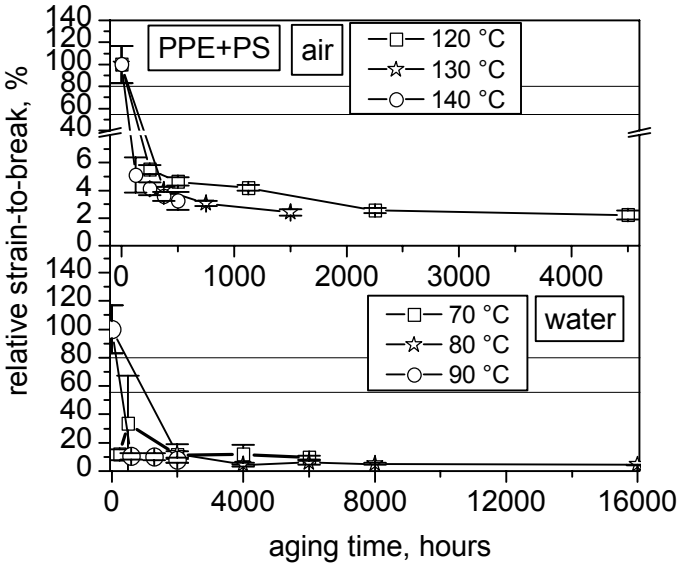

Fig. 1: Relative strain-to-break for PPE+PS versus aging time in air and in water at various temperatures. Also indicated in the diagram are the limit lines for lifetime modeling.

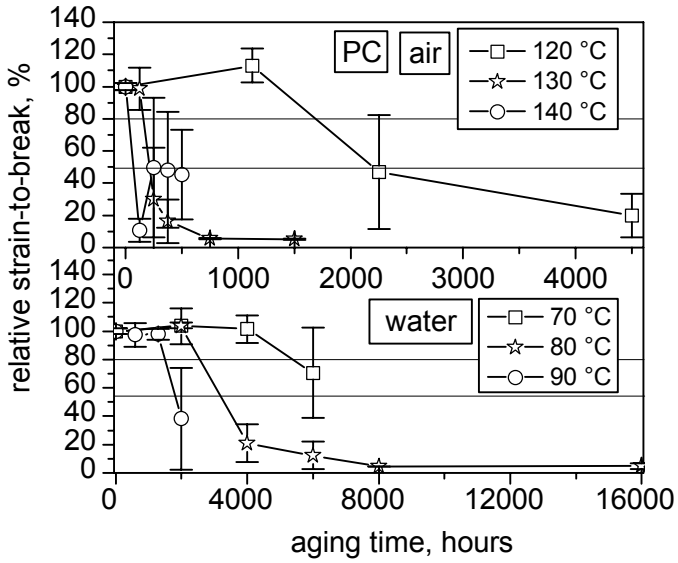

Fig. 2: Relative strain-to-break for PC versus aging time in air and in water at various temperatures. Also indicated in the diagram are the limit lines for lifetime modeling.

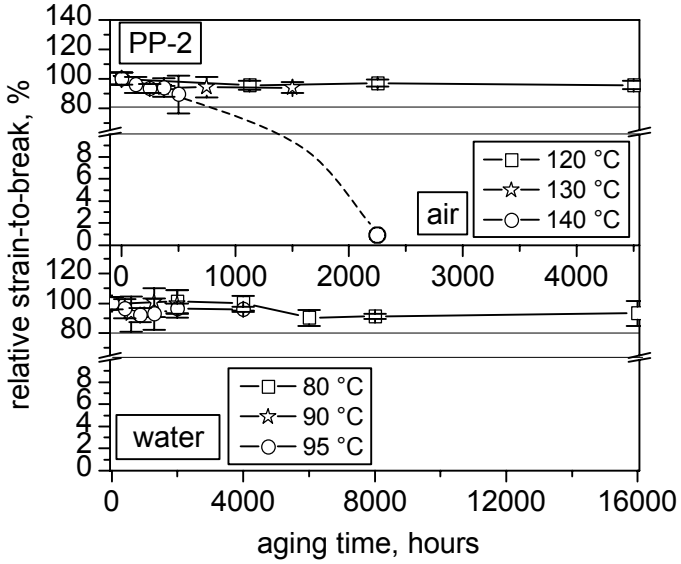

Fig. 3: Relative strain-to-break for PP-2 versus aging time in air and in water at various temperatures. Also indicated in the diagram are the limit lines for lifetime modeling (relative strain-to-break reduction to 80 % and 50 %, respectively).

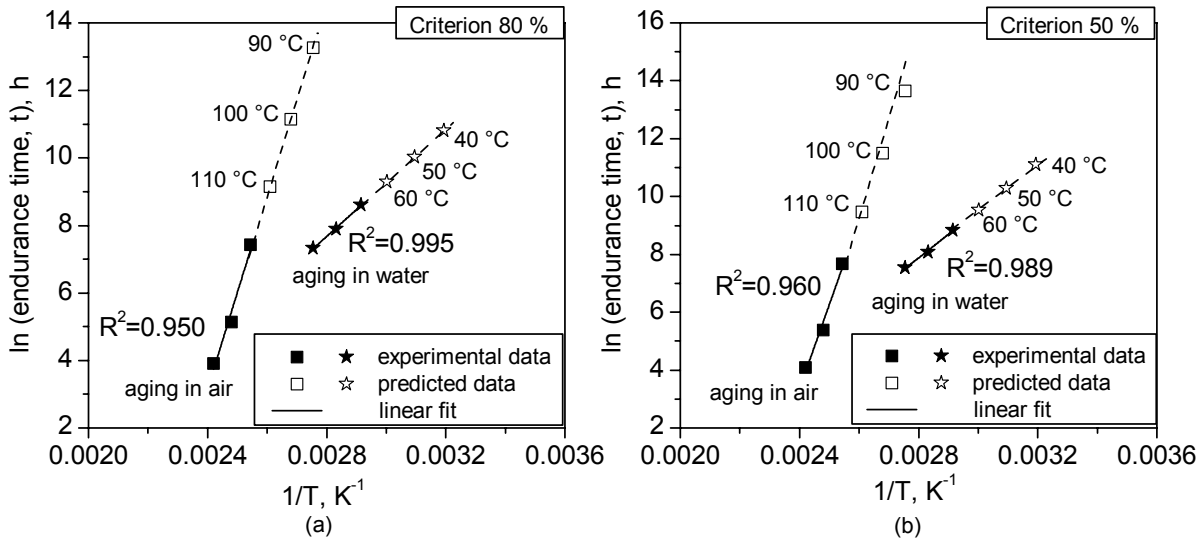

Fig. 4: Arrhenius type diagram for PC according to ISO 2578 for hot air and hot water aging, respectively using two different criteria as aging indicators. (a) reduction in relative strain-to-break to 50 %; (b) reduction in relative strain-to-break to 80 %.

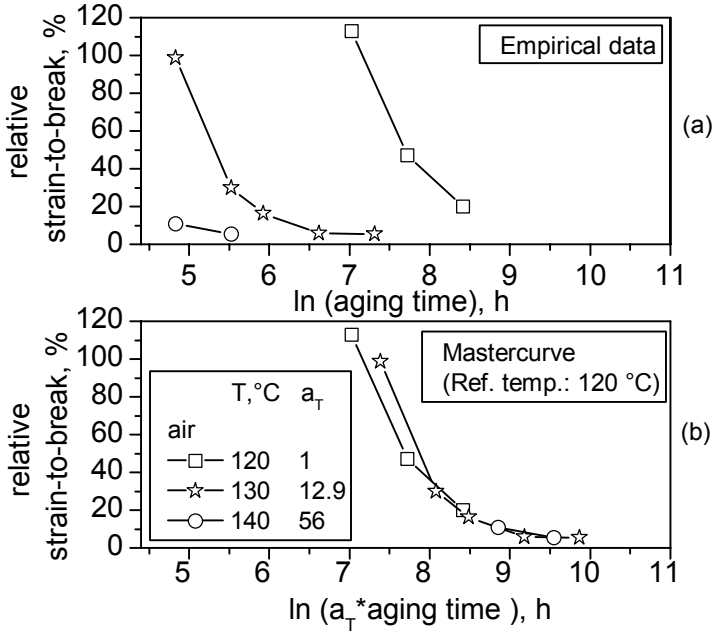

Fig. 5: (a) relative strain-to-break vs. aging time for PC after hot air and hot water exposure; (b) mastercurves for relative strain-to-break vs. aging time for a reference temperature of 120 °C in air and 70 °°C in water.

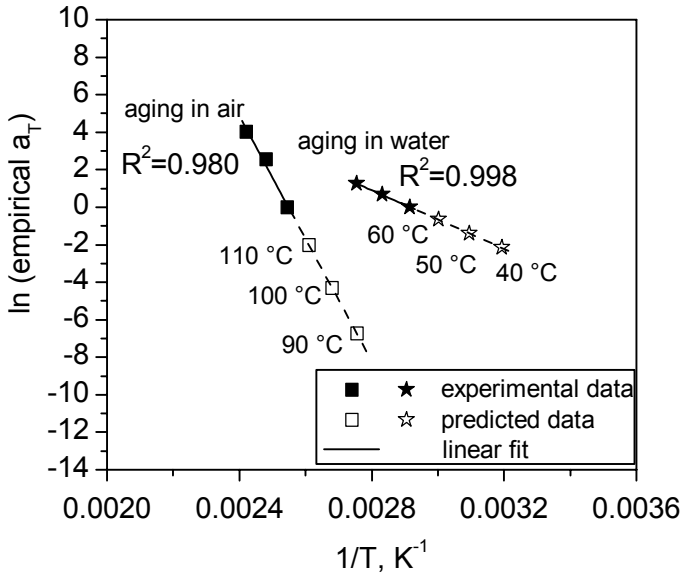

Fig. 6: Arrhenius type diagram for PC according to Gillen et al. (1997) for hot air and hot water aging, respectively, using the empirical shift factor concept.

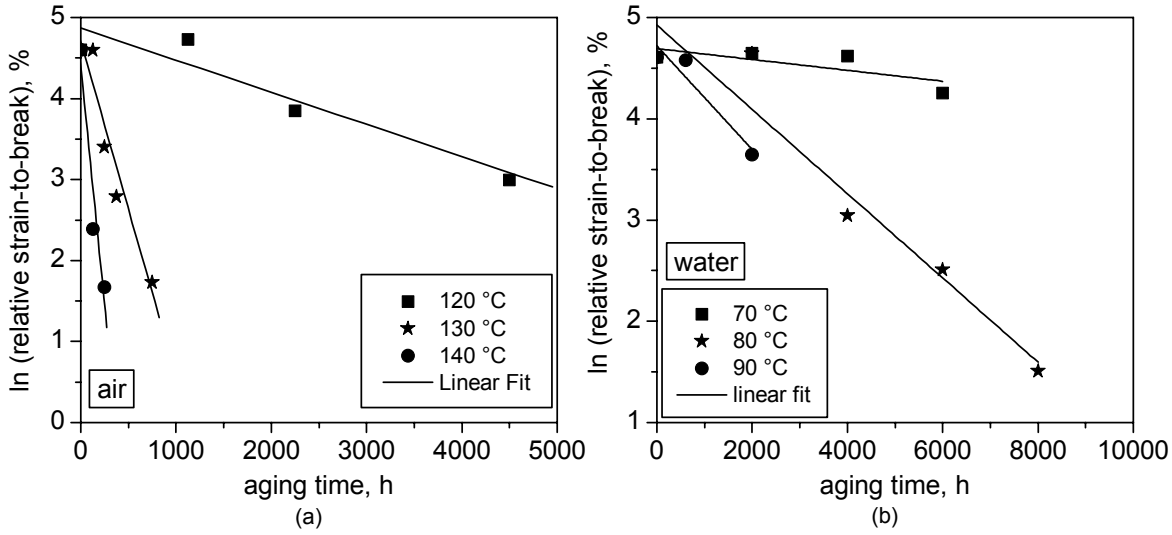

Fig. 7: Relative strain-to-break vs. aging time for PC after exposure to (a) hot air and (b) hot water.

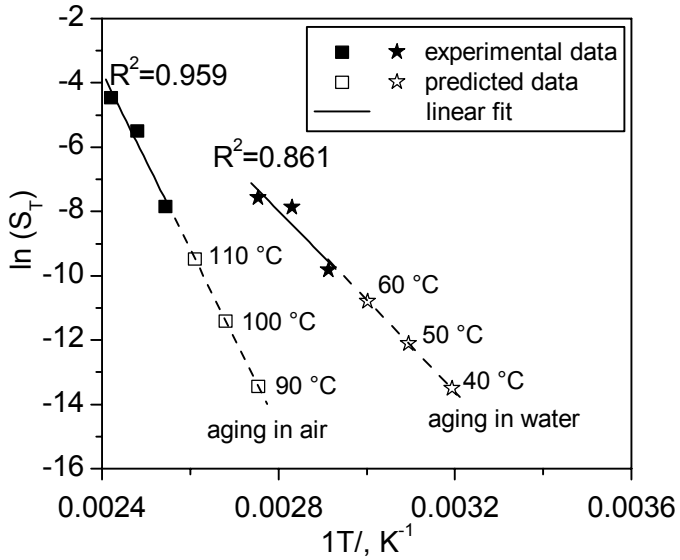

Fig. 8: Arrhenius type diagram for PC according to Hoang et al. (2008) for hot air and hot water aging, respectively, using the empirical reaction rate concept.

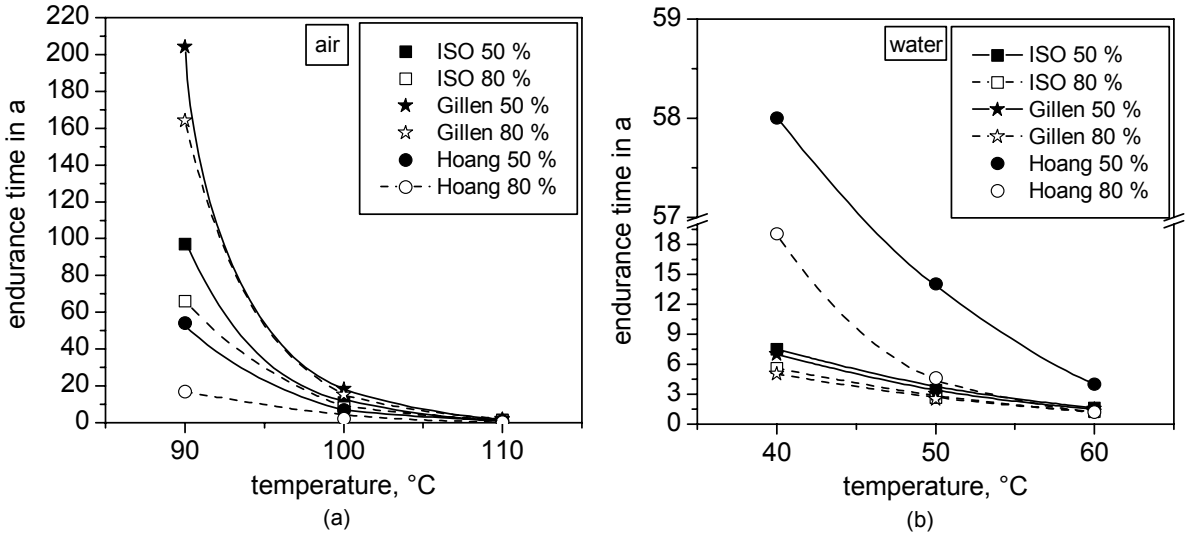

Fig. 9: Predicted lifetimes (endurance limits) for PC exposed to temperatures ranging (a) from 90 to 110 °C in air and (b) from 40 to 60 °C in water according to various models and assumptions (residual strain-to-break after aging).

PAPER 5°

Aging Behavior of Polymeric Solar Absorber Materials: Aging on the Component Level

S. Kahlen[a)*], G. M. Wallner[b)], R. W. Lang[b)], M. Meir[c)], J. Rekstad[c)]

[a)] Polymer Competence Center Leoben GmbH, Roseggerstrasse 12, Leoben, 8700, Austria

[b)] Institute of Materials Science and Testing of Plastics, University of Leoben, Franz-Josef Strasse 18, Leoben, 8700, Austria

[c)] Department of Physics, University of Oslo, POBox 1048, Blindern, Oslo, 0316, Norway

ABSTRACT

Within this study, the aging behavior of a PPE+PS absorber material was investigated on the absorber component level. To indicate aging, characteristic mechanical values were determined by indentation tests of specimens taken from components and exposed to laboratory aging (140 °C in air, 80 °C in water) and service near outdoor aging conditions (stagnation in northern climate). In addition to the mechanical tests, the unaged and aged specimens were also characterized thermo-analytically via differential scanning calorimetry (DSC). The results indicate that reductions in both characteristic mechanical values of the indentation tests, i.e. load of the first transition and ultimate indentation, reflect at least some physical aging although chemical aging may also be of importance based on previous analytical investigations of laboratory aged polymer films. While laboratory aging in air at 140 °C and service exposure at a test facility in Oslo (N) under stagnation conditions led to a significant reduction in the mechanical indentation resistance, no influence of laboratory aging in water at 80 °C on the mechanical behavior of the absorber sheet was found. Depending on the ultimate failure criterion applied (reduction of characteristic mechanical values to 80 % and

---

° To be published in “Solar Energy”.

* Corresponding author. Tel.: +43 (0) 3842 42962 50
Email address: kahlen@pccl.at

50 %, respectively), the technical service life found for hot air laboratory and stagnation service conditions was found to be less than 51 h and 159 h, respectively. As these durations are significantly below the estimated stagnation conditions accumulated in the desired operation lifetime for such a collector, the PPE+PS type investigated does not seem to be a proper material candidate for solar thermal absorbers. Finally, based on the results obtained, a relation between laboratory aging time in air at 140 °C and cumulated irradiation energy during exposure on the test facility in Oslo was established.

Keywords: polymers, solar thermal application, component testing, aging.

1 INTRODUCTION

The evaluation and certification of solar thermal collectors is usually performed according to EN 12975-2 (2006). However, as to the use of polymeric materials, only unglazed collectors (swimming pool absorbers) are considered in this standard. So far, no standard exists for the use of plastics in glazed collectors. For an all-polymeric collector, several adaptations such as a drain-back design in combination with low-pressure levels are usually needed (Meir and Rekstad, 2003). As a result, the operating conditions of a collector with an absorber made of plastics and a conventional collector are different.

Different testing and evaluation methods have to be implemented to predict the applicability and the long-term performance of a polymeric absorber in a glazed collector. Olivares et al. (2008) developed a method to determine the long-term stability of a polymeric absorber sheet. Segments of the polymeric absorber were exposed to water or air at elevated temperatures. After accelerated aging the component was tested by a mechanical indentation method. To evaluate the component (i.e., compression of the inner walls and the deflection of the surface in one test) an indentation test with a prismatic indenter was proposed. Olivares et al. (2008) defined the “surface strength” which corresponds to indentation failure as characteristic values for the evaluation of the plastics absorber sheet under operation.

To study the influence of aging at elevated temperatures in air and water, Kahlen et al. (2009a+b+c+d) performed tests on polymer film specimens. Different commercially available engineering and commodity plastics potentially suitable for the application in solar thermal absorbers were chosen and investigated as to their performance behavior. Several mechanical parameters such as the modulus, characteristic for the small strain regime, the yield strength and the strain-to-break were determined and interpreted in terms of physical and chemical aging, respectively. With regard to the classification of aging, size exclusion chromatography (SEC) to determine changes in molecular mass and differential scanning calorimetry (DSC) were applied.

This work is a continuation of the previous papers and extends the investigations from film specimens aged under laboratory conditions to component sections aged under laboratory and outdoor service stagnation conditions. The main objectives are (1) to apply and evaluate the practical engineering methodology originally proposed by Olivares et al. (2008) to describe the performance of plastics absorber sheets in the unaged state to laboratory and service aged specimens and (2) to interpret the results in terms of absorber lifetime expectations.

2 EXPERIMENTAL

The experimental program described in detail below included aging exposure of specimens taken from extruded absorber sheets, which were characterized mechanically by a special indentation test and analytically by DSC.

2.1 Materials and Exposure

The specimens investigated were taken from extruded absorber sheets of a blend of polyphenylene ether and polystyrene (PPE+PS). The raw material was supplied by Sabic (Sabic Innovative Plastics Holding BV; Bergen op Zoom; The Netherlands), the extrusion of the absorber sheets with a thickness of approximately 10 mm was performed by Solarnor (Solarnor AS; Oslo; N). First, sections were cut from the absorber sheets perpendicular to the extrusion direction with a width of 72 mm. Specimens were then obtained by cutting these sections into 6 segments with a width of 87 mm. As to labeling, the letters A to F

were used according to the nomenclature of Olivares et al. (2008). For laboratory aging, specimens were exposed to hot air at 140 °C up to 500 h and to hot water at 80 °C up to 16000 h. In addition, identical absorber sheets were exposed on the roof of the laboratory site at the University of Oslo in Norway (referred to as Sollab) under stagnation conditions (latitude 59.98 °, azimuth 17 °, tilt angle 32 °; no water running through the absorber). The absorber sheets were placed on the roof at the Sollab according to the Solarnor installation standards and were exposed to solar irradiation for different time intervals, i.e. ½ winter, ½ summer, 1 winter, 1 summer, 1 year and 2 years. On the back of the absorber sheets and placed on the top of the stand a temperature sensor with an accuracy of 0.2 – 0.5 K (type: PT1000; Tritec group; Allschwil/Basel; CH) was mounted. Furthermore, the incoming irradiation was measured using an irradiation sensor (type: Tritec SIC 100; Tritec group, Allschwil/Basel, CH). In Table 2 the measured cumulated irradiation energies are depicted. After the outdoor aging exposure, specimens of equivalent dimensions and nomenclature as described above were cut from the aged absorber sheets.

When comparing the results of this study on the absorber component level with previous results obtained on the film specimen level produced from the same raw material, the following findings on the molecular weight for the different processing conditions should be kept in mind. While compared to the PPE+PS compound in granule form, for the film specimens a reduction in weight average molecular mass (M_w) by about 20 % was found, probably due to improper processing conditions, the absorber sheets revealed only a decrease of 5 % in M_w compared to the original state.

2.2 Mechanical Testing

In terms of mechanical testing, indentation tests according to Olivares et al. (2008) were performed using a screw driven universal testing machine (type: Instron 4505; Instron International Ltd.; High Wycombe; UK) (see Fig. 1*). A prismatic indenter (oriented with the contact edge in the extrusion direction) was used. The indentation speed was 1 mm/min. For reproducibility reasons, 3 samples of each segment were tested.

As depicted in Fig. 2, load/indentation curves did not always show a pronounced maximum. Hence, for the evaluation of the load/indentation curves in terms of a first local failure criterion, a method analogous to the theory of the Considère's construction (Boyce and Haward, 1997) was applied to determine the first knee (transition) in the load/indentation curves (Fig. 3). According to this procedure, the intersection of the first derivative of the load/indentation curve with the curve itself was determined. This knee or first transition point is referred to as force transition point F_T in the subsequent discussion. Furthermore, in terms of a characteristic ultimate value, the indentation at break I_B, accompanied by a drop in the load by more than 300 N and defined in terms of the associated displacement was chosen (see Fig. 2). Due to the initial thickness of 10 mm of the absorber sheet, the indentation measurement was limited to a maximum displacement value of 9 mm.

2.3 Differential Scanning Calorimetry (DSC)

Thermal analysis was carried out using a Mettler Toledo DSC 821e instrument (type: Mettler Toledo GmbH; Schwerzenbach, CH). Samples with a mass in the range between 8 and 12 mg were put in a 40 µl pan and closed with a perforated lid. The thermograms were recorded under static air applying a heating/cooling/heating cycle at a heating/cooling rate of 10 K/min. To analyze any effects of the aging exposure, only results of the initial (1^{st}) heat-up were considered. In other words, all diagrams shown in the section on results and discussion correspond to the 1^{st} heating scan. The oxidation temperature T_{ox} was determined with the tangent method by determining the intercept point of the baseline and the slope to the final exothermal ascent of the DSC curve.

3 RESULTS

3.1 Laboratory Aging

3.1.1 Mechanical Indentation Tests

The indentation tests on the segments A to F yielded the highest reproducibility for segment D. In the following, load/indentation curves determined for segment D are described and discussed in detail (see Fig. 2). Characteristic mechanical

properties including the force value of the first transition and the indentation at break in the unaged state and the fully aged state in air at 140 ° and in water at 80 °C are listed in Table 1 and shown in Fig. 4.

Table 1: Characteristic mechanical properties in the unaged and fully aged condition (air at 140 °C for 500 h and water at 80 °C for 16000 h) determined for segment D.

Aging conditions	**Force value of first transition, F_T** in N	**Indentation at break, I_B** in mm
unaged	1202 ± 10	9 ± 0
air (500 h, 140 °C)	693 ± 16	1.16 ± 0.03
water (16000 h, 80 °C)	1210 ± 31	9 ± 0

While after aging in hot air a significant decrease in the first transition load by 30 % and 42 % after 250 h and 500 h, respectively, was obtained, hot water aging had nearly no effect on the first transition point of the absorber sheet. Similarly, indentation at break values decrease significantly after aging in air at 140 °C by 87 % after 500 h where fracture of the components occurred close to the transition point. After hot water exposure also no changes in ultimate indentation were determined. The maximum displacement level of 9 mm was achieved. Thus, only hot air exposure led to changes (i.e., a decrease) in the first transition in the load indentation and in ultimate indentation results. The indentation test results after aging in hot air are in accordance with Olivares et al. (2009) who reported a drastic decrease in load already within the first 200 h of aging in air at 140 °C.

As described in a previous paper (Kahlen et al., 2009b), on the film specimen level a significant embrittlement (drop in ultimate strain values below yield point) was obtained after exposure to air at 140 °C and to water at 80 °C within the first measurement interval (125 h in air at 140 °C, 2000 h in water at 80 °C) and no determination of the yield point was possible. In accordance with other analytical test results, the aging behavior of PPE+PS on the film specimen level after hot air and hot water exposure indicated significant chemical aging, accompanied by substantial reductions in strain-to-break values. Analogous to the ultimate mechanical elongation results on the film specimen level, indentation at break on the component specimen level may have been caused by chemical degradation.

As for the component level the same tendency after aging in hot air was observed for the indentation at break I_B and the transition point F_T, the latter may presumably also be attributed to irreversible degradation. Moreover, in agreement with results on the film specimen level, exposure in air at 140 °C was identified to be more harmful than water exposure at 80 °C. However, in all these comparisons the differences in the initial state of degradation of film specimens and component specimens due to processing must be kept in mind. Thus, it may well be that due to the more significant irreversible degradation of PPE+PS films during extrusion (by a decrease of 20 % in weight average molecular mass) compared to the component level (by a decrease of 5 % in weight average molecular mass), the lower temperature of hot water exposure affected the mechanical properties of the film specimens to a stronger extent and no influence on the component level was observed. Hence, at this point only a limited correlation between the aging behavior of the component and the specimen level can be established. In further studies special focus should be given on comparable processing conditions on film specimen and component level.

3.1.2 Differential Scanning Calorimetry

DSC diagrams obtained from testing of the absorber sheets exposed for specific times to hot air and hot water, respectively, are shown in Fig. 5. The unaged reference absorber sheet specimen exhibits a glass transition of 160 °C and a value for T_{ox} of about 292 °C. Already after 125 h exposure to hot air an endothermic peak appears, indicating physical aging by free volume diffusion (Hutchinson, 1995; Wallner et al., 2004). No further change in the peak size was determined up to 500 h, indicating that the main physical aging process occurs within the initial period of aging. In contrast, based on the observations by DSC, hot water aging exhibited no significant physical aging phenomena. Moreover, for both aging conditions no clear indication for chemical aging can be deduced from the DSC results. It must be mentioned, however, that the oxidation temperature was difficult to determine. Nevertheless, these results are in good agreement with DSC results reported before for a laboratory aging investigation on the film specimen level (Kahlen et al., 2009b). This implies that the different state of pre-aging induced by the extrusion process for films (reduction in molecular mass by

about 20 %) vs. absorber sheets (reduction in molecular mass by about 5 %) apparently has no influence on the thermo-analytical properties. Consequently, the decrease in F_T and I_B found after hot air exposure in indentation tests may thus be attributed at least in part to physical aging. At his point it should be mentioned that in the previous investigation of laboratory aged film specimens, clear evidence for chemical aging was found for equivalent exposure conditions (Kahlen et al, 2009b). However, further analytical investigations as to chemical aging on the component level are needed to unambiguously clarify the existence of chemical aging mechanisms on the absorber sheet level.

3.2 Outdoor Aging

3.2.1 Mechanical Indentation Tests

The exposure time, the cumulated irradiation energy in kWh/m^2 calculated over the exposure time and the maximum temperatures of the absorber sheets investigated (numbered from 1 to 7) are provided in Table 2.

Table 2: Comparison of the investigated absorber sheet exposed to outdoor conditions on the Sollab.

Absorber number	**Exposure time**	**T_{max}** in °C	**Exposure interval** (dates)	**E_{cum}** in kWh/m^2
1	1 winter	115	28.09.2005 - 10.04.2006	233
2	½ summer	110	07.03.2005 – 18.07.2005	635
3	1 summer	115	07.03.2005 – 29.09.2005	901
4	1 year	131	25.04.2006 – 27.04.2007	928
5	1 year	115	07.03.2005 – 25.04.2006	1159
6	2 years	128	20.07.2005 – 12.03.2007	1327
7	2 years	131	07.03.2005 – 12.03.2007	1883

Typical load indentation curves of segment D of the absorber sheets 1 to 7 exposed to outdoor aging are shown in Fig. 6. Specimen R refers to the unaged reference sheet. The characteristic mechanical properties values, the force value of the first transition point F_T and the indentation at break I_B, for these absorber sheets are listed in Table 3.

Table 3: Characteristic mechanical properties in the unaged state and in the aged state (outdoor exposure at the Sollab under service stagnation conditions) determined for segment D.

Absorber number	**Exposure time**	**T_{max}** in °C	**E_{cum}** in kWh/m²	**Force value of first transition, F_T** in N	**Indentation at break, l_B** in mm
1	1 winter	115	233	1213 ± 22	9 ± 0
2	½ summer	110	635	1094 ± 17	3.9 ± 0.3
3	1 summer	115	901	1073 ± 3	3.6
4	1 year	131	928	1104 ± 166	1.2 ± 0.2
5	1 year	115	1159	1166 ± 2	-*)
6	2 years	128	1327	706 ± 67	0.7
7	2 years	131	1883	544 ± 39	0.7

*) No determination of indentation at break possible due to high scatter in the experiments.

Up to an accumulated irradiation energy of 1159 kWh/m² (absorber 5) no significant change in F_T (Fig. 7) was determined for segment D. For specimens taken from absorber 6 (exposure of 2 years, accumulated irradiation energy of 1883 kWh/m²) and from absorber 7 (exposure of 2 years, accumulated irradiation energy of 1327 kWh/m²) F_T values dropped by 41 % and 55 %, respectively (Fig. 7). This is in accordance with the force transition results of the absorber sheets aged in the laboratory in air at 140 °C which also indicated a significant drop in force after a certain period of exposure. Also indentation at break values for segment D indicate a decrease already after 635 kWh/m² (1/2 summer) by 55 % and further full embrittlement after 1327 kWh/m² (2 years) by a decrease of 92 % (compare Fig. 7). In this analysis, results of sheet number 5 (corresponding to an accumulated irradiation energy of 1159 kWh/m²) were not included due to high scatter in indentation at break values. Thus, in accordance with the l_B results of the laboratory aged absorber sheets exposed to air at 140 °C, outdoor exposure also led to significant changes in ultimate indentation at break. Hence, results of the absorber sheets exposed at the Sollab indicate the same trend as laboratory oven experiments on absorber sheets exposed to air at 140 °C. Interestingly, force values of the first transition decrease simultaneously with indentation at break values, the latter being associated with total embrittlement of the Sollab exposed sheets. Hence, both parameters, transition point and indentation at break, may be

considered to indicate and reflect degradation also by chemical aging. However, it seems that under outdoor stagnation conditions indentation at break values are slightly more affected.

3.2.2 Differential Scanning Calorimetry

Typical DSC thermograms of the outdoor exposed absorber sheet specimens and the unaged reference absorber sheet are illustrated in Fig. 8. While initially no significant influence of exposure on the glass transition was found, absorber sheet number 6 and 7, which were outdoor exposed for 2 years, exhibit pronounced physical aging. With reference to the previously described mechanical indentation test results, this corresponds to a significant reduction in the force transition value F_T and the indentation at break l_B, which was also observed only for absorber sheets 6 and 7. Simultaneously, for all sheets exposed on the Sollab no influence on the oxidation temperature was found, so that at least from the DSC measurements again no indication for chemical aging can be deduced. And yet, based on the previously cited study on laboratory aged film specimens, the occurrence of chemical aging is rather likely. Here too, however, further analytical investigations are needed to unambiguously identify or exclude chemical aging under the chosen outdoor conditions.

3.2.3 Correlation between laboratory and outdoor aging

To check potential correlations between aging exposure under laboratory and outdoor conditions, the ultimate indentation values are compared in Fig. 9. The relative indentation at break values after outdoor aging are plotted as a function of cumulated irradiation energy, whereas the same values are plotted for laboratory aging conditions at 140 °C in air as a function of time. By comparison, it should be noted that under outdoor conditions, temperatures above 120 °C occurred over a time span of 85.5 h and none of the outdoor aged sheets experienced temperatures higher than 131 °C within the time span of exposure (compare Table 2).

To correlate the effects of outdoor aging (varying temperature profile up to 2 years) and laboratory aging (constant temperature of 140 °C up to 500 h), the

relative change in I_B values is plotted in Fig. 9 in a manner so that the functional form of the curves corresponds to one another for both aging procedures.

In both cases the curves were fitted with an exponential relationship y = 100*exp (-A*x). Based on the exponential decay function obtained for both cases, the following approximate inter-conversion between laboratory aging time t_L (in h) and accumulated outdoor irradiation exposure E_{cum} (in kWh/m^2) was obtained:

$$E_{cum} \cong 0.229 * t_L$$

Not considered in the above fitting and inter-conversion calculation was absorber 5 (1159 kWh/m^2) due to high scatter in the indentation test results. Assuming an analogous criterion for determining the endurance limit as in a previous study by Kahlen et al. (2009d), the reduction in relative I_B values to 50 % and 80 %, respectively, may be chosen. For these reductions, limits for the accumulated irradiation energy under outdoor exposure of 529 kWh/m^2 (50 %) and 170 kWh/m^2 (80 %) corresponding to a laboratory aging time at 140 °C in air of 159 h (50 %) and 51 h (80 %) are obtained. In practical terms this implies, that absorbers produced out of the PPE+PS compound investigated may fail well before the required service life of 20 years corresponding to an accumulated time under stagnation of about 500 h.

4 SUMMARY AND CONCLUSIONS

Specimens taken from PPE+PS absorber sheets were characterized as to their aging behavior comparing the effect of laboratory aging conditions (in air at 140 °C up to 500 h and in water at 80 °C up to 16000 h) and outdoor exposure in northern climate up to 2 years. In performing indentation tests, two characteristic mechanical properties were determined including the load of the first transition (F_T) and the indentation at break (I_B). While no influence on these indentation properties was found for laboratory oven tests in hot water, after hot air exposure both, F_T and I_B values decreased significantly after a short period of aging time. In DSC experiments performed with the same unaged and laboratory as well as outdoor aged specimens, clear indications for physical aging were found at least hot air laboratory exposure and outdoor exposure. Although in accordance with

previous investigations, no clear indication for chemical aging was deducible from DSC experiments, results on the film specimen level of PPE+PS described elsewhere (Kahlen et al., 2009b) also revealed significant reductions in strain-to-break after hot air and hot water exposure within the shortest measurement interval (125 h in air at 140 °C and 2000 h in water at 80 °C). In that study, which also included further analytical tests such as size exclusion chromatography (SEC), this behavior was attributed to chemical aging. Hence, analogous with the behavior of ultimate elongation results found on film specimens, indentation at break values determined by testing absorber sheets indicating a significant deterioration in material performance may be interpreted also in terms of a contribution of chemical aging. Since F_T values exhibited the same trend as I_B values, these mechanical properties may also well be a result of irreversible degradation by chemical aging. However, final evidence for chemical aging under these aging conditions still remains to be shown. In accordance with laboratory aging tests at 140 °C in air, the outdoor aging experiments also led to significant changes in ultimate indentation at break values by a sudden decrease after a certain period of exposure. The experimental data of indentation at break determined with outdoor aging experiments and with laboratory oven tests were then fitted with an exponential decay function, and a relation between accumulated irradiation energy of outdoor aging and laboratory aging time was determined. Using a criterion of 80 % and 50 % reduction in the indentation at break value for the aged state relative to the unaged state, 51 h and 159 h, respectively, were predicted as service life. Over all, based on these results the investigated PPE+PS material does not seem to be suitable for glazed solar thermal absorber applications without overheating protection.

Acknowledgments

The research work of this paper was performed within the project S. 11 “Aging of polymers in solar-thermal applications” at the Polymer Competence Center Leoben GmbH within the framework of the K_{plus} Program of the Austrian Ministry of Traffic, Innovation and Technology with contributions by the University of Leoben, Graz University of Technology, Johannes Kepler University Linz, JOANNEUM RESEARCH ForschungsgmbH and Upper Austrian Research GmbH. The PCCL is funded by the Austrian Government and the State Governments of Styria and Upper Austria.

Literature

Boyce, M.C., Haward, R.N., 1997. The post-yield deformation of glassy polymers. In: Haward, R.N., Young, R.J. (Eds.), The physics of glassy polymers, second edition. Chapman and Hall, London, United Kingdom, p. 221.

EN 12975-2, 2006. Thermische Solaranlagen und ihre Bauteile-Kollektoren. Teil 1: Allgemeine Anforderungen.

Hutchinson, J.M., 1995. Physical aging of polymers. Prog. Polym. Sci. 20, 703-760.

Kahlen, S., Jerabek, M., Steinberger, R., Wallner, G.M., Lang, R.W., 2009a. Characterization of Physical and Chemical Aging of Polymeric Solar Materials by Advanced Mechanical Testing. To be submitted in Polym. Test.

Kahlen, S., Wallner, G.M., Lang, R.W., 2009b. Aging behavior of polymeric solar absorber materials – part 1: engineering plastics. Submitted to Sol. Energy.

Kahlen, S., Wallner, G.M., Lang, R.W., 2009c. Aging behavior of polymeric solar absorber materials – part 2: commodity plastics. Submitted to Sol. Energy.

Kahlen, S., Wallner, G.M., Lang, R.W., Meir, M., Rekstad, J., 2009d. Aging Behavior and Lifetime Modeling for Polymeric Solar Absorber Materials. Submitted to Sol. Energy.

Meir, M.G., Rekstad, J., 2003. Der Solarnor® Kunststoffkollektor - the development of a polymer collector with glazing. In: Wallner, G.M, Lang, R.W. (Eds.), Proceedings of 1st Leobener Symposium Polymeric Solar Materials, pp. II-1-II-8.

Olivares, A., Rekstad, J., Meir, M., Kahlen, S., Wallner, G., 2008. A test procedure for extruded polymeric solar thermal absorbers. Sol. Energy Mater. Sol. Cells 92, 445-452.

Olivares, A., Rekstad, J., Meir, M., Kahlen, S., Wallner, G., 2009. Degradation model for an extruded polymeric solar thermal absorber. Sol. Energy, submitted.

Wallner, G.M., Lang, R.W., 2005. Guest editorial. Sol. Energy 79 (6), 571-572.

Fig. 1: Indentation test set-up with a prismatic indenter applied to the absorber sheet specimen.

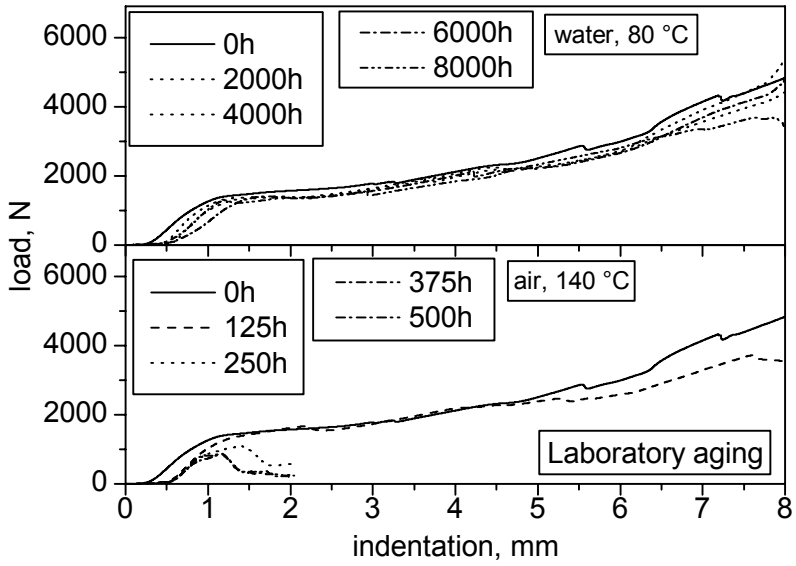

Fig. 2: Load-indentation curves for segment D after laboratory aging in air at 140 °C and in water at 80 °C.

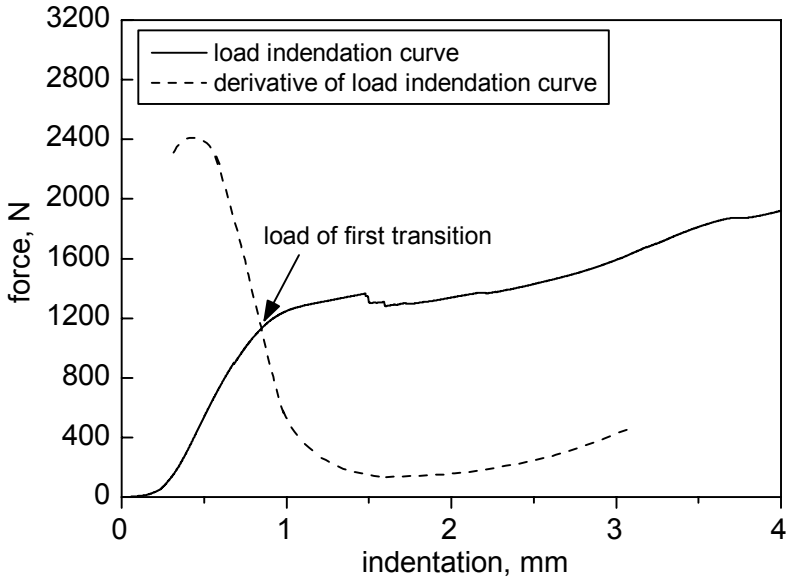

Fig. 3: Illustration of the determination for the load of first transition for segment D.

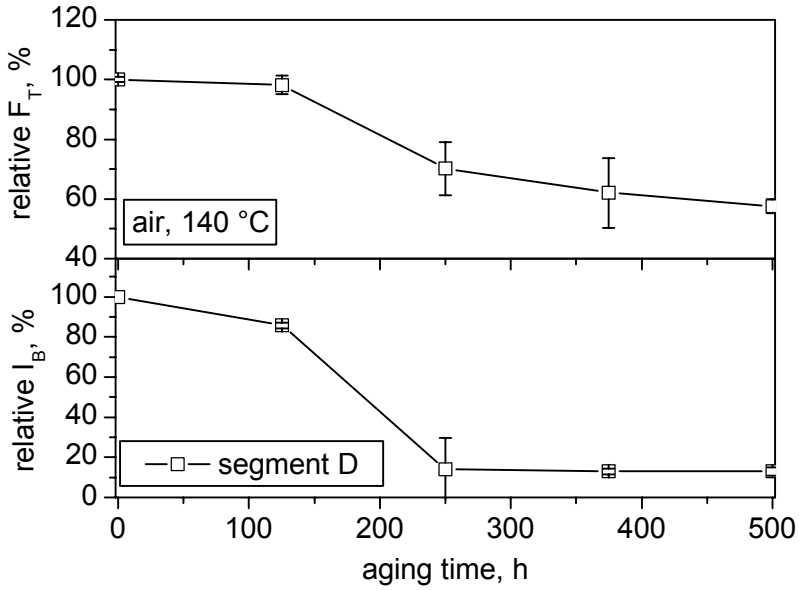

Fig. 4: Load at transition point (F_T) and indentation at break (I_B) in relative units versus aging time for segment D after laboratory aging in air at 140 °C.

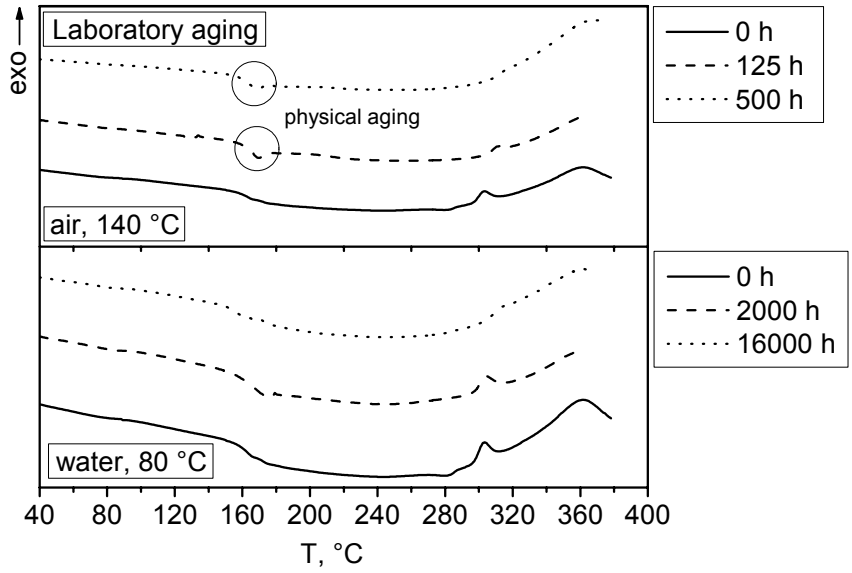

Fig. 5: DSC thermograms of PPE+PS absorber sheets exposed to air at 140 °C (0, 125 and 500 h) and to water at 80 °C (0, 2000 and 16000 h).

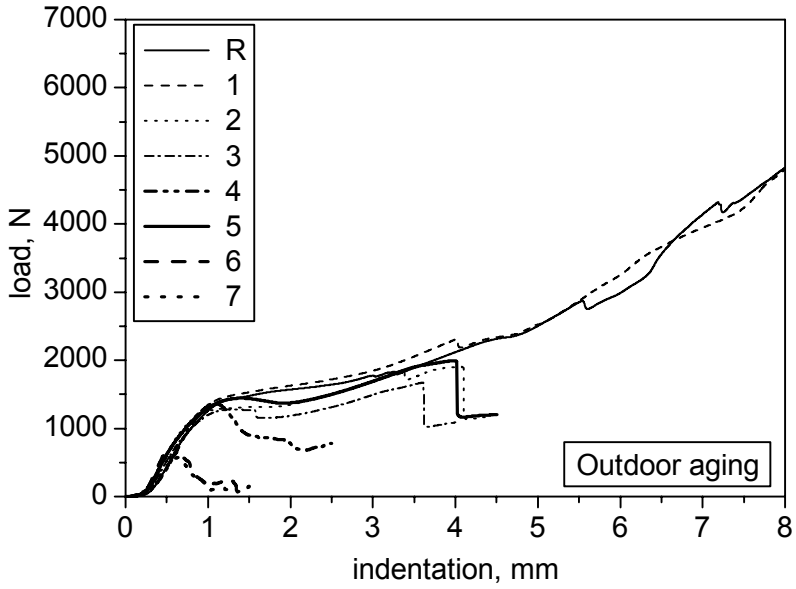

Fig. 6: Load-indentation curves for absorber sheet segment D after aging under outdoor conditions in comparison to an unaged absorber sheet reference specimen R. For a detailed description of outdoor aging conditions see Table 2.

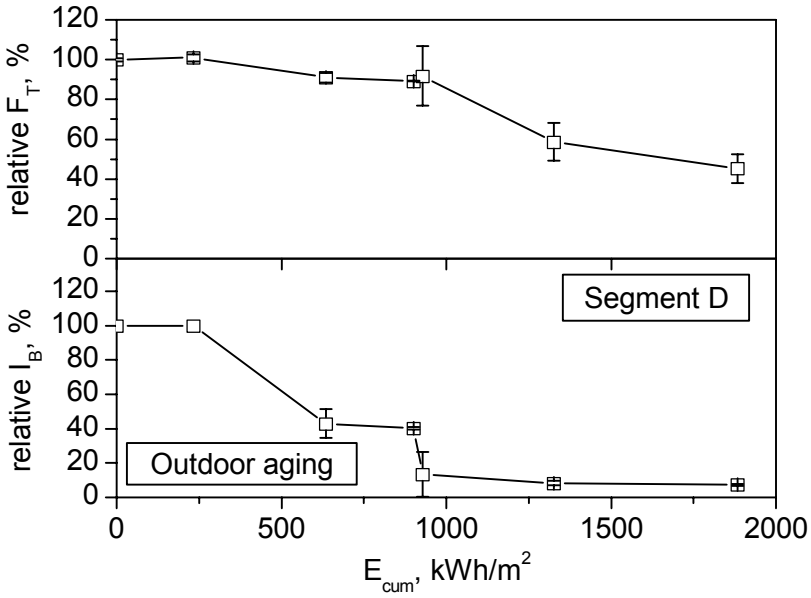

Fig. 7: Change in load at first transition (F_t) and indentation at break (I_B) in relative units versus cumulated irradiation energy for segment D after outdoor aging exposure.

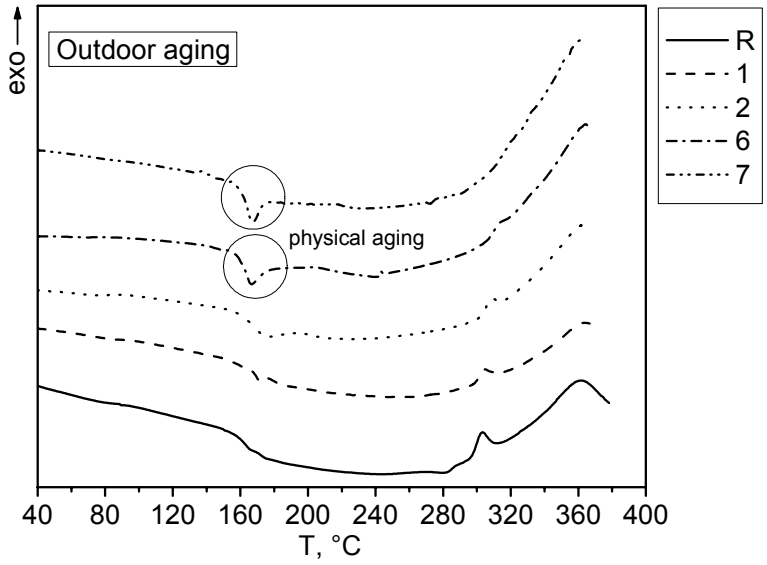

Fig. 8: DSC thermograms of PPE+PS absorber sheets after outdoor aging exposure.

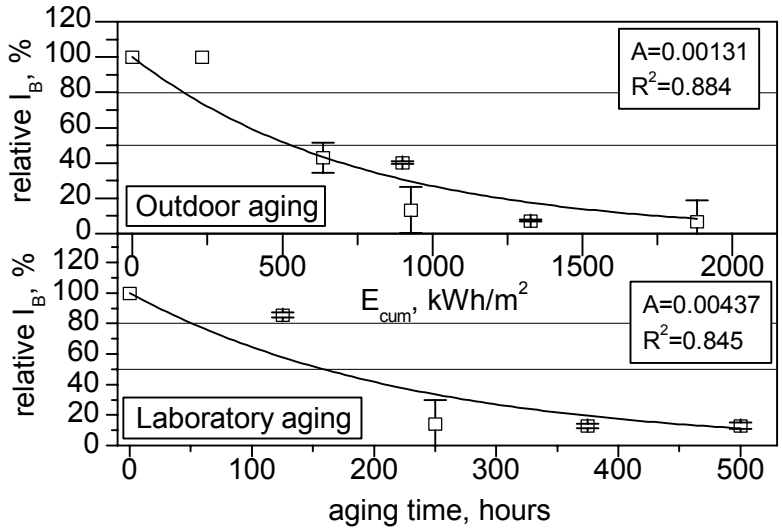

Fig. 9: Relative indentation at break (I_B) versus laboratory aging time at 140 °C in air in h (bottom) and versus the accumulated irradiation energy in kWh/m^2 for outdoor aging (top) for segment D. Experimental data are fitted with the exponential decay function y = 100*exp (-A*x). The constant A and the linear regression coefficient (R^2) for this fit are displayed.